University of Kentucky

UKnowledge

University of Kentucky Master's Theses   Graduate School

2011

DEVELOPMENT OF NOVEL ELECTROPHILIC RUTHENIUM(II) AND IRIDIUM(III) COMPLEXES AND THEIR APPLICATIONS AS HOMOGENEOUS CATALYSTS

Ryan R. Ketcham
University of Kentucky, rrketc2@uky.edu

Right click to open a feedback form in a new tab to let us know how this document benefits you.

ABSTRACT OF THESIS

DEVELOPMENT OF NOVEL ELECTROPHILIC RUTHENIUM(II) AND IRIDIUM(III) COMPLEXES AND THEIR APPLICATIONS AS HOMOGENEOUS CATALYSTS

Our aim was to develop the synthetic potential and reaction chemistry of Ir^{3+} and Ru^{2+} electrophiles by preparing well-characterized complexes whose properties are controllable by modification of the ancillary ligand environment Specifically, we prepared a series of ruthenium complexes to serve as selective hydrogenation and hydrogenolysis catalysts of furan derivatives. We also expanded the synthesis of electrophilic Ir^{3+} di-thiolate complexes. These types of compounds could eventually serve as catalysts precursors for the addition of weak nucleophiles to alkynes and nitriles.

KEYWORDS: Biofuels, Ruthenium Dihydrogen Complexes, Iridium Di-thiolate complexes, Hyrdrogenation of Furans, Heterolytic Activation of Dihydrogen

Ryan Robley Ketcham

04/05/2011

DEVELOPMENT OF NOVEL ELECTROPHILIC RUTHENIUM(II) AND IRIDIUM(III) COMPLEXES AND THEIR APPLICATIONS AS HOMOGENEOUS CATALYSTS

By

Ryan R Ketcham

Dr. Folami Ladipo

—————————————

Director of Thesis

Dr. John Anthony

—————————————

Director of Graduate Studies

RULES FOR USE OF THIS THESIS

Unpublished theses submitted for the Master's degree and deposited in the University of Kentucky Library are, as a rule, open for inspection, but are to be used only with due regard to the rights of the authors. Bibliographical references may be noted, but quotations or summaries or parts may be published only with the permission of the author, and with the usual scholarly acknowledgments.

Extensive copying or publication of the theses in whole or in part also requires the consent of the Dean of the Graduate School of the University of Kentucky.

A library that borrows this thesis for the use of its patrons is expected to secure the signature of each user.

Name   Date

_____

_____

_____

_____

_____

_____

_____

_____

_____

_____

_____

_____

_____

_____

THESIS

Ryan Robley Ketcham

The Graduate School

University of Kentucky

2011

DEVELOPMENT OF NOVEL ELECTROPHILIC RUTHENIUM(II) AND
IRIDIUM(III) COMPLEXES AND THEIR APPLICATIONS AS HOMOGENEOUS
CATALYSTS

_____

THESIS

_____

A thesis submitted in partial fulfillment

of the requirements for the degree of

Master of Science at the University of Kentucky

By

Ryan R Ketcham

Advisor: Dr. Folami Ladipo, Asscociate Professor of Chemistry,

Lexington, Kentucky

2011

ACKNOWLEDGEMENTS

I would like to thank my advisor, Dr. Folami. T. Ladipo, for his guidance and encouragement. I would also like to thank my committee members for their help and support. My lab mates were very important to my success as were my colleagues from other synthetic laboratories. My family's support throughout this test of endurance was also very important.

Table of Contents

List of Figures

List of Schemes

CHAPTER 1

The Development of Electrophilic Ruthenium-Based Hydrogenation/ Hydrogenolysis Catalytic Systems

Introduction

The use of fossil fuels is well documented since the dawn of technology. Much of early forms of fossil fuels were coal, and oil. Only in the past 150 years have coal, natural gas, and petroleum grown to their more principal roles as sources of usable energy.[1] The expansion and full realization of the petrochemical industry can be considered one of the greatest technological success stories.

Since the development of the world's first commercial oil field in Azerbaijan (1848), the exploitation, refinement, and chemical transformation of crude oil has not only provided fuel for heating, but also electricity for light and eventually gasoline for transportation.

However, due to these oil and fossil fuel stocks diminishing in supply and the growing concern about overall environmental impacts, a more sustainable energy source is needed.

For continued world economic growth, it seems likely that in the near future, a renewable energy source will be required to complement fossil fuels.

Abundant biomass resources offer a promising alternative for the production of sustainable fuel and essential industrial chemicals.[2] With recent advances in conversion technology, biomass resources now have the potential to gain a central position as a primary energy feedstock for civilization. A fructose dehydration product, 5-

hydroxymethylfurfural (HMF), will likely fulfill a role in this bio-based rebirth. From HMF, 2,5-dimethylfuran (DMF) can be obtained. DMF has the potential to replace ethanol in the near future as a fuel additive.

Fructose can be made readily available from lignocellulosic biomass material with use of ionic liquids.[3] Watanabe et al. have recently reported the catalytic conversion of the furanose form of fructose to HMF via an ion-exchange resin and microwave heating.[4]

From HMF, DMF can be obtained with the use of certain homogenous catalytic systems. The development of these types of catalysts is a tantalizing area of chemical research. DMF has the potential for use as a bio-derived transportation fuel and could complement the use of gasoline. DMF has many advantages over ethanol, the current biofuel additive.

Ethanol has hydroscopic properties, which can cause the absorption of water from the air, thus, contamination of the fuel is an issue. It has a relatively low boiling point which can limit its storage due to the relative ease of evaporation from reservoir tanks. Also, the energy of combustion of ethanol is somewhat low in comparison to 2,5-dimethylfuran.

Due to these shortcomings of this present bio-fuel, a more suitable system is desired. Compared to ethanol, 2,5-dimethylfuran has about a 40% higher energy density, a higher boiling point by 20 K, and is not as nearly miscible with water. These properties make the use of DMF in the transportation sector an attractive bio-based

alternative.   The platform chemical, HMF, can be converted into a plethora of synthetically useful aldehydes, acids, alcohols, and amines.

Currently there is less ongoing focus on the design and development of catalytic systems that can convert HMF into the above mentioned chemicals. There is a present need for the development of new soluble and well-defined catalysts for the hydrogenation and hydrogenolysis of furan derivatives and the production of 2,5-dimethylfuran. These catalyst systems must act via well understood mechanistic pathways and exhibit high activity and product selectivity.

Our effort focused on the design and development of efficient catalytic systems for the conversion of 5-hydroxymethylfurfural to 2,5-dimethylfuran and furfural to 2-methylfuran.

Scheme 1. Generalized scheme for 2,5-DMF production.
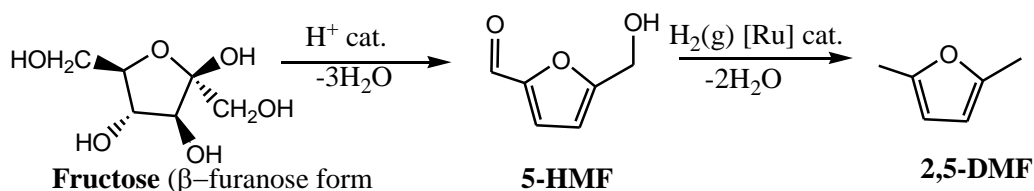
In particular, we desired to develop a series of electrophilic transition metal phosphine complexes that are discrete, well characterized, easily studied, and capable of heterolytically activating $H_2(g)$.

To date, the synthesis and study of phosphine-transition metal complexes that can selectively hydrogenate furan derivatives is lacking. The design and synthesis of electrophilic ruthenium complexes that permit synthetically facile tuning of the metal center is an area that needs to be further developed. Ligand modification on the metal complex would affect the overall capability of the complexes as hydrogenation/hydrogenolysis catalysts. An easily modified catalyst that can support a dihydrogen-metal interaction and sufficiently activate the bound dihydrogen is desired. The catalyst would need to be sufficiently electrophilic to heterolytically cleave dihydrogen in the presence of substrate under high pressures and at high temperatures. A ligand system that can guard the metal against reduction and oxidation under these conditions is another important design requirement.

The Ru^{2+} complexes need to be sufficiently electrophilic to support a dihydrogen η^2 bonding interaction. We desired that the ligand sets used were stable under acidic conditions, high temperature, and high pressure. Another requirement was facile tuning of the metal center so that the electrophilicity could be controlled.

In this way the acidity of the bound dihydrogen molecule as well as the hydricity of the metal hydride can be controlled. As will be discussed later, this acidity and hydricity are crucial parameters affecting the ability of the catalyst to selectively hydrogenate the substrate.

Background

Late transition metals with lower oxidation states tend to give more stable complexes with π acceptor ligands. There are many examples of the iron group triad supporting stable or semi-stable dihydrogen complexes.[5-8]

Bautista et al. have demonstrated, from a spectroscopic comparison within the iron group triad, that ruthenium phosphine complexes have the strongest H-H to metal σ donation and the weakest metal to dihydrogen back bonding interaction in comparison with the corresponding iron and osmium systems.[9] They found that the $[RuHL_2]^+$ fragments are poorer π-back-bonders with dihydrogen than the analogous complexes of Fe and Os and form weaker σ-bonds than the Os complexes.[9]

Chin et al. performed an investigation to examine the influence of acidity of ligands trans to the bound dihydrogen. This study was done on a series of ruthenium dihydrogen complexes containing bidentate phosphine ligands.

By modulating the ancillary ligands *trans* to the bound dihydrogen, they were effectively able to tune the pK_a of the dihydrogen complex. By comparing *trans*-Cl^- vs. *trans*-H^-, they found that acidic nature was more enhanced by the chloride ligand over the hydride.[10] The higher pK_a of the complex with the *trans*-H^- ligand most likely arises from the (H)-$d\pi$(Ru) repulsions that enhance $d\pi$(Ru)$\rightarrow\sigma^*$(H$_2$) back-bonding. Thus, the longer and hence weaker H-H bond gives rise to a less acidic complex.

These considerations are important to the design of our catalysts. If the assumed first step of the catalytic hydrogenation of furan derivatives involves heterolytic cleavage of dihydrogen and protonation of the substrate then enhanced acidity would be beneficial.

Curtis et al. studied a series of $[M(diphosphine)_2]^{2+}$ complexes (where M = Ni and Pt) to determine kinetic hydricity or metal-hydride donor ability. They reacted these complexes with dihydrogen in the presence of a base to form the corresponding hydrides, $[HM(diphosphine)_2]^+$. They were then able to calculate $\Delta G^\circ_{H^-}$ using pK_a measurements and electrochemical half-wave potentials.[11] In doing so, it was confirmed that the complexes with more electron-donating phosphine ligand sets were more hydridic in nature. This can be explained by reasoning that higher electron density at the metal center gives greater electron density to the hydride. This hydride, with enhanced electron density, is likely to be more reactive. Quantitative values of $\Delta G^\circ_{H^-}$ for transition metal hydride complexes are useful for predicting the following: (1) the stability of hydride complexes to acids of different strengths, (2) the ability of these compounds to act as hydride donors toward organic substrates and other metal complexes, and (3) the conditions required for heterolytic cleavage of H_2 by the conjugate hydride acceptor of the transition metal hydride.

All of the above are very important considerations for our catalyst to function properly as a selective hydrogenation and/or hydrogenolysis system.

Figure 1. Targeted catalyst framework.

X= Cl, H,Tolyl

R= Pyr, Ph,Me

X= Cl, H, Tolyl

R= Pyr, Ph,Me

L=H_2

BAr^{F-}
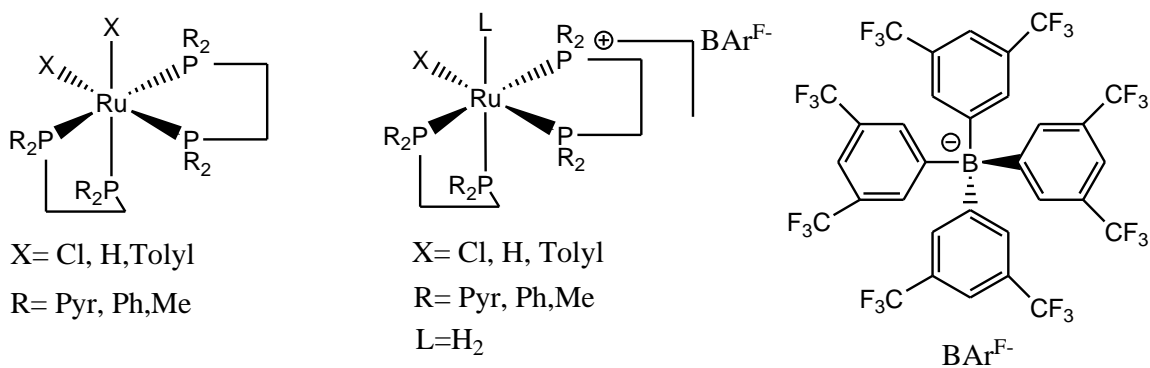
Scheme 2. The generic series of steps for the catalytic hydrogenation of a carbonyl.
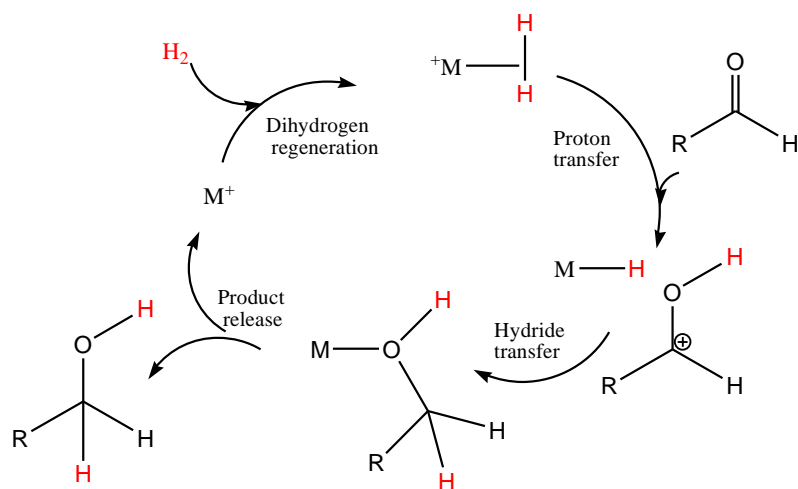
In the generic mechanism depicted in **Scheme 2**, a carbonyl system is hydrogenated via an initial protonation of the substrate and a sequential hydride transfer from the metal to the carbonyl carbon of the substrate. It is possible that a subtrate-oxygen to metal interaction is needed to stabilize this intermediate or to bring the substrate in close proximity for hydride transfer to be more energetically favorable. Product release gives the alcohol and in the presence of dihydrogen, the metal di-hydrogen is regenerated.

If the catalyst were to coordinate or interact with the substrate in this way, then obviously this interaction mustn't be too strong. Oxophilic metals would be poor choices for these types of systems. With a metal of this type, the interaction between the carbonyl oxygen and the metal could stifle coordination of H_2 and/or the release of the product.

The patented, $[(P-P)Pd(OAc)_2]$ and $[Rh(CO)_2(acac)]/H_2WO_4$ systems have recently been demonstrated as active species for selective hydrogenation.[12,13] The ruthenium complex, $[Cp*Ru(CO)_2]_2(\mu-H)^+[OTf]$ $Cp*=C_5Me_5$ and $OTf = CF_3SO_3^-$ has been reported to be an effective catalyst for the deoxygenation of 1,2-propanediol under acidic conditions to yield *n*-propanol.[14] Two equivalents of the dihydrogen complex $[Cp*Ru(CO)_2(\eta^2-H_2)]^+$ are presumed to be the active species and are formed from the hydride bridged dimer by thermal dissociation and hydrogen uptake and protonation by HOTf. The system cannot be observed under catalytic conditions, but can be generated independently at 220 K by protonating the corresponding hydride $Cp*Ru(CO)_2H$ with

HBF$_4$ in CD$_2$Cl$_2$. The hydride complex Cp*Ru(CO)$_2$H has also been shown to be an efficient hydride transfer reagent to the trityl cation.[15]

Taken together these observations strongly suggest that the catalyst does indeed hydrogenate carbonyl functions by an ionic mechanism in which, the substrate never coordinates to the metal center.[16]

Scheme 3. The assumed mechanism for the deoxygenation of 1,2-propanediol to n-propanol.
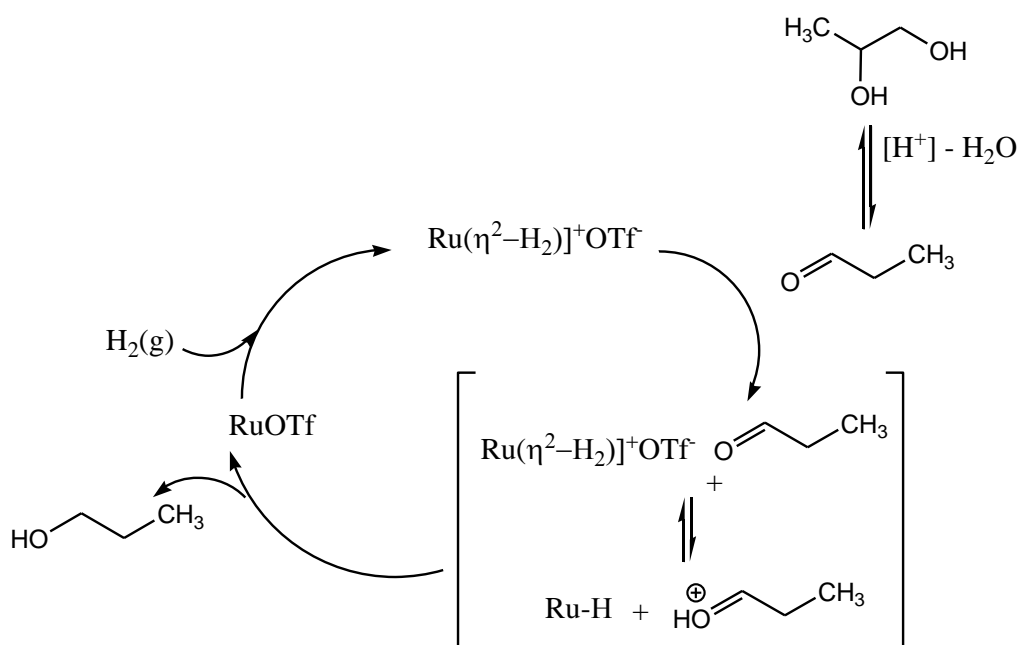
As seen in **Scheme 3**, a ruthenium dihydrogen complex is generated and in the presence of triflic acid the carbonyl oxygen is protonated. Subsequent attack of the carbonyl carbon by the nucleophilic hydride produces the corresponding alcohol.

Takei et al. have reported novel catalytic hydrogenolysis of trialkylsilyl enol ethers with H$_2$ and acidic ruthenium complexes such as [RuCl(η^2-H$_2$)(S)-BINAP)$_2$][OTf] and [Ru(Cl)(η^2-H$_2$)(dppe)$_2$][OTf]. [17] The reaction is believed to be initiated by the

nucleophilic attack of the oxygen atom of the enol ether on the coordinated H_2 on the ruthenium atom. This induces the heterolytic cleavage of the H_2 and results in the formation of the ketone and Me_3SiOTf together with the corresponding ruthenium hydride. The following reaction of Me_3SiOTf with the hydride under 1 atm of H_2 regenerates the starting dihydrogen complex concurrent with the formation of Me_3SiH. It is presumed that a delicate balance of the acidity of dihydrogen complex, $[Ru(Cl)(\eta^2\text{-}H_2)(dppe)_2][OTf]$, and the nucleophilicity of the hydride complex might realize this novel catalytic hydrogenolysis of silyl enol ethers. However, the Takei group could not rule out the possibility that a concerted transfer of a proton and a hydride from the H_2 ligand to the oxygen and silicon atoms of the enol ether, respectively, could give rise to the formation of the ketone and Me_3SiH.

Scheme 4. Catalytic hydrogenolysis of trialkylsilyl enol ethers with $[Ru(dppe)_2Cl(\eta^2\text{-}H_2)][OTf]$.
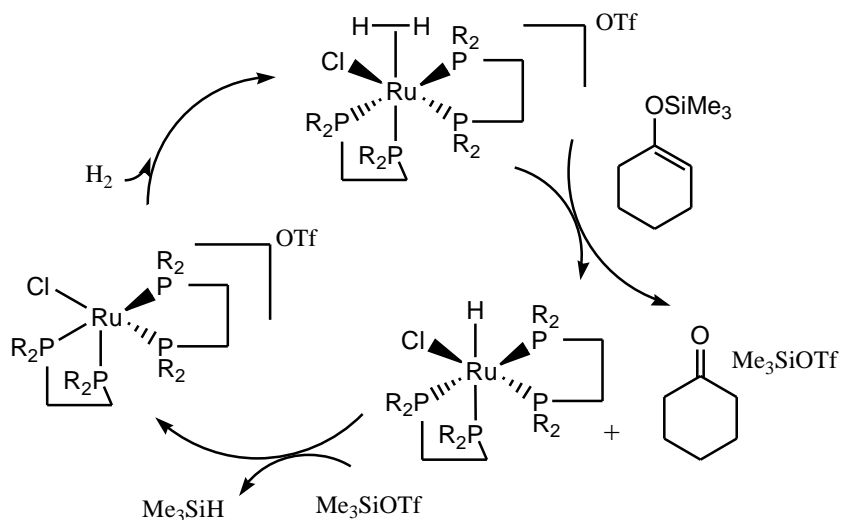
We wished to employ a similar methodology that was based in these previously published reports that would meet the above stated criteria for an effective selective hydrogenation/hydrogenolysis catalyst for the transformation of HMF and FFR derivatives to 2,5-dimethylfuran and 2-methylfuran. We also wanted to study, in detail, the ruthenium systems that were prepared for their specific properties as hydrogenation catalysts and to gain more insight into how these properties are related to the proposed catalytic cycle.

In this work, I will attempt to describe a series of active ruthenium-based hydrogenation catalysts that were prepared. These systems showed promise toward the hydrogenation and hydrogenolysis of FFR to FFA and MF.

This series of catalysts that were prepared offered a range of electrophilicity of the metal center. These different electronic properties were due to the different types of ancillary bidentate phosphine ligands that supported the metal center.

Scheme 5. Possible catalytic pathway for the catalytic hydrogenation and selective hydrogenolysis of HMF.
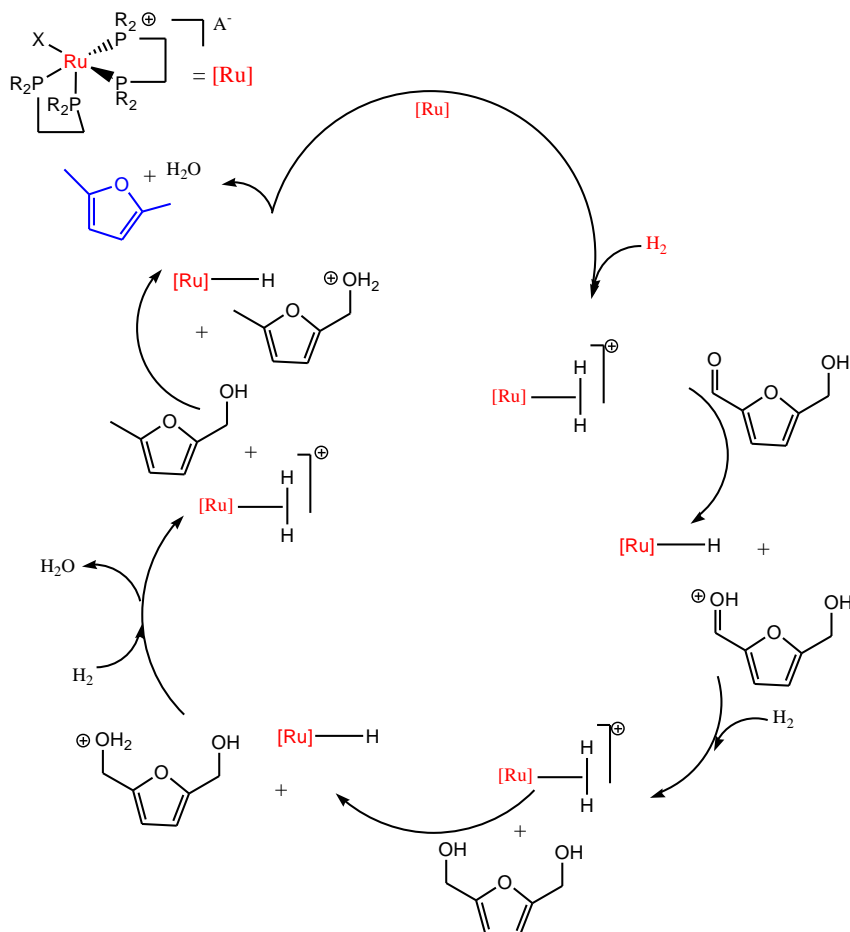
Scheme 5 shown above depicts a possible mechanism for catalytic hydrogenation and hydrogenolysis of 5-hydroxymethylfurfural (HMF) to 2,5-dimethylfuran (DMF). The pathway to hydrogenation and hydrogenolysis of HMF is assumed to function via a sequential series of proton/hydride transfer steps depicted above. The initial step involves coordination of one molecule of hydrogen to the catalyst. Subsequent heterolytic cleavage of H_2 results in a proton transfer to the substrate and formation of a ruthenium hydride. This protonated substrate undergoes nucleophilic attack by the hydride resulting in alcohol formation from aldehyde. In other words, the substrate is hydrogenated.

12

The second step can be considered as an acid assisted reduction of the corresponding alcohol. Protonation of the OH functionality results in the formation of H_2O^+-R, which through another hydride attack results in dehydration of the substrate.

If a catalytic system is to operate through this pathway, then it is clear that a number of design criteria must first be instituted for the catalyst to function effectively. First, the system must be able to not only maintain a sigma interaction with a dihydrogen molecule but also activate it toward heterolytic cleavage, producing a metal hydride and a proton. Second, the ligand environment must also be able to tolerate both acidic conditions and a reducing environment at high temperatures and H_2(g) pressures. Third, the catalyst itself must be stable in an acidic media. Lastly, the counter-ion that will stabilize the cationic catalyst species must be non-nucleophilic, non-coordinating, and sufficiently stable under the reaction conditions.

Results and Discussion

We began our investigations by synthesizing several electrophilic ruthenium complexes and examining their efficiency as hydrogenation and hydrogenolysis catalysts for furan derivatives. We used 2-furfural instead of 5-hydroxymethylfurfural because of the ready availability and low cost of this material.

Section A. Synthesis of pre-catalysts

A series of electrophilic ruthenium^{2+} compounds were prepared. The pre-catalysts were made by unsaturating *hexa* coordinate octahedral *di*-chloro ruthenium phosphine

complexes with the use of NaBAr^F (Bar^F) = B-[3,5-(CF$_3$)$_2$C$_6$H$_3$]$_4^-$. The unsaturation of the *hexa*-coordinate complexs produced the, *penta*-coordinate 'mono' chloride complexes as seen in **Scheme 6**. The assumed actual catalyst would be the hexa-coordinate octahedral *mono*-chloride ruthenium dihydrogen species depicted in **Scheme 7**.

Scheme 6. The general synthesis of the pre-catalysts (1b) and 2a).
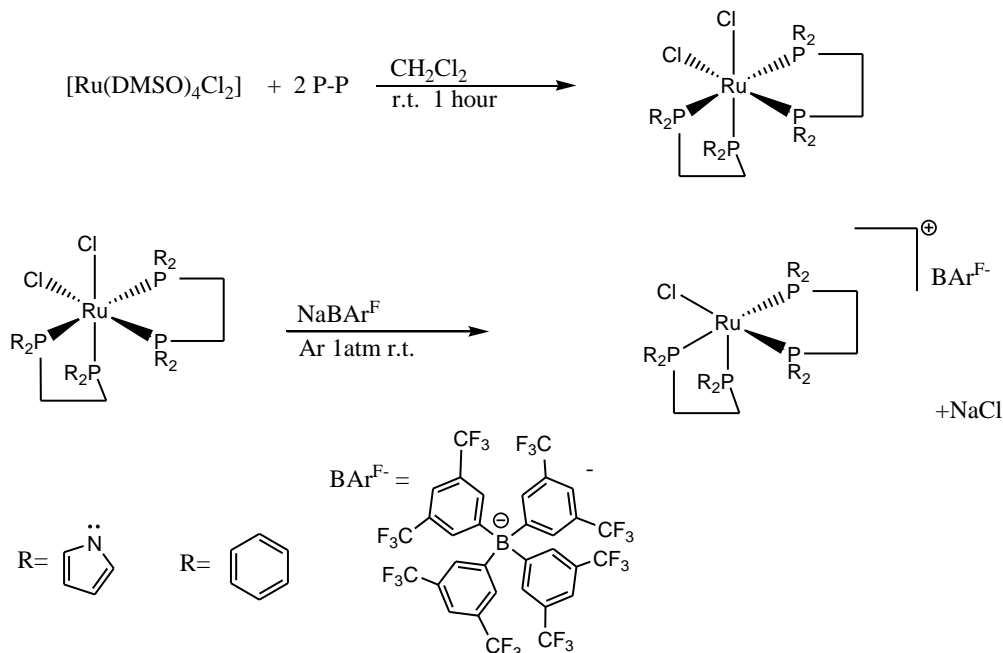
As shown in **Scheme 6**, the known synthetic precursor, [Ru(DMSO)$_4$Cl$_2$] was mixed with 2 equivalents of a bidentate phosphine to obtain the octahedral *di*-chloride phosphine complex. This synthesis afforded the *cis*-dichloride as well as the *trans* complex in a 3:1 ratio. Recrystallization from THF/hexanes was used to obtain *cis* isomer in 100%. This yellow compound was then mixed with one equivalent of NaBAr^F to give the trigonal bipyramidal *penta*-coordinate *mono*-chloride complex. When R=Ph (1,2-bis(diphenylphosphino)ethane) (**1b**), this 5-coordinate species was deep red in color.

When R = pyrrolyl (1,2-bis(dipyrrolylphosphino)ethane) (**2b**), the unsaturated complex was pale yellow in color.

We wanted to make a series of catalysts that differed in electrophilicity. We decided to use the dppe (R = Ph) and the pyrrolyl ligand sets to gain a direct comparison between the two complexes for hydrogenation/hydrogenolysis activity. Due to better back-bonding capability of the $P(pyr)_2(alkyl)$ vs. $P(Ph_2(alkyl)$, the ruthenium metal center was much more electron deficient in the pyrrolyl complex than the corresponding *dppe* complex. Greater electrophilic character could influence the activity of the catalytic hydrogenation/hydrogenolysis of fufural differently. It is possible that more electron-withdrawing ability of the pyrrolyl system could make heterolytic cleavage of H_2 more facile, thus producing a more acidic catalyst.

Scheme 7. The presumed active catalytic species.
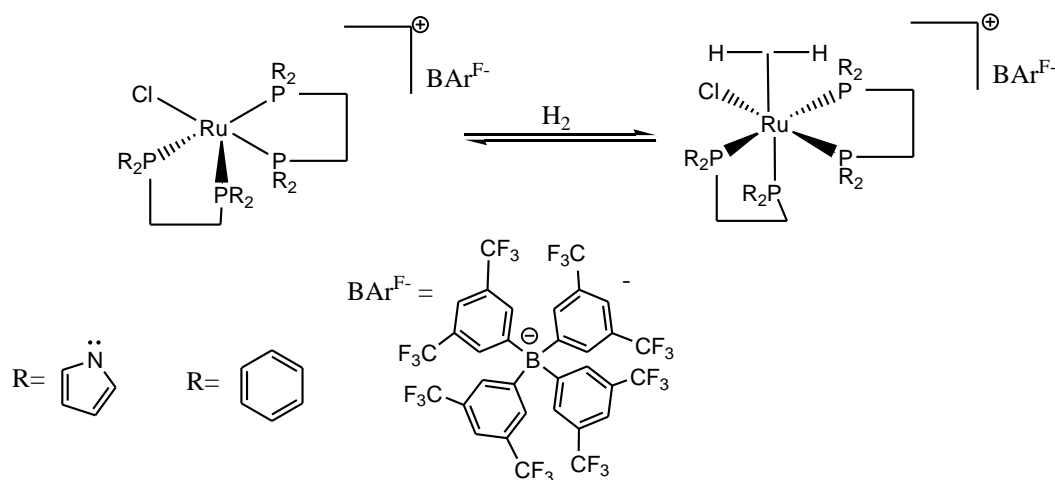
From **Scheme 7**, it is seen how the pre-catalyst would coordinate a dihydrogen molecule in the presence of $H_2(g)$. This interaction is presumed to occur through σ donation of H_2 to the metal.

It was observed through proton NMR techniques, that the catalyst, under H_2 pressure most likely forms a ruthenium hydride-dihydrogen via the elimination HCl. Thus, perhaps the first step in the catalytic hydrogenation reaction is the elimination of HCl and subsequent protonation of substrate by HCl.

Scheme 8. Elimination of HCl by the pre-catalyst to give [Ru(dppe)$_2$(H)(H$_2$)][BAr^F].
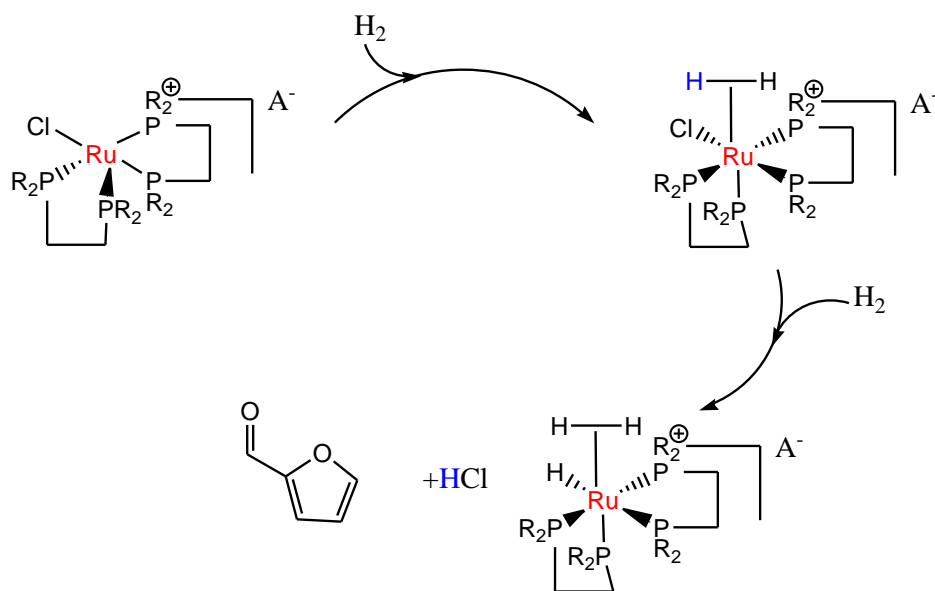
This was further tested by the synthetic preparation of $[Ru(dppe)_2(H)(H_2)][BAr^F]$ and testing the species for catalytic activity. Indeed, the system seemed much less active without the initial HCl to protonate and thus activate the substrate in the first step of the reaction.

To avoid the elimination of HCl and to maintain a neutral catalytic intermediate, the organometallic complex, $[Ru(dppe)_2(tolyl)][BAr^F]$ (**3b**) was synthesized. We wanted to prepare a catalyst that would perhaps go through a neutral intermediate and thus provide a more nucleophilic Ru-H.

Scheme 9. Proposed first step in the protonation of furfural with $[Ru(dppe)_2(tolyl)(H_2)][BAr^F]$.
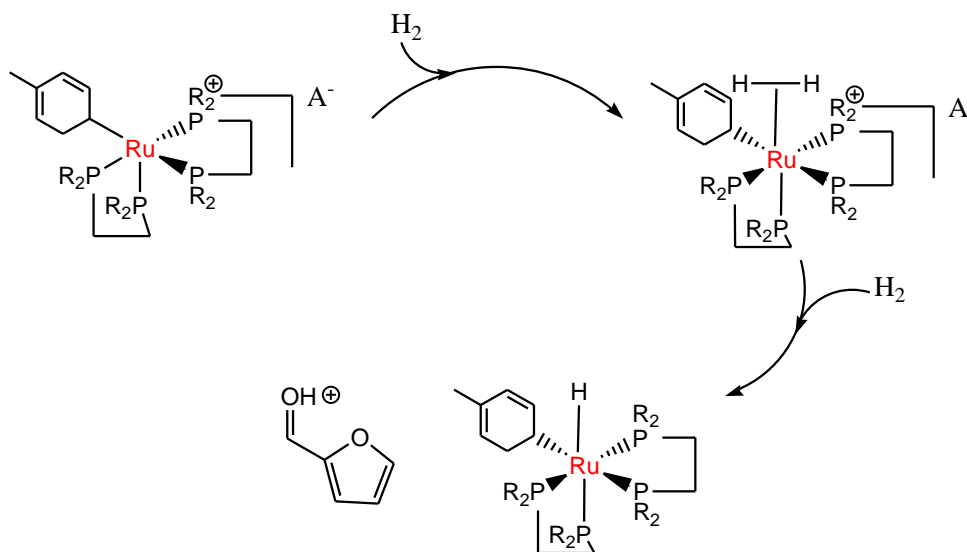
The $[Ru(dppe)_2(tolyl)(H_2)][BAr^F]$ catalyst was observed without substrate in $CDCl_3$ in a screw-capped NMR tube to see if the elimination of toluene would occur analogous to the elimination of HCl observed with the 'monochloride' catalyst. Preliminary evidence suggests that the elimination of toluene did not take place at room temperature or $110\,^oC$.

As shown in **Scheme 9**, the hydrogen, once coordinated, is heterolytically cleaved to protonate the substrate and yield the neutral hydridic complex. We postulated that this neutral species would be more hydridic than a cationic hydride. In other words, the hydride transfer from the catalyst to the substrate would be more favorable.

17

This aryl system was synthesized by adding to the *cis*-dichloride starting complex dropwise at 78 °C a dilute solution of tolyl-MgBr. After subsequent workup steps, the complex was reacted with NaBA^{rF} to afford the pre-catalyst *[Ru(dppe)$_2$(tolyl)][BAr^F]*.

A slight modification to this system was attempted by changing the ruthenium-bound tolyl group to the more electron-withdrawing *para*-fluoro phenyl group. We attempted to prepare the pre-catalyst, [Ru(*para*-fluoro-phenyl)dppe]$_2$][BAr^F] system. However, we were unable to remove trace amounts of impurities and purification procedures are ongoing.

Figure 2. Modification to the more electron-withdrawing para-fluoro system.

R=Ph   Modification to fluoro system
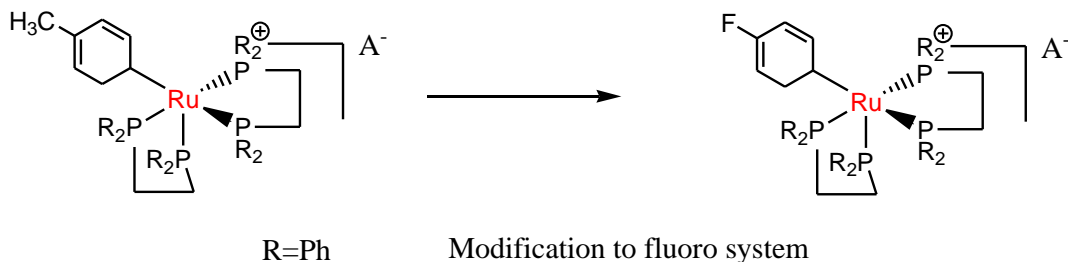
An attempt was made to prepare the electron-rich, [Ru(depe)$_2$(Cl)[BAr^F] from the fully saturated, [Ru(depe)$_2$(Cl)$_2$] precursor. This would have provided a direct comparison between one end of the spectrum in the electron poor, *bis*-pyrrolyl system, (**2a**) to the electron-rich 1,2-bisdiethylphosphinoethane complex. However, due to the exceedingly electron-rich character of this species, dimerization through the chloride ligands was observed. This made unsaturation and hence gaining catalytic information on the species difficult.

Section B. Characterization of pre-catalysts

The pre-catalysts, in all cases, by ^{31}P NMR, gave 2 triplet resonances from the dppe ligands. This is consistent with *penta*-coordinate trigonal bipyramidal geometry. One resonance resulted from P_{ax} and the other resonance from P_{eq}. Evidence in the literature suggests that due to the large steric hindrance of the dppe ligands, that Y distortion occurs from the normal tbp geometry.[10] These triplets for (**1b**) appeared downfield at 85 and 56 ppm relative to H_3PO_4. A further downfield shift was observed for complex (**2b**) at 130 and 115 ppm. This extreme shift of (**2b**) might have resulted from the more electrophilic character of the complex due to better Ru-P(pyr)$_3$ back bonding as a result of the pyrrolyl groups. The aryl complex (**3b**) and had similar chemical shifts. They both resonated at 80 and 60 ppm. Elemental analyses were carried out on (**1b**), (**2a**), and (**2b**) were consistent with the theoretical percentages. However, (**3b**) has still not completely been isolated in a pure state. Some impurity from the reactants seems to create a small amount (5%) of (**1b**) with the product. Therefore to date, the aryl pre-catalyst has only been prepared at 95% purity.

Figure 3. Molecular structure of cis-[Ru(dipyrrolyl)$_2$(Cl)$_2$] (2a).
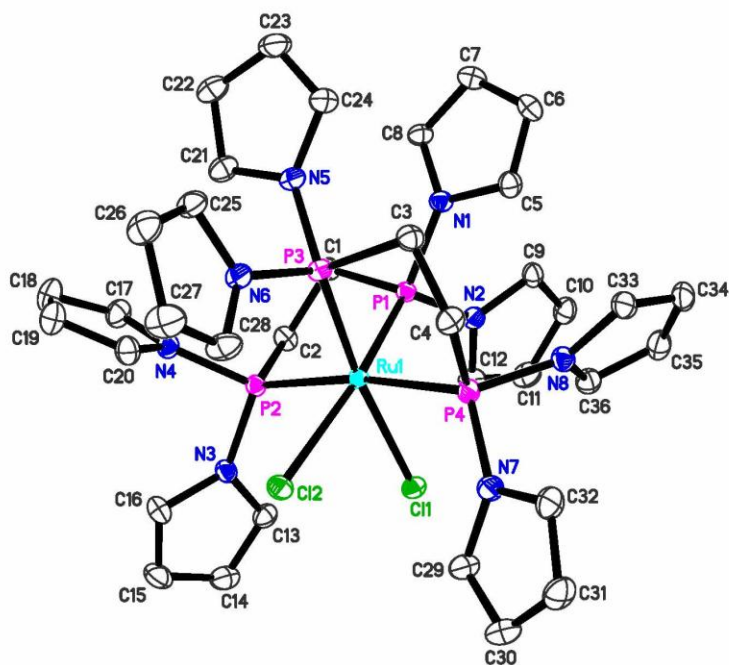
It was observed that, if the *mono*-chloride, (**2b**), was placed in a NMR tube in acetone d$_6$ with one equivalent of lithium chloride for 5 minutes at room temperature, then the saturated dichloride complex would be once again obtained. However, a new *trans*-[Ru(dipyrrolyl)$_2$(Cl)$_2$] (**2a'**) was observed.

Figure 4. Molecular structure of trans-[Ru(dipyrrolyl)₂(Cl)₂] (2a`).
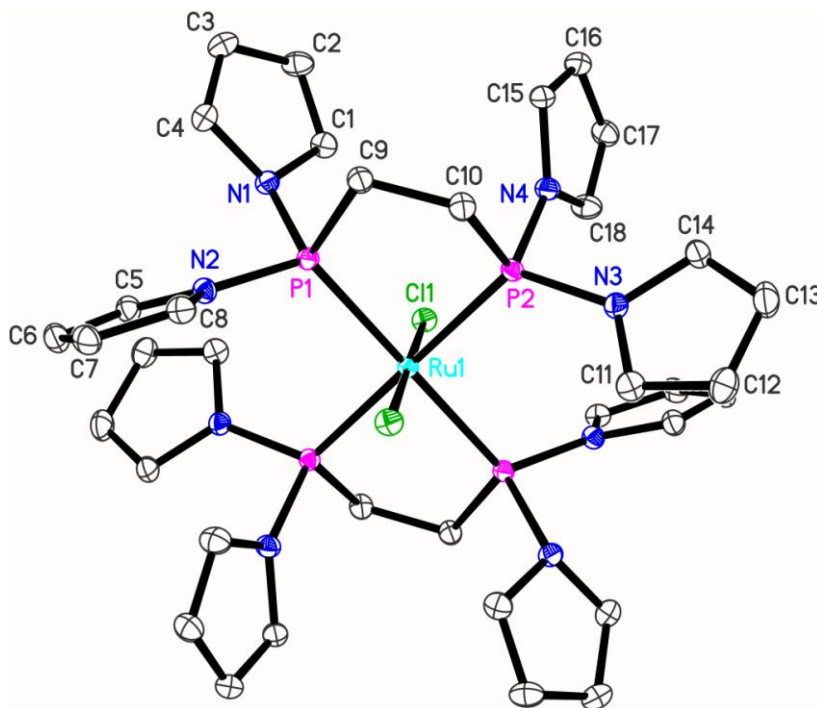
Section C. T_1 Measurements

An estimation of H-H distances of a Ru-H₂ system can be obtained from T_1 measurements using NMR techniques.[18] T_1 measurements were made on the dihydrogen complex of (**1b**) to gain insight into the effect of the ligands on the H-H distances. From a comparison with other species listed in publications, we could gain some insight into the acidic nature of some of the pre-catalyst.

The pre-catalyst was placed in an NMR tube and dissolved in CDCl₃. The system was then cooled to -45 °C and was subjected to a steady stream of H₂(g). The cooling was necessary to retard HCl elimination from the complex. The T_1 values were obtained from the ¹H NMR inversion-recovery method. With this method, the Ru-H₂ complex

was subjected to an inversion pulse that flipped the magnetic nuclear spin state of the bound H_2 molecule 180°. The time that it took the system to relax back into the positive z orientation was the measured T_1 value.

Scheme 10. Preparation of the Ru-H_2 complex for T_1 analysis.
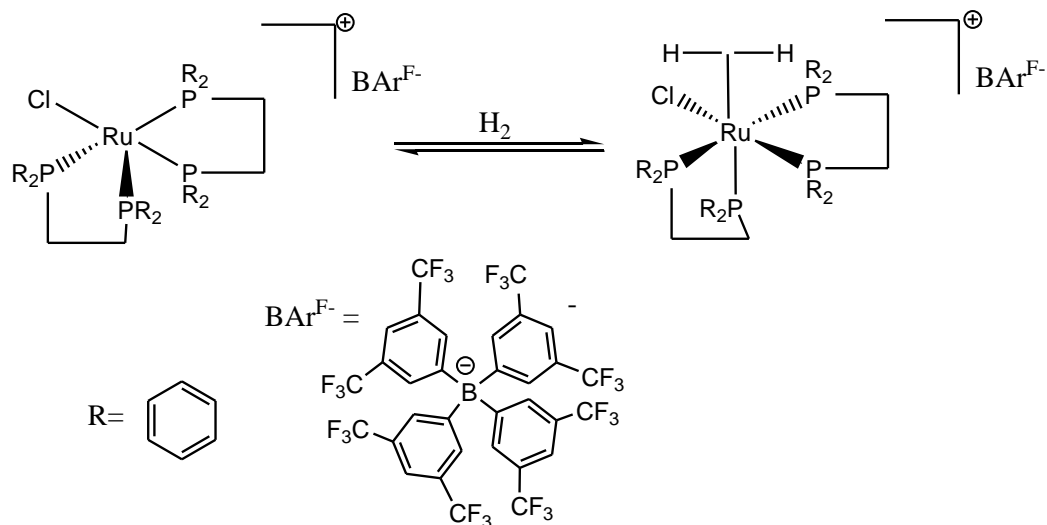
The T_1 value for dihydrogen-bound (**1b**) was 26.8 ms. Similar compounds that were subjected to these conditions were found to have T_1 values around 21 ms.[9] With this, it was determined that the H-H distance 0.89 Å   This suggests that the greater electrophilicity of the metal then the greater the σ donation from the H-H bond to the ruthenium metal. This would cause an elongation and weakening of the bound dihydrogen molecule.

Section D.Catalytic data

Scheme 11. Possible mechanism for the hydrogenation and hydrogenolysis of furfural to 2-MF.
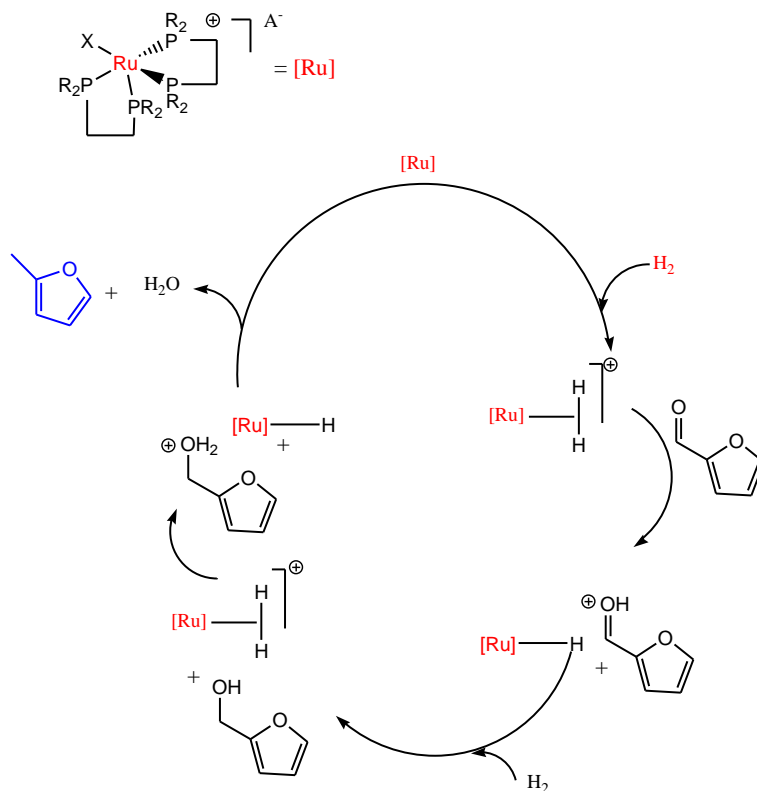
Initially, we tested the well-known complex, [Ru(dppe)$_2$(Cl)][OTf] (**1a**)-(where OTf = CF$_3$SO$_3^-$), as a catalyst for the hydrogenation and hydrogenolysis of furfural. This species was assessed at 700 psi H$_2$(g) pressure, 100 :1 substrate to catalyst loading, 80-100 ^{o}C, and in ethanol.   However, this system was not effective. It was thought that the catalyst was deactivated at these temperatures. Indeed, the appearance of the complex changed from an initial red color to black. This indicated that possibly the complex was decomposing.

It seemed that the catalyst was not stable under the above stated conditions. Below 80 ^{o}C, the catalyst was not very active. It is also possible that the OTf anion might

be competing with the coordination of molecular hydrogen by interacting with the inner sphere of the metal center. This type of interaction would limit the availability of the open site on the catalyst. It has been observed by ^{19}F NMR, that in some Ru^{2+} complexes, triflate coordination is a factor.[19]

Table 1. Selected results with [Ru(dppe)$_2$Cl][OTf] catalyst.(1a)

Reaction #	temperature [^{0}C]	pressure [psi H$_2$]	Time [h]	solvent	conversion %	FFA %	acetal %	tetrahydro-MF
414	135	750	5	10 ml DCM	0	0	0	0
418	82	750	24	10 ml DCM	0	0	0	0
430	55	750	48	5 ml EtOH/10 mlDCM	50	0	50	0
431	70	700	18	5ml PhMe/10 ml DCM	20	0	0	20

As shown in the table above, there appeared to be no conversion of furfural (FFR) when dichloromethane (DCM) was used as the sole reaction solvent. It is possible that DCM was not polar enough to aid in the formation of intermediates that needed to be accessed for the reaction to go to completion. In fact, when most other non-alcoholic solvents were used, then either no conversion or poor substrate conversion was observed. It could also be that protic solvents aided in the delivery of H$^+$ to the substrate better than the non-protic solvents.

However, when ethanol was used, there was conversion of the substrate but the corresponding acetal, 2-(diethoxymethyl)furan, was the only product formed at the reaction temperature. This corresponding acetal is believed to have been formed through

a protonation and thus activation of the substrate by the catalyst and then subsequent nucleophilic attack by the solvent (ethanol).

It was postulated that the nucleophilic attack of the substrate from lone-pairs of the oxygen of ethanol was more facile than the ruthenium hydride transfer from the catalyst. From the mechanism below, it can be seen that if the nucleophilic attack of a solvent molecule were more favorable, then more of the corresponding acetal product would be observed than methyl-furan or furfuryl alcohol.

Scheme 12. Possible catalytic pathway for acetal formation from furfural.
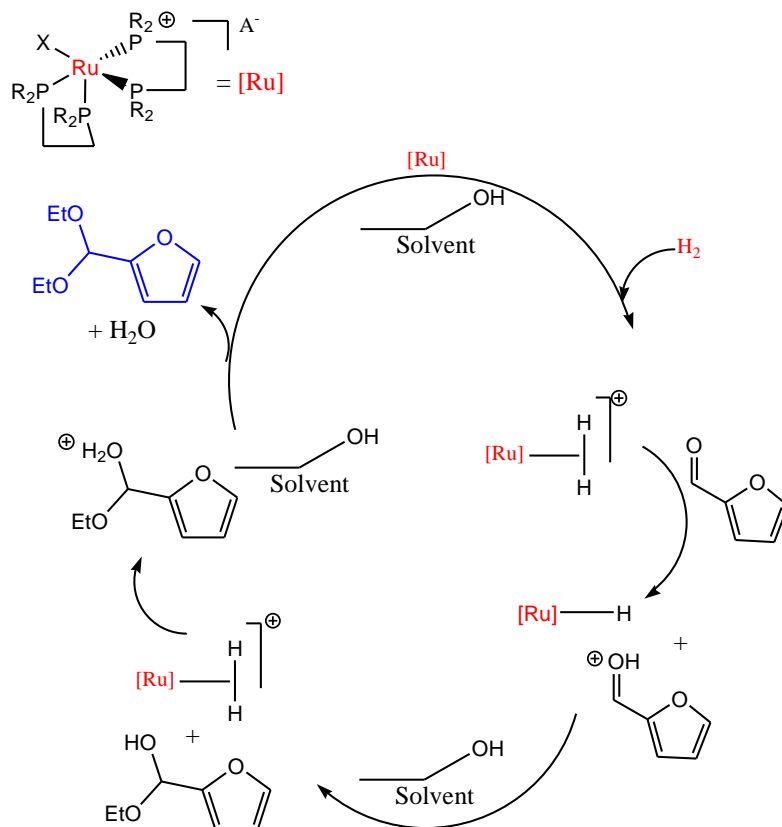
From the proposed mechanism depicted above, it can be seen that the metal assisted heterolytic activation of dihydrogen results in a protonated substrate. Ethanol

can then attack the protonated carbonyl carbon which produces the hemi-acetal. Either tautomerization or another protonation from a ruthenium-H_2 can give a good leaving group in water, which ripens the substrate for another attack by ethanol to yield the acetal product.

Hindering of acetal formation was attempted by using the solvent system, CF_3CH_2OH. The oxygen is less nucleophilic due to the induction from the electron-withdrawing CF_3 group. This would reduce attack on the substrate. Indeed, acetal production was curbed but substrate conversion was also minimized.

We then decided to change the counter ion to a system that would have less ability to coordinate or interact with the metal. We wanted to promote further thermal stability of the catalyst. The new catalyst precursor, $[Ru(dppe)_2(Cl)][BAr^F]$, $(Bar^F) = B$-$[3,5-(CF_3)_2C_6H_3]_4^-$ (**1b**) was then prepared and tested. The results clearly showed that the catalyst could withstand higher temperatures and was more active toward hydrogenation and hydrogenolysis of the furfural than the triflate stabilized species. As shown in **Table 2**, the 'BAr^F' catalyst was more active when the temperature was elevated beyond 100 ^{o}C. From **Table 2**, it is seen that tetrahydromethyl furan (TETMF) was formed in good yield and in some cases as high as 70 %. It seemed reasonable that methylfuran must first be made before the ring hydrogenation occurs. In other words, most likely, ring hydrogenation was taking place after the desired methylfuran product was produced. If this were true, then one would expect that if the reaction were done at a shortened time interval, then less ring hydrogenation would occur and perhaps methyl furan would be selectively produced. In reaction RK #565, it is seen that indeed this was

the case. The reaction was performed more than half of the time as RK#551 and ring hydrogenation was much less pronounced, giving only partial ring hydrogenation by GCMS. When the reaction was performed under the same conditions but at even shorter times, such as in RK #566, only furfuryl alcohol (FFA) was observed along with unreacted starting material.

Table 2. Selected results with [Ru(dppe)$_2$Cl][BAr^F] catalyst. (1b)

Reaction #	pressure [psi H2]	solvent		conversion %		FFA %	tetrahydro-MF %		dihydro-M %	ether/acetal %		tetrahydr-F %
$_a$496	800	3ml EtOH/10mlDCM		53.6		0	0		0	27		26.6
$_a$519	600	5ml ^{t}BuOH/10mlDCM		100		0	47		14	39		0
526	700	5ml ^{t}BuOH/10mlDCM		76		30	6.6		2.5	36.9		0
$_b$551	650	2.5ml ^{t}BuOH/5mlDCM		100		1	73		0	26		0
$_b$*562	650	2.5ml ^{t}BuOH/5mlDCM		100		0	95		0	5		0
*565	650	2.5ml ^{t}BuOH/5mlDCM		73		0	59		0	14		0
* FFA was used as a substrate												
a= 18 hours, b=19 hours, RK #526 was 14 hours and 565 was 7 hours.												

To lend support to the assumed mechanism that is sketched out in **Scheme 11**, we tested the catalyst with furfuryl alcohol as the starting substrate.

From the mechanism depicted in **Scheme 11,** it can be seen that if methylfuran or tetrahydromethyl furan is being produced then firstly furfuryl alcohol must be made as an intermediate product. So, by using furfuryl alcohol (FFA) as the initial substrate we might expect to see faster formation of methyl furan and tetrahydromethyl furan due to the fact that the intermediary FFA was not first needed to be produced by the catalyst.

As shown in RK#562, when FFA was used as the substrate, 95% partially ring hydrogenated methylfuran was produced. This result, at least, validates that FFA must be accessed first from FFR to obtain the desired furan derivative.

Figure 5. Products formed from [Ru(dppe)₂(Cl)][BAr^F] catalyst.

FFA   2-methyl-tetrahydrofuran   tert-butylt ether di-hydro tert-butyl ether
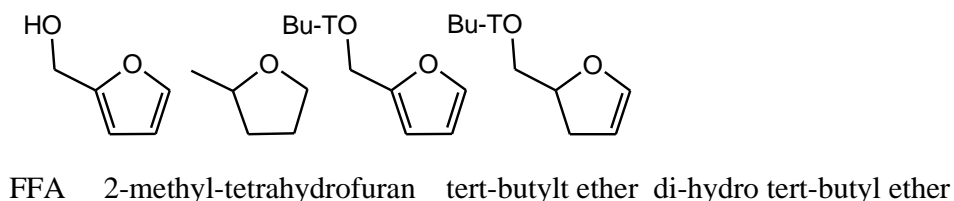
By switching from ethanol to *t*-butanol, acetal formation was avoided but the corresponding ether, 2-(tert-butoxymethyl)furan, was generated instead. Ether formation is believed to occur through the heterolytic cleavage of H_2 that results in the protonation of a solvent molecule rather than the substrate. Elimination of water gives a resonance stabilized carbocation that can then be attacked by the oxygen atom of the substrate. Subsequent ruthenium hydride nucleophilic attack at the carbonyl carbon gives the corresponding ether.

Scheme 13. Assumed pathway for the formation of the corresponding ether from furfural when tert-butanol was used as a solvent.
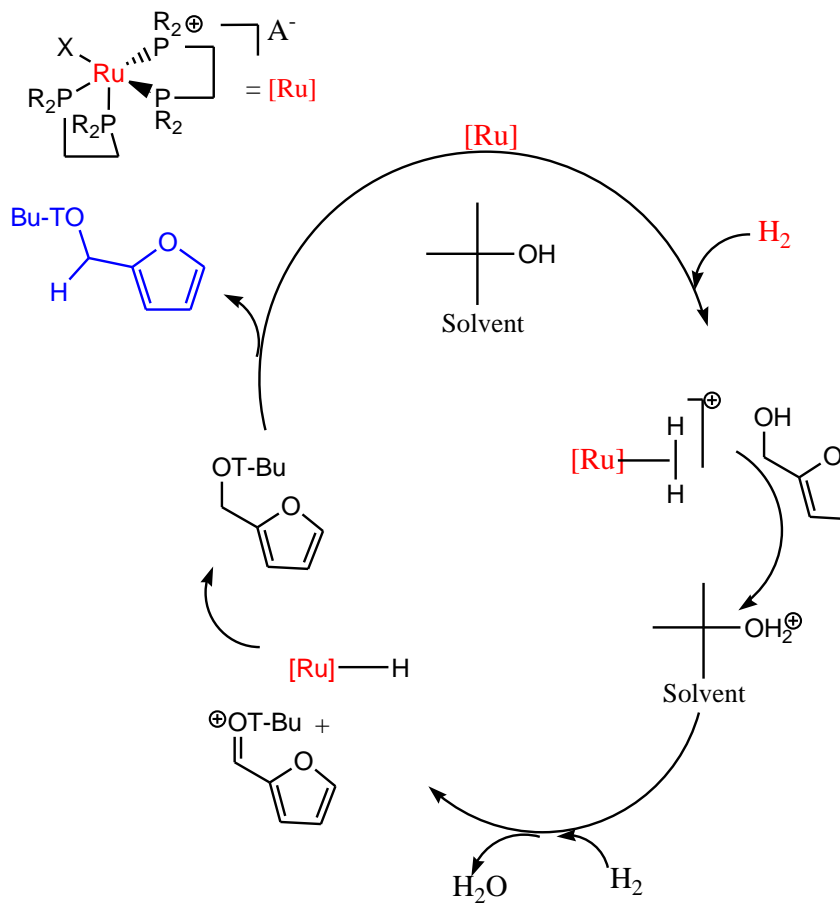
Preliminary data in **Table 4** indicates that the system was active towards the hydrogenation and hydrogenolysis of the furfuryl substrate when alcoholic solvent systems were used.

In RK# 533, 95% ethanol was used to see if the 5% water may have a rate enhancing effect on the transfer of the proton produced from the cleaved H_2. In catalytic trial, RK# 534, pure ethanol was used as a control and there seemed to be no substantial change in product distribution.

29

Table 3. Results from [Ru(dipyrrolyl)$_2$(Cl)][BAr^F] catalyst (2b).

Reaction	time	conversion	FFA	MF	ether	di-hydro ether
#	[h]	%	%	%	%	%
570	9	19	8	0	11	
571	18	50	24	1.2	25	
572	23	85	22	2.5	36	
573	47	92	20	2.5	16	54
*576	18	72	x	3.6	60	8

* FFA was used as a substrate

In all reaction 2.5 ml ^{t}BuOH/5ml DCM was used as solvent.

As shown above in **table 3**, the catalyst (**2b**) was tested under similar conditions as (**1b**) for the hydrogenation and hydrogenolysis reaction of FFR and FFA. It is seen that this catalyst was much less active that (**1b**). Most likely, this was due to the higher electrophilic nature of this species due to greater π-acidity of the ligand framework. This electrophilicity produced a weaker hydridic character in the Ru-H intermediate thus hindering the nucleophilic attack of the activated substrate. Under very similar reaction conditions catalyst (**2b**) mostly produced the corresponding ether signaling that the enhanced electrophilicity gave a strongly acidic species but a less hydridic one.

Our continuing efforts to find a solvent system for these catalytic reactions that was less reactive with the substrate but was still polar enough to allow for the needed substrate conversion finally was realized with the use of 1-methyl-2-pyrrolidone also

known as 'NMP'. As shown in **Table 4**, the catalyst, *(1b)* in NMP was active in the

generation of significant amounts of FFA from FFR at low temperatures (100 ^{o}C) and did

not react with the FFR substrate the way the alcoholic solvents did. We were pleased to

find that with the use of NMP, catalytic selectivity was enhanced relative to the trials in

which ^{t}BuOH was used. However, at 100 ^{o}C activity was generally poor given that the

reaction had to go two days to generate significant amounts of the desired product. When

the temperature was increased by 20 ^{o}C as in RK# 594, activity was seen to increase and

some methyl furan production occured. However, as the temperature was increased, it

was observed that substrate conversion was declining.   Perhaps the catalyst was

unreactive at these higher temperatures due to decomposition. Indeed the pre-catalyst in

the crystalline state decomposes at 156 ^{o}C.

Table 4. Results from the use of 1-Methyl-2-pyrrolidone (NMP) as a solvent.

Reaction	temperature	pressure	time	conversion	FFA	MF	tetrahydro-MF
#	[^{0}C]	[psi H$_2$]	[h]	%	%	%	
587	100	600	23	49	49	0	
592	100	500	46	93	93		
594	120	600	23	~80		80	trace	trace
596	150	650	23	53	27	25	3

Conclusions

Novel catalysts were developed, fully characterized, and tested for their ability as

hydrogenation and hydrogenolysis of furan derivatives. The properties of the catalysts

were explored in terms of the Ru-H$_2$ (H-H) bond length via T$_1$ measurements through [1]H

NMR techniques. The catalyst (**1b**) did indeed show promise as active

hydrogenation/hydrogenolysis catalysts toward some furan derivatives in alcohols.

However, due to side reactions with the solvent, these systems were not especially

selective. Better selectivity was demonstrated with these catalytic systems when the

solvent, NMP, was used, but the hydrogenolysis step to give methylfuran was not as

accessible under the above mentioned conditions. At higher temperatures the catalyst

apparently underwent decomposition. Catalyst (**1b**) was not as effective as (**2b**) was

toward hydrogenation of furan derivatives. Most likely, this was due to the higher

electrophilic nature of this species due to greater π acidity of the ligand framework. This

electrophilicity contributed to weaker hydridic character of the Ru-H intermediate thus

hindering the nucleophilic attack of the activated substrate.

Future Work

The next phase of work on these catalytic systems should involve the

development of more complex phosphine ligand systems to provide for the electronic

considerations at the metal center. A ligand system that would provide for more

thermally stable catalysts is beckoning. More tuning about the metal center for these

electronic factors could provide a balanced catalyst whereby heterolytic cleavage of

dihydrogen and subsequent proton transfer is attained as easily as hydride transfer step.

A new multidentate and more versatile ligand set could offer some promise in

hydrogenation reactivity. It was postulated that one of the larger energy barriers to the

transfer of the ruthenium hydride to the activated substrate was that the substrate must be

in spatially close to the catalyst. This may be difficult to attain due to the steric

interactions of the ligand system and the charge on the ruthenium species. The synthesis outlined in **Scheme 14**, details the theoretic preparation of the catalyst system.

Scheme 14. Synthesis of the 'tethered base system.
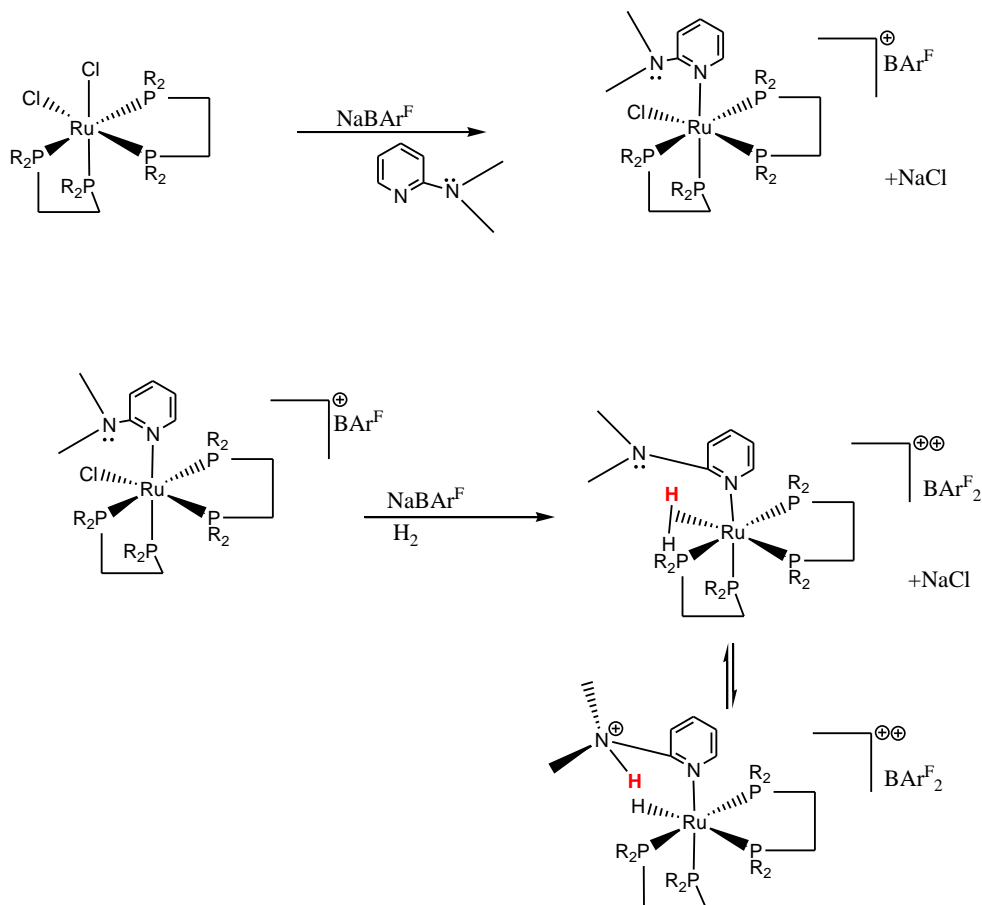
We postulated that a tether on the catalyst could aid in the heterolytic cleavage of H_2 and transfer of a proton to the furfural substrate. One could imagine the tether extending further out into space thus increasing the chances of interacting with the

substrate. Therefore a type of catalyst could prove to be a more facile pathway for

protonation and hydride transfer from catalyst to substrate.

Scheme 15. Possible mechanism of hydrogenation and hydrogenolysis of furfural by the tethered base catalyst.
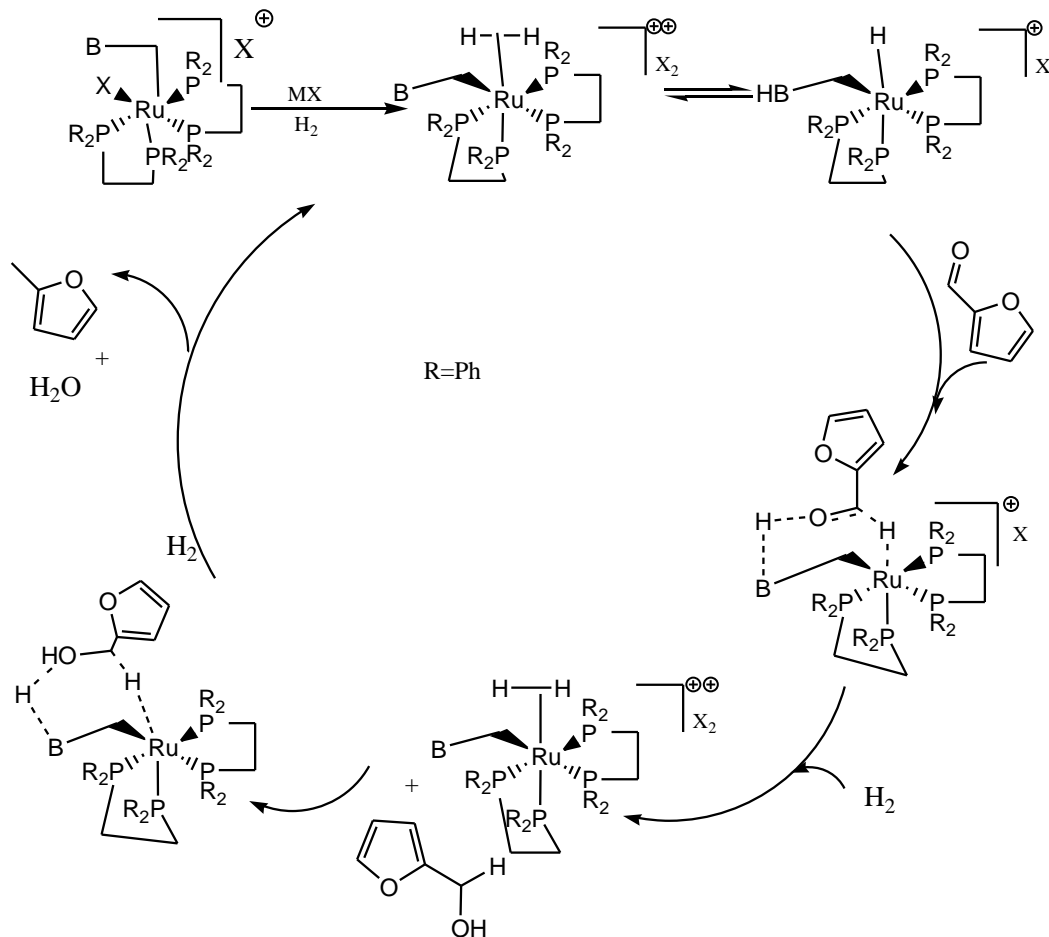
As depicted above, one may envision coordination of dihydrogen to the metal and

subsequent heterolytic cleavage. The cleavage then results in an acidic tether and a

ruthenium hydride. This tether may function as a sort of arm that can extend outside of

the outer-coordination sphere of the metal center to protonate the substrate. The action of

bringing the substrate close to the metal center may facilitate the hydride transfer step thus aiding in the hydrogenation and hydrogenolysis of the furfural.

A complete investigation of the tethered base system could give more facile conversion of substrate to product by a more concerted transfer mechanism.

The ruthenium-aryl catalysts need to be more adequately developed and characterized so the neutral ruthenium-hydride complex can be investigated as a more facile hydride transfer system than the cationic one. The exploration of these catalysts with not only FFR substrate but also with HMF needs to be realized. Perhaps to lower overall costs, catalytic iron analogues need to be developed.

At this point, conditions in the field do seem right for methyl furan production and indeed seem to be within our grasp. Hopefully, a world with a new renewable energy is also on the way.

Experimental Section (part 1)

Oxygen and water were at all times excluded from all operations by use of glove box and Schlenk techniques supplied by purified nitrogen unless otherwise noted. Benzene, ethyl ether, tetrahydrofuran (THF), and hexanes were all dried and distilled from sodium-benzophenone ketyl. Ethanol was distilled from activated magnesium turnings. Dichloromethane was dried and distilled from calcium hydride. Deuterated solvents were distilled and stored over type 4A molecular sieves. The phosphine ligands were purchased from Sigma Aldrich or Strem Chemicals unless otherwise stated. The

complexes [RuCl$_2$(DMSO)$_4$], *cis*-[RuCl$_2$(dppe)$_2$],   and cis-[RuCl$_2$(depe)$_2$] were prepared by literature methods.[9-10]

All NMR spectra were recorded on a Varian XL-400 (400 MHz for ^{1}H, 181 MHz for ^{31}P) spectrometer. All ^{31}P NMR were proton decoupled, unless otherwise mentioned. ^{31}P NMR chemical shifts were referenced to 85% H$_3$PO$_4$ via a sealed coaxial capillary tube. ^{1}H NMR shifts were measured relative to partially deuterated solvent peaks but are reported relative to tetramethylsilane. T$_1$ measurements were made at 400 MHz using the inversion recovery method. Microanalyses were performed by Robertson Microlit services. Quantitative GLC analyses were performed on a Shimadzu GC-14A instrument equipped with a flame ionization detector using a 25mm x 0.25 mm CBP-10, 14% cyanopropylphenylpolysiloxane in a fused capillary column. GC-MS analyses were carried out on a Shimadzu GC-MS QP-5000 spectrometer. In general, all catalytic hydrogenation reactions were performed in a glass liner that was placed inside a steel Parr bomb chamber. Ultra-pure hydrogen purchased from Scott Gross gas supplies was used. In all cases the chamber was placed half way into a heated silicone oil bath while stirring of the oil was performed for heat distribution. In all cases, after the catalyst, solvents, and substrate were added, the system was purged thrice to rid the vessel of air. In almost all cases, a 1:100 molar ratio of catalyst to substrate was used.

1b. *Preparation of [RuCl(dppe)$_2$][BAr^F]*

To a solution of 0.134 g [RuCl$_2$(dppe)$_2$],(0.103 mmol) in 15 mL of dichloromethane was added a solution of one equivalent of NaBAr^F (0.11 g) in 5 mL of dichloromethane. The resulting deep red solution was allowed to stir at room temperature for a period of one hour. After this period, the red solution was passed through a column of Celite to remove NaCl generated from the reaction. The solvent was then evaporated leaving 150 mg of the red solid. (62% yield)

^{1}H NMR (CDCl$_3$, 400MHz): δ 7.8-6.7 (m, PC$_6$H$_5$), 2.7 (br s, 2H), 2.5 (br s, 4H), 1.6 (br s, 2H) (PCH$_2$CH$_2$P). ^{31}P{^{1}H} NMR (CDCl$_3$): δ 83.5 (t), 56.8 (t) ^{13}C NMR (CDCl$_3$, 400MHz): δ 162-131 (m PC6H5), 128-117 (m, B(C$_8$H$_3$F$_6$)$_3$), 29.9 (m PCH$_2$CH$_2$P). 18.6 (m (PCH$_2$CH$_2$P).

[RuCl(dppe)$_2$][BAr^F] • DMSO

Anal. Calcd. For C$_{86}$H$_{66}$BClF$_{24}$OP$_4$RuS, C, 55.1; H, 3.55. Found: C, 54.01; H, 3.25.

T$_1$ measurements of [RuCl(H$_2$)(dppe)$_2$][BAr^F](RK# 547)

To a screw capped NMR tube was added 20 mg of [RuCl(dppe)$_2$][BArF] and 1 mL of CDCl$_3$. This deep red solution was then cooled to -40 ^{o}C with use of a CHCl$_3$/CO$_2$ bath. The cooled solution then had H$_2$(g) bubbled through for 2 minutes. The resulting orange

solution, $[RuCl(H_2)(dppe)_2][BAr^F]$ was then observed via an inversion recovery method at 243 K.

2a. *Preparation of cis-[RuCl₂(dipyrrolyl)₂](RK# 512)*

To a solution of 0.056 g, (0.116 mmol) of $[RuCl_2(DMSO)_4]$ in 10 mL of dichloromethane was added 2 equivalents of dipyrrolyl ligand, (0.085 g) in 5 mL of dichloromethane. The golden yellow solution turned an immediate pale yellow. This solution was then allowed to react for one hour at room temperature. After this period, the solvent was evaporated and the pale material was recrystallized from THF/hexanes. (48% yield)

^1H NMR (CDCl₃, 400MHz): δ 7.1-5.5 (m, P(NC₄H₄)), 2.9 (br s, 2H), 2.57 (br s, 4H), 1.8 (br s, 2H) (PCH₂CH₂P). $^{31}P\{^1H\}$ NMR (CDCl₃): δ 130.3 (t), 118.5 (t) ^{13}C NMR (CDCl₃, 400MHz): δ 125-112 (m PC6H5), 40.5 (m (PCH₂CH₂P), 20.6 (m PCH₂CH₂P).

cis-[RuCl₂(bis-pyrrolyl)₂] • DMSO

Anal. Calcd. For $C_{38}H_{46}Cl_2N_8OP_4RuS$ C, 47.67; H, 4.60 ; N, 11.70. Found: C, 47.66; H, 4.60; N, 12.08.

2b. *Preparation of [RuCl(dipyrrolyl)₂][BAr^F](RK# 468)*

To a solution of 0.04 g, of **2a** in 10 mL of dichloromethane was added one equivalent of NaBAr^F, (0.039 g), in 5 mL of dichloromethane. The pale solution was stirred at room temperature for 1 hour. After this period, the golden brown liquid was filtered through Celite to remove residual NaCl. (56 % yield)

^{1}H NMR (CDCl$_3$, 400MHz): δ 7.31-7.2 (m B(C$_8$H$_3$F$_6$)$_3$), 6.45-5.5 (m, P(NC$_4$H$_4$)), 2.9 (br s, 2H), 2.57 (br s, 4H), 1.8 (br s, 2H) (PCH$_2$CH$_2$P). ^{31}P{^{1}H} NMR (CDCl$_3$): δ 134.6 (t), 133.4 (t)

^{13}C NMR (CDCl$_3$, 400MHz): δ 162-124 (m P(NC$_4$H$_4$)), 124-112 (m B(C$_8$H$_3$F$_6$)$_3$), 68.4 (m (PCH$_2$CH$_2$P), 25.5 (m PCH$_2$CH$_2$P).

[RuCl(bis-pyrrolyl)$_2$][Barf] •DMSO

Anal. Calcd. For C$_{70}$H$_{58}$BClF$_{24}$N$_8$OP$_4$RuS. C, 47.06; H, 3.27 ; N, 6.27. Found: C, 45.87; H, 2.97; N, 6.11.

2a'. *Preparation of trans-[RuCl$_2$(dipyrrolyl)$_2$](RK# 516)*

To a solution of (**2b**) in acetone d$_6$ was added one equivalent of LiCl in a screw-capped NMR tube. Immediately, it was observed by ^{31}P NMR that (**2b**) had been converted to (**2a**) but a small amount of new material was observed as a singlet at δ 131.3. This new material, *trans* (**2a'**) crystallized along with the *cis-[RuCl$_2$(dipyrrolyl)$_2$]*). It was never observed in an isolated state.

^{31}P{^{1}H} NMR (CDCl$_3$): δ 131.3 (s)

3a. *Synthesis of [Ru(tolyl)(Cl)(dppe)$_2$](RK#539)*

To a flask was added 0.2 g of [RuCl$_2$(dppe)$_2$] and 25 mL of THF. This yellow mixture was cooled to -78 ^{o}C. A slight excess (0.27 mL in 20 mL THF) of 1M *p*-tolyl-MgBr in ethyl ether was added to the cooled mixture drop wise over a period of one hour. The material was allowed to warm to room temperature and was stirred overnight. The yellow solution then had added wet THF to deactivate any remaining starting materials. This solution was then passed through a plug of silica. The solvent was then evaporated and the material was observed via NMR. (36 % yield)

^{1}H NMR (CDCl$_3$, 400MHz): δ 7.7-6.6 (m, PC$_6$H$_5$), 2.5 (br s, 2H), 2.3(br s, 4H), 1.6 (br s, 2H), (PCH$_2$CH$_2$P), 2.1 (s 3H), PhCH$_3$. ^{31}P{^{1}H} NMR (CDCl$_3$): δ 58.3 (t), 42.7 (t), 37 (t), 35 (t).

3b. *Synthesis of [Ru(tolyl)(dppe)$_2$][BAr^F](RK# 549)*

To a flask was added 0.048 g, (0.0345 mmol), of [Ru(tolyl)(Cl)(dppe)$_2$]and 10 mL of dichloromethane. To that yellow solution was added a solution of 0.038 g NaBAr^F in 5 mL of dichloromethane. The resulting deep red solution was allowed to stir at room temperature for one hour. After this period, the solution was passed through Celite and had the solvent evacuated. There was 5% of (**1b**) observed via ^{31}P NMR. This (**1b**) was most likely due to some unreacted precursor that was carried through the synthetic steps.

^{1}H NMR (CDCl$_3$, 400MHz): δ 7.7-6.6 (m, PC$_6$H$_5$), 2.5 (br s, 2H), 2.3(br s, 4H), 1.6 (br s, 2H), (PCH$_2$CH$_2$P), 2.1 (s 3H), PhCH$_3$. ^{31}P{^{1}H} NMR (CDCl$_3$): δ 81.6 (t), 60.1 (t). (31% yield)

CHAPTER 2.

The Synthesis and Characterization of Electrophilic Iridium Dithiolate Complexes

Introduction

The active design, synthesis, and characterization of electrophilic late transition metal complexes for mediating bond activation chemistry has been an area of active interest in organometallic chemistry and catalysis. This interest stems from examples of late transition metal complexes that were capable of electrophilically driving bond activation transformations. One of the best known examples is the well characterized Pd^{2+} system, $[Pd(NCMe)_4]-[BF_4]_2$ which, due to the lability of the ligand system, the electrophilic nature as a Pd^{2+} cation, C=C bond polarization, and activation, was found to polymerize styrene,[20] oligomerize ethylene, [21]and isomerize 1-butene into *tran*s- and *cis*-2-butene.[22] All of these types of conversions are of scientific and industrial interest. The activation and functionalization of the C-H bonds of different organic substrates using electrophilic late transition metals is an area that has recently begun to tantalize the industrial and academic arena. However, the synthesis and chemistry of electrophilic group 9 metal complexes are, at present, inadequately studied. This is mainly due to the overwhelming inertness of low spin d^6 complexes. Preliminary evidence suggests that this substitutive inertness may be overcome through the use of weakly coordinating ligands as well as strong electron donating ligands *trans* to the substrate coordination site

on the metal. With the use of a thiolate rich environment, the rates of ligand dissociation, which would be necessary in the first step of a catalytic reaction, may be enhanced.

Some examples of these systems that are being pursued by chemists in academia and industry describe the use of $[(Cp*)IrMe(PMe_3)(CH_2Cl_2)]^+$ and $[PtMe(sol)(NN)]^+$ complexes (NN=Me$_4$en and (sol= a weakly coordination solvent) to activate methane and arene C-H bonds.[23]

As a d^6 metal ion Ir[III] is thought to possess electrophilic character similar to that of Pd[II] but due to its electron configuration in a coordinatively saturated environment with high field ligands it gives a low spin inert cationic species.

We have proposed here, that this inertness can be overcome by designing an Ir[III] complex that maintains a thiolate rich environment that is a *trans*-directing multi-dentate ligand system. We wished to probe the ancillary ligand effects on reactivity and to demonstrate facile tunability at the metal center by use of monodentate and multi-dentate phosphine auxiliary ligands.

Figure 6. Targeted system framework.
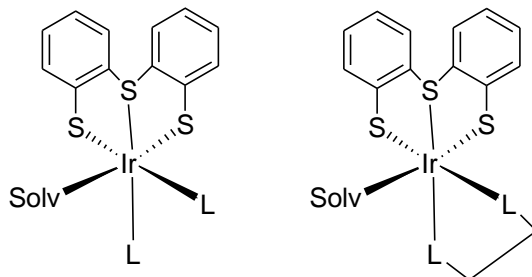
The system framework can be described as maintaining a thiolate rich environment and tunability at the (L) positions (when L = PR_3 and L~L = a bidentate phosphine) by varying the (R) groups of the phosphine ligands. We also wanted to demonstrate the capability of unsaturating the position *trans* to the electron-donating thiolate ligand.

Here, we have designed a new class of Ir^{III} metal thiolate complexes that have been synthesized and fully characterized. We were able to demonstrate tunability at the metal center for steric and electronic factors via the use of PR_3 ligands (R=Phenyl, pyrrolyl) and multidentate ligand systems. We believe that the basic framework of these systems offers a platform for future investigation of these catalyst precursors to mediate additions of weak nucleophiles such as water, alcohols, and organic acids to activated substrates. The additions to alkynes, organonitriles, and ketones were evaluated. With this study, we hoped that the groundwork for the synthesis and organic chemistry of group 9 metal electrophiles can be expanded upon. Ultimately, their aptitude as catalysts for nucleophilic addition reactions could pose as an interesting tool for the synthetic organic chemist.

Background

Many group 9 transition metal complexes have similar electrophilic character as the well-known Pd^{2+} catalytic systems. However, despite the extensive chemistry of these systems [24-25] the potential for group 9 systems remains insufficiently studied.[26-29] This can primarily be attributed to the anticipated substitutive inertness of low-spin d^6 metal complexes in saturated environments. There is recent evidence that suggests that

43

this inertness may be overcome through the use of a thiolate-rich ligand system that is *trans* to the substrate binding site.[30] In fact, the labilizing effect of a *trans*-thiolate donor has recently been demonstrated [31] and suggests a reasonable explanation for high activity of the nitrile hydratase (NHase) in the hydration of nitriles to primary amides. [32] NHase is a metalloenzyme and is found in bacterial cell lines such as *Rhodococcus* sp. R312 and N771 and *Pseudomona chlorophis* that live near under water volcanic vents.[33] With recent crystallographic data, these enzymes have been found to contain a non-corrinoid low-spin Co^{3+} or a non-heme Fe^{2+} center at the active site.[34] Kovacs has recently reported a series of well-studied Co-NHase and Fe-NHase model compounds that maintain a distorted trigonal bipyramidal geometry with two thiolate sulfurs position in the basal plane and two imino in the axial positions.[35]

Figure 7. The proposed active site of nitrile hydratase.
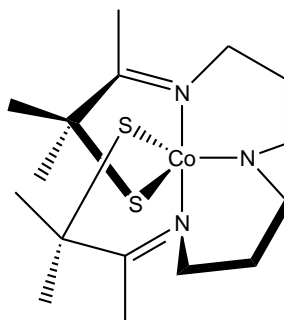
The possibility and potential for these systems to be mimicked or harvested for use as nitrile-containing waste remediation is beckoning. Industrial catalytic applications of these systems could revolutionize the field of enantioselective amide syntheses. [36] Currently, in Japan, microbial NHase accounts for the annual kiloton production of

acrylamide.[37]   There is an enormous effort being directed toward the development of structural and functional models of these metalloenzymes.[38]

The mechanism of action of the NHases is not yet known.   However, some possibilities have been described.[38]   In the pathway depicted in **Scheme 16**, the Co-OH is first protonated to give water that can then be displaced by the nitrile.   The nitrile is then activated by the electrophilic metal center and is subsequently attacked by water to give imine-like species.   Tautomerization then gives the oxonium and with the addition of an additional water molecule, the amide product is eliminated.   The Kovacs group has demonstrated that reversible coordination of nitriles, alcohols, and amines to the Fe^{3+} center of $[Fe(S_2Me_2N_3)(Et,Pr)][PF_6]$ is possible, thereby lending support to this mechanistic pathway.[39]   Competitive binding studies seem to indicate that MeCN binds preferably to MeOH, suggesting that nitriles could displace a coordinated water molecule.

Scheme 16. Possible mechanism for catalytic conversion of a nitrile derivative to the corresponding amide.
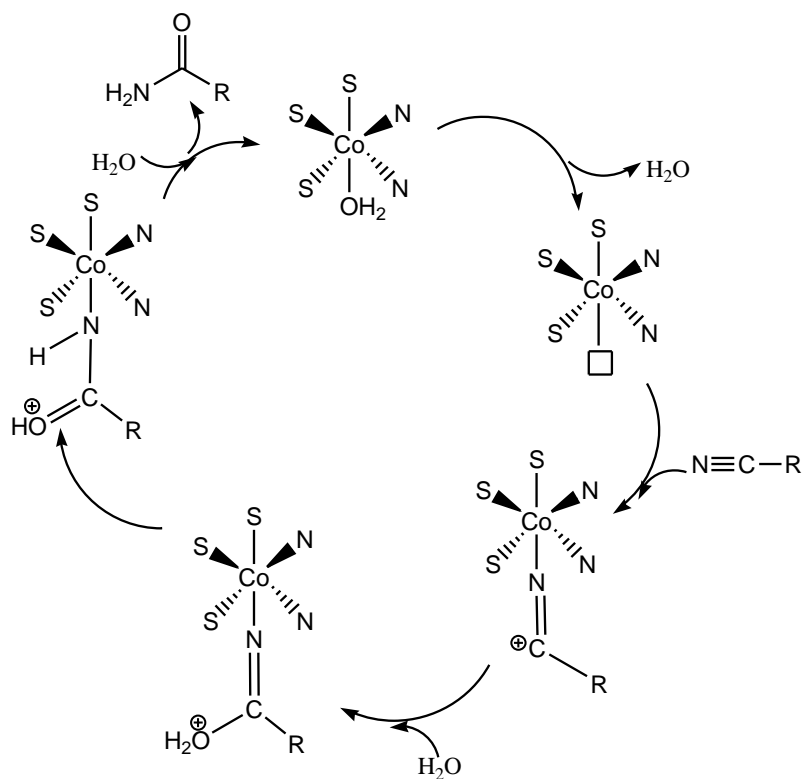
From these thiolate-rich nitrile hydration systems, there is much interest in the coordination chemistry of transition metal sulfur complexes. These systems can find use in applications such as hydrosulfurization.[40] There is a range of structural complexity involving these thiolate systems due to the tendency of the ligands to bridge metal centers.[41] However, there is evidence that through the use of bulky tertiary phosphine ligands and multidentate ligand systems, that this dimerization may be overcome.[42]

There is a possibility that these of systems can be used in types of electrophilically driven reactions. The addition of water to activated organonitriles offers an attractive pathway for the creation of new C-O bonds. The facile catalytic addition of

carboxylic acids to alkynes to generate vinyl and enol esters represents an extremely valuable pathway to obtain important intermediates in synthetic schemes. These types of transformations have been achieved under mild conditions using rhodium catalysts. So far, the *E*-isomer of the vinyl ester has been obtained in a selective fashion but to date, the *Z*-isomers are difficult to achieve.[43] The proposed mechanism, as detailed in **Scheme 17**, involves the generation of the 16 electron species, [RhL]$^+$ which forms an adduct with the alkyne substrate. This alkyne is then electrophilically activated toward nucleophilic attack by the carboxylate. This results in the Rh$^{\mathrm{I}}$ σ-alkenyl species being protonated at the metal to give an unstable Rh$^{\mathrm{III}}$ complex that can reductively eliminate the product to regenerate the catalyst. Currently, the reaction of carboxylic acids with terminal alkynes at 100$^{\mathrm{o}}$C in the presence of [Ir(COD)Cl]$_2$ and Na$_2$CO$_3$ was shown to produce the corresponding vinyl and enol esters but little selectivity was observed.[44]

Scheme 17. Proposed mechanism for rhodium catalyzed enol-ester formation.
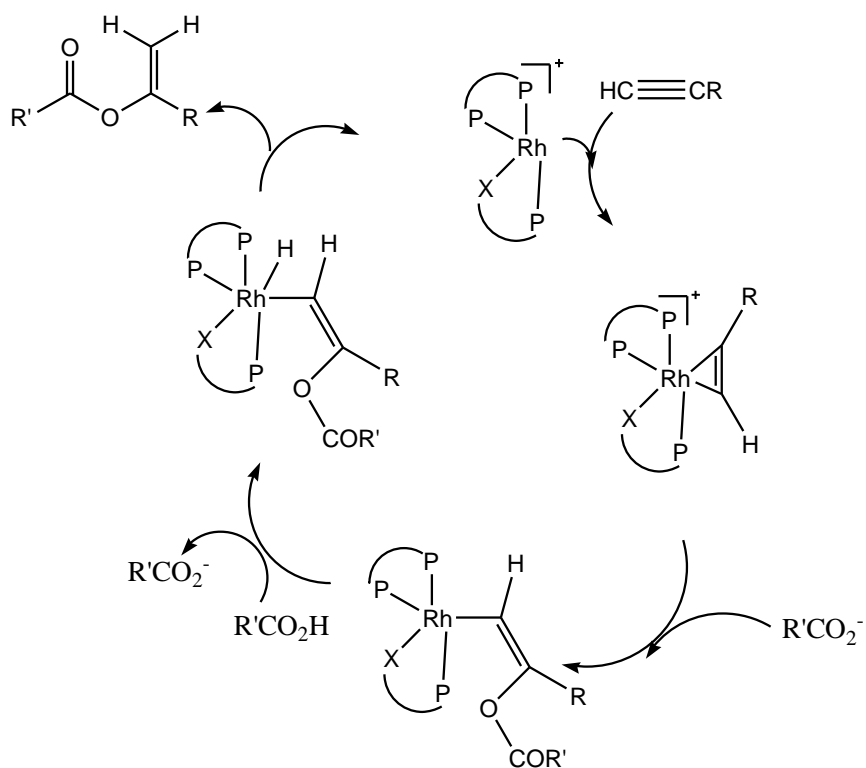
Results and Discussion

Thiolate ligand synthesis was a multi-step process that is outlined below. It was chosen for its *trans* directing function as well as being a tridentate ligand system that maintains a facial orientation about the metal coordination sphere. No modifications of the synthesis of this species were performed to the preparation detailed by Sellman et al.[45]

Scheme 18. Synthesis of thiolate ligand H_2S_3.
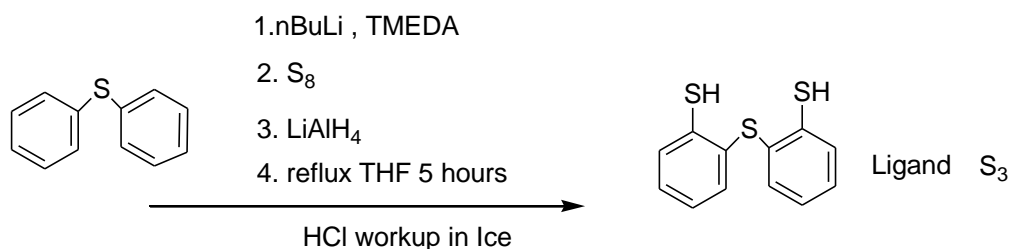
The thiolate ligand, H_2S_3, was then deprotonated and reacted with one equivalent of the tris-phosphine complex, $[Ir(PPh_3)_3H(Cl)_2]$ which was prepared via the method of Simpson et al.[27]

Scheme 19. Synthesis of complex $[Ir(PPh_3)_2HS_3]$.

(**4a**)
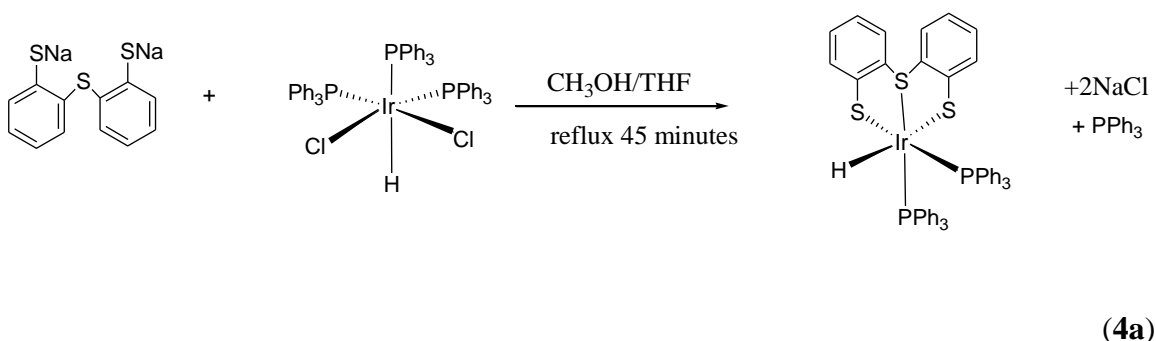
The complex $[Ir(PPh_3)_2HS_3]$ was prepared by first reacting the H_2S_3 species with 2 equivalents of sodium methoxide, $(NaOCH_3)$, in methanol to deprotonate the thiolate hydrogens. The Na_2S_3 bronze methanol solution was then added to the yellow THF suspension of $[Ir(PPh_3)_3H(Cl)_2]$ and refluxed for 15 minutes to afford the red solution, containing $[Ir(PPh_3)_2HS_3]$. The precipitation of 2 equivalents of NaCl from the organic medium is thought to drive the reaction thermodynamically. Subsequent washing with THF and then ether gives the pure yellow complex.

Figure 8. Molecular structure of [Ir(PPh₃)₂HS₃](4a).
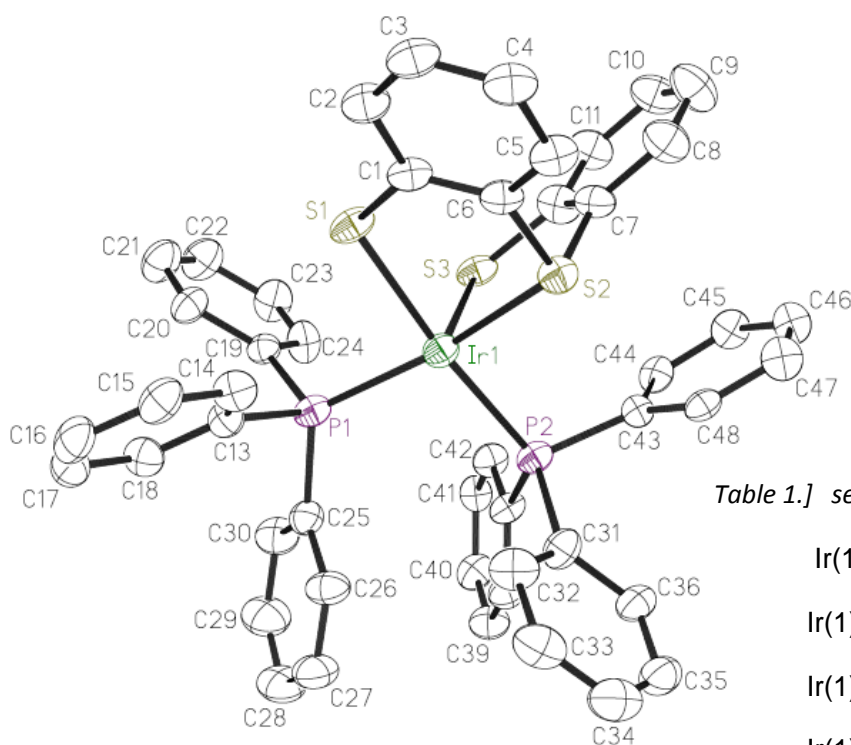
Table 1.] selected Bond lengths [Å].

Ir(1)-P(1)	2.303(3)
Ir(1)-P(2)	2.314(3)
Ir(1)-S(2)	2.353(3)
Ir(1)-S(1)	2.388(3)
Ir(1)-S(3)	2.418(4)

The isomerization of [Ir(PPh₃)₂HS₃] was explored due to the potential of the complex to lose a triphenylphosphine ligand at high temperatures. The loss of phosphine would unsaturate the complex producing a *penta*-coordinate species.

Also, loss of phosphine would change the geometry of the complex. This was of particular interest due to the sterochemical rigidity of these complexes could be important in terms of general reactivity.

Scheme 20. Isomerization reaction of [Ir(PPh₃)₂HS₃].

(4a) C_6D_6 / 100° C 24 hours   (4b)
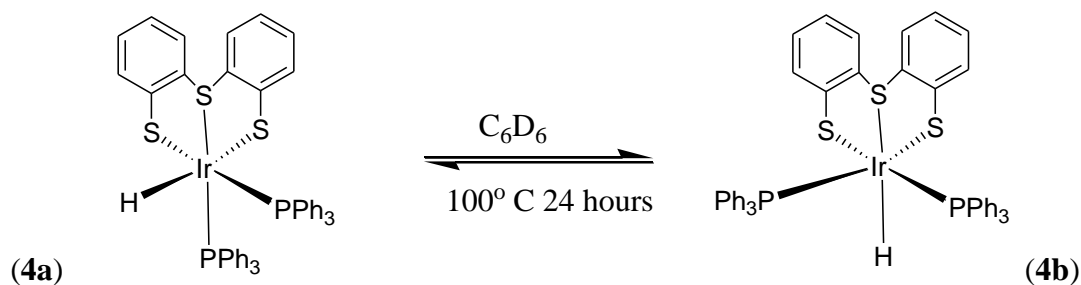
Isomerization of complex (**4a**) to complex (**4b**) occurs, after 24 hours at 100 ^{o}C to give an equilibrium distribution of 40% (**4a**) to 60% (**4b**). These percentages were obtained via hydride integrations from a 400 MHz ^{1}H-NMR instrument after 24 hours of being allowed to react at the above stated temperature.

Scheme 21. Newman projection of the isomerization reaction of [Ir(PPh₃)₂HS₃].

4a   4b
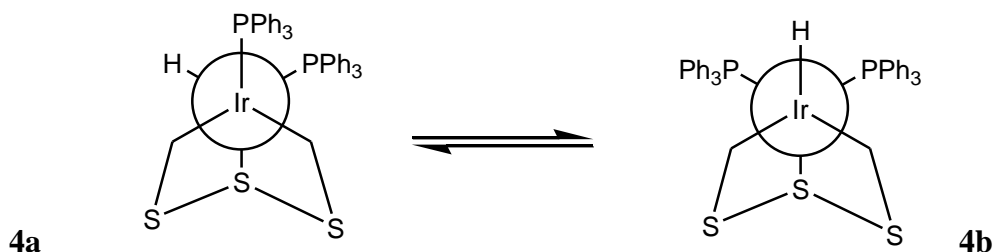
Preliminary results of these trials indicate that the isomerization is most likely proceeding via an intramolecular mechanism. It was found that, at these conditions, with the addition of one stoichiometric equivalent of PPh₃ no observed change in the equilibrium distribution between (**4a**) and (**4b**) was observed. If the reaction was proceeding via an intermolecular rate determining loss of PPh₃, then one could expect a possible change in the equilibrium product distribution with the presence of the PPh₃. For

this reason, an intramolecular isomerization seems, at present, a more viable avenue for the isomerization reaction to take place. A bailar twist mechanism is one possibility where a trigonal prismatic transition state is accessed. This is probably due to the lack of steric interactions around the coordination sphere of the metal as well as strong electron-donating capability from the triphenylphosphine ligands.

Figure 9. Molecular structure of [Ir(PPh3)2HS3](4b).

Selected Bond lengths [Å].

Ir(1)-P(2)	2.3106(9)
Ir(1)-P(1)	2.3136(9)
Ir(1)-S(3)	2.3832(9)
Ir(1)-S(1)	2.3872(9)
Ir(1)-S(2)	2.3929(9)
Ir(1)-H(1)	1.34(3)
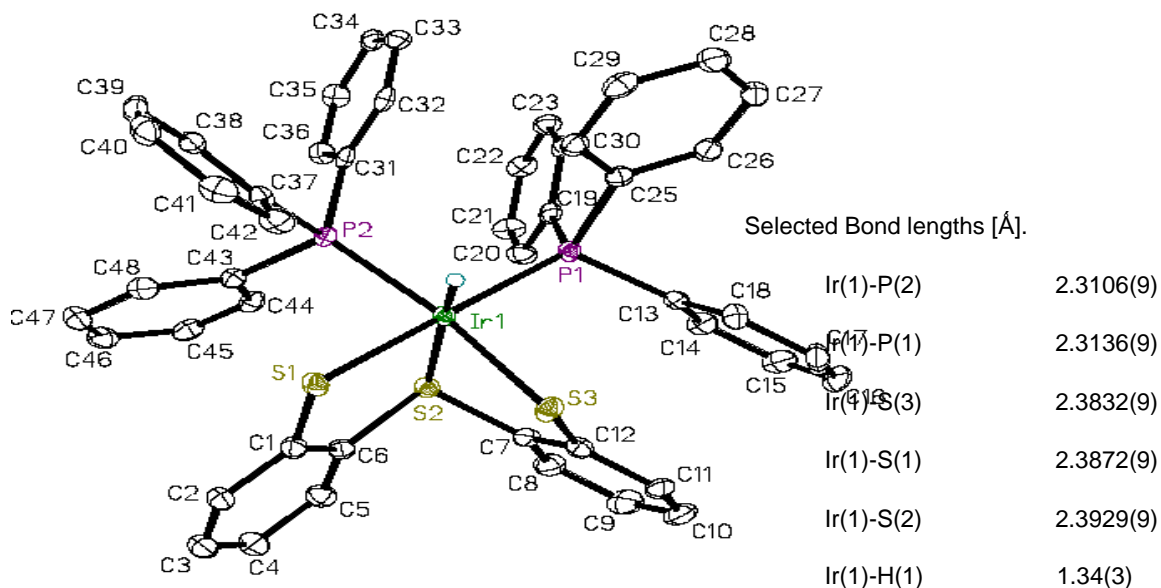
The molecular structure, (**4b**)**, Figure 9,** shows that the complex gained an element of symmetry due to the mirror plane that makes the phosphine ligands equivalent. The thiolate positions are now visibly *trans* to the less electron-donating phosphine indicating a more thermodynamically stable species.

Scheme 22. Possible mechanistic pathways for the isomerization of [Ir(PPh$_3$)$_2$HS$_3$].
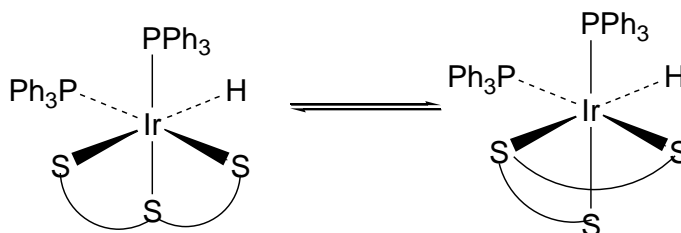
Bailar twist mechanism
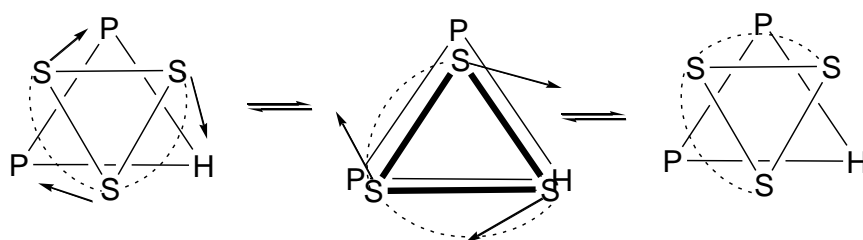
Dissociative mechanism
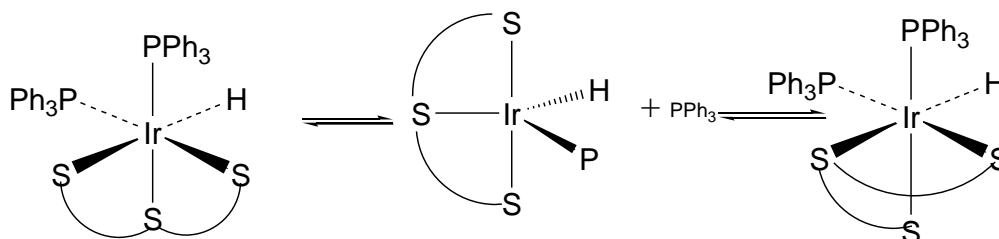
A possible mechanistic pathway for the isomerization of (**4a**) to the more thermodynamically stable (**4b**) system is outlined above in **scheme 22**.

In order to generate an open coordination site at the metal center we explored the conversion of the hydride ligand to a halide ligand.

The complex was brominated in order to position to explore opportunities for unsaturating the system with a large non-coordinating counter ionic species that would precipitate NaBr as a salt in an organic medium and stabilize the metal cation.

Scheme 23. Bromination reaction of [Ir(PPh₃)₂HS₃].

(**4a**)   (**5a**)
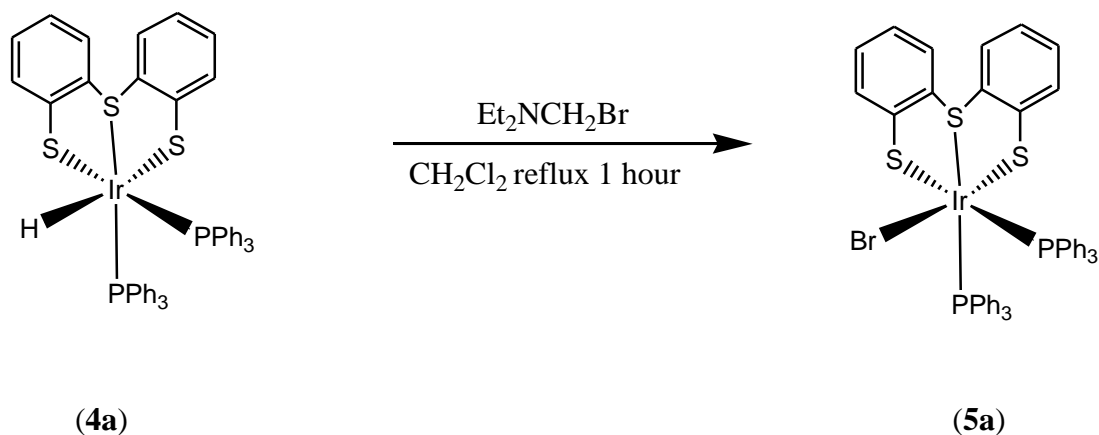
The complex was brominated using an excess of an iminium bromide salt and one equivalent of triphenylphosphine in methylene dichloride. It was then refluxed for 1 hour and stripped to dryness and dissolved into benzene. The red/orange benzene solution was the passed through a flash column in nitrogen atmosphere with a gradient of elutions (15 mL) each. First a 9:1 hexane/ ethyl acetate mixture was flushed through the column, then a 8:2 mix of the same solvents, then 7:3, 3:2, and finally a 1:1. This afforded an analytically pure sample of a [Ir(PPh₃)₂BrS₃] at 11.5% yield. The excess reagent was used due to the extreme water sensitivity of the brominating reagent.

The extra phosphine was added to suppress dissociation triphenylphosphine from the metal center. It was found that the increased steric bulk about the metal sphere from the larger bromide increased the rates of phosphine dissociation. After the reaction had

54

taken place phosphine would dissociate at the reflux temperature and nucleophilic attack of the amine bi-product to the metal center would result in an undesirable product distribution.

Figure 10. The molecular structure of [Ir(PPh$_3$)$_2$BrS$_3$] (5a).

Selected Bond lengths [Å].

Ir(1)-S(2)	2.3106(17)
Ir(1)-P(2)	2.3387(17)
Ir(1)-S(3)	2.3510(17)
Ir(1)-S(1)	2.3528(16)
Ir(1)-P(1)	2.3749(17)
Ir(1)-Br(1)	2.5664(9)
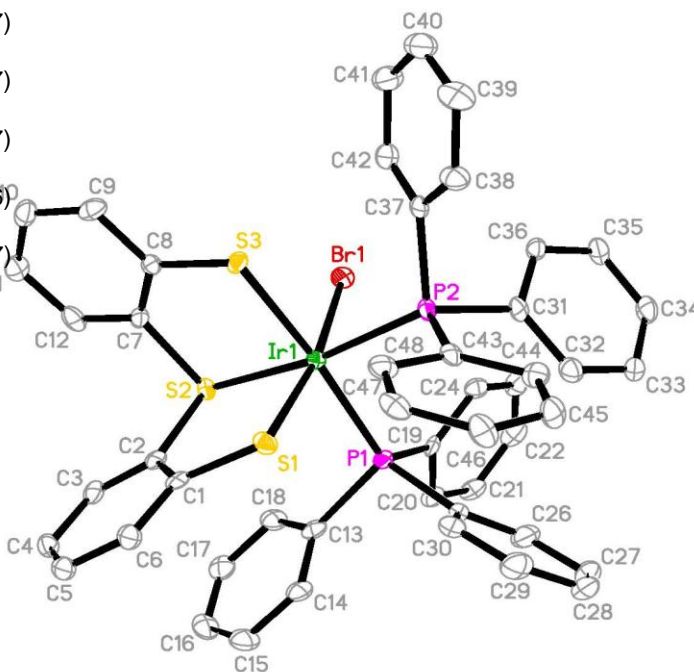
Due to the increased steric bulk about the metal center that is introduced by the bromide ligand, the iridium-thiolate bond distance was substantially elongated in comparison to the hydrido complex. This brominated species was then reacted with one equivalent of NaBAr^F and catalytic conversions were then attempted.

Complex (**5a**), [Ir(PPh₃)₂BrS₃], and NaBAr^F was placed into a sealed pressure tube with deutero-benzene and various substrates and a catalytic amount of base was added. The vessel was then heated to 100 °C for a period of 24 hours. It was determined through the substrate conversions that this catalyst gave poor selectivity.   Also, the reaction proceeded quite sluggishly leading us to conclude that the catalyst was not very active. Desired selectivity was not gained with this particular system.

Scheme 24. The proposed catalytic pathway for electrophilically driven enol-ester formation.
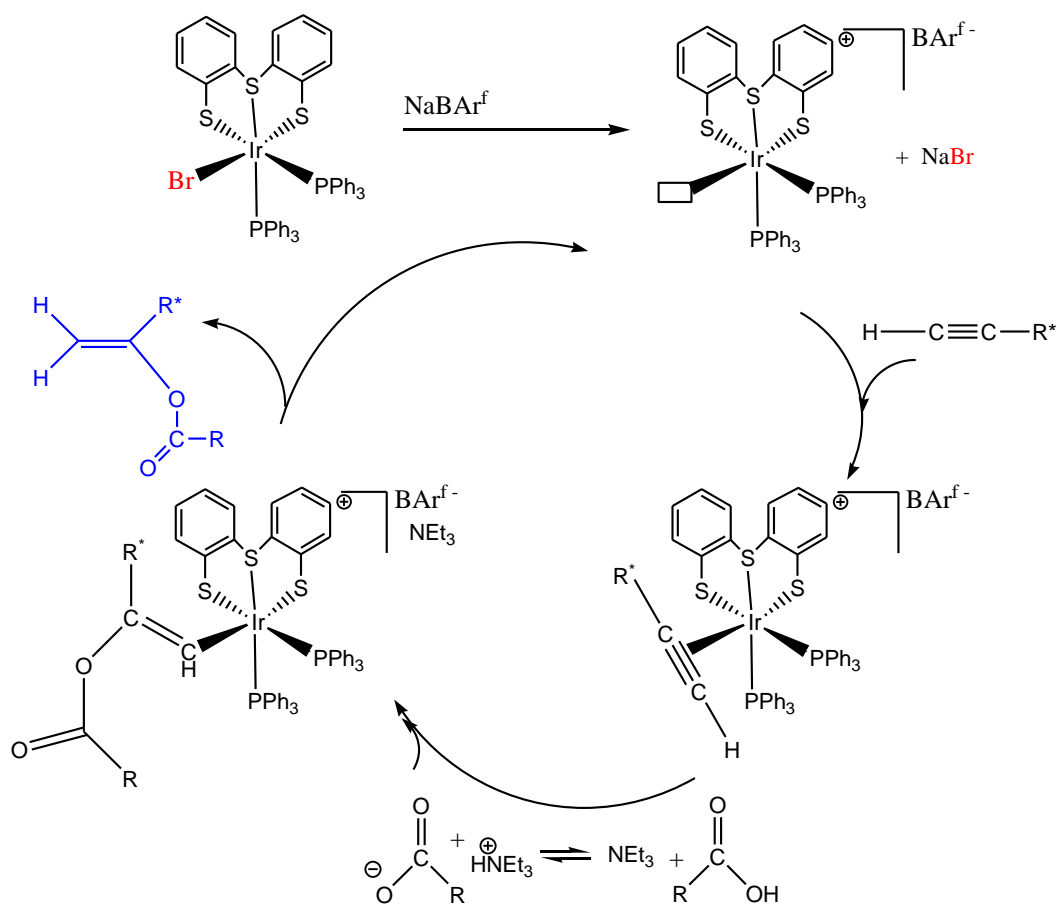
The proposed pathway for the catalytic electrophilically driven enol-ester production proceeds via an unsaturation of the complex so that substrate can bind. The

56

substrate is then activated for nucleophilic attack due to the electron-withdrawing ability of the electrophilic iridium cation. Catalytic amounts of base, then deprotonate the acid substrate and the deprotonated acid will attack the alkyne on the most activated carbon. A subsequent elimination then affords the product and the catalyst. The regenerated catalyst can then go through more production cycles.

It was observed that the catalyst could afford various isomers of the product; hence, selectivity was somewhat poor. Also, the catalyst was not particularly active, low turnover rates were observed hinting at high activation barriers in some of the catalytic steps. It seemed plausible that the system was too electron-rich for facile electrophilic activation of the substrate. Also, steric hindrance at the metal center from bulky R-groups on the phosphine ligands could impede the rate of substrate coordination or even nucleophilic attack on a coordinated substrate. Another issue that could have contributed to the lack of selectivity, besides the reaction conditions, was the possibility geometric rearrangement of the complex. This could have affording a less reactive substrate binding position.

Due to the lackluster results of the catalytic system that was designed, modifications were then deemed to be necessary to increase the catalysts potential activities and product selectivity. Therefore, demonstrating tunability was essential. We wished to tune the system's original framework for electronic and steric factors that influence the nature of the above stated shortcomings.

We were able to develop an alternative synthetic route to obtaining the [Ir(PPh$_3$)$_2$HS$_3$] complex. Work done by Morris, et al.[46] demonstrated that starting with IrCl$_3$ that DMSO could be refluxed in a protic medium to afford [Ir(DMSO)$_3$(Cl)$_2$H]. Due to the substitutive labile nature of the DMSO ligands, we were able to use this system as a starting point to tune the ligand environment about the iridium metal center.

Scheme 25. Addition of thiolate ligand to [Ir(DMSO)$_3$(Cl)$_2$H].

$$[Ir(DMSO)_3HCl_2] + Na_2S_3 \xrightarrow[\text{stir 30 minutes r.t}]{\text{THF/CH}_3\text{OH}}$$

(6a)

+2NaCl
+DMSO
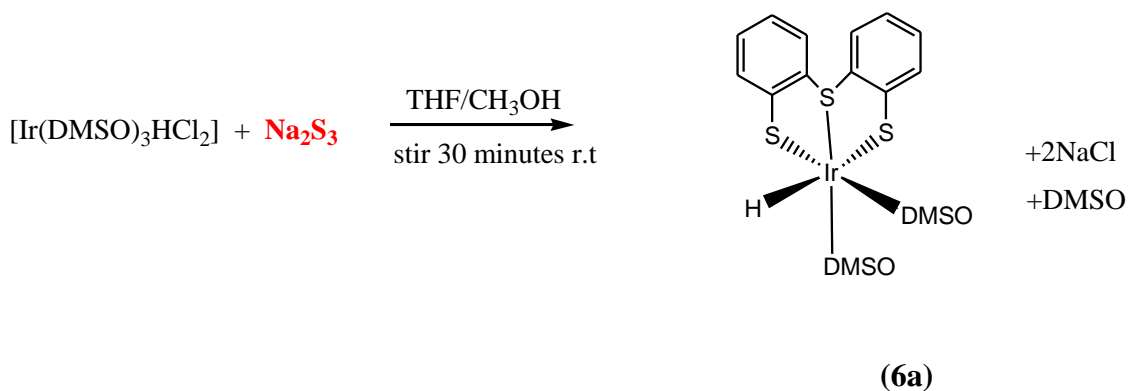
The tris-DMSO complex, [Ir(DMSO)$_3$(Cl)$_2$H], was then reacted with one equivalent of the sodium salt of the dithiolate ligand at room temperature in a one to one mixture of THF and MeOH for 30 minutes to afford the red [Ir(DMSO)$_2$HS$_3$], at 77% yield.

With [Ir(DMSO)$_2$HS$_3$] (**6a**), lability of the DMSO ligands was demonstrated by substitution with 2 equivalents of PPh$_3$. This afforded an alternative synthetic route to obtain the complex, [Ir(PPh$_3$)$_2$HS$_3$] (**4a**). We were then able to tune the complex by substituting the DMSO ligands with one equivalent of 1,2-bis(diphenylphosphino)ethane.

Scheme 26. Bidentate framework synthesis of [Ir(dppe)HS₃].

(**6a**)   (**7a**)
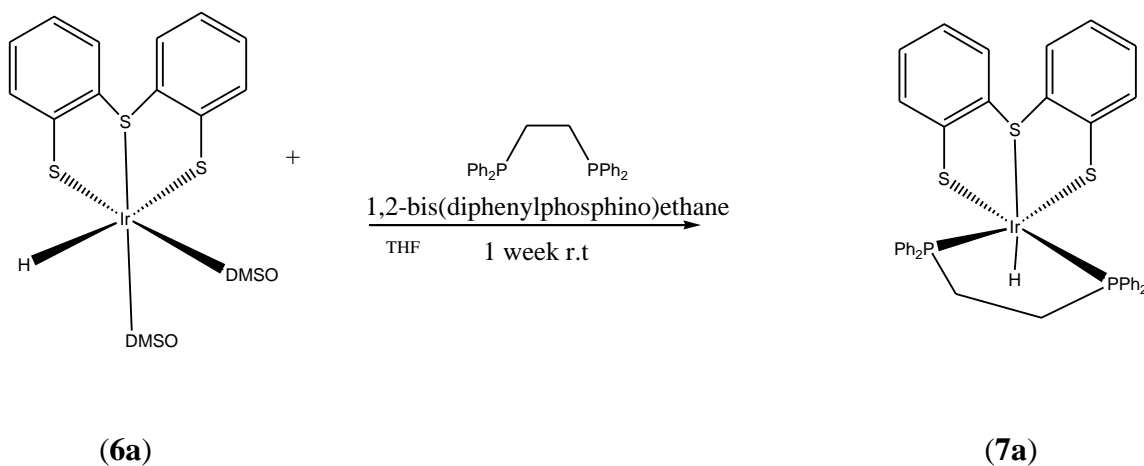
   With this synthesis, the system framework of multidentate ligand systems was

obtained. The complex, [Ir(DMSO)₂HS₃] (**6a**) was stirred in THF at room temperature in

the presence of one equivalent of 1,2-bis(diphenylphosphino)ethane. For the clean

preparation of the complex [Ir(dppe)HS₃] (**7a**), it was necessary to let the mixture stir at

room temperature for one week. We attempted to speed up the reaction via heating, but

isomerization and other issues gave multiple products that were difficult to separate. We

were only able to obtain a system where the hydride was *trans* to the thioether. We

desired the complex to be more reactive with the potential substrate binding site *trans* to

the thiolate. Due to this shortcoming an alternative synthesis was devised.

Scheme 27. Addition of 1,2-bis(diphenylphosphino)ethane(dppe) to [Ir(COD)Cl]₂.

(**8a**)
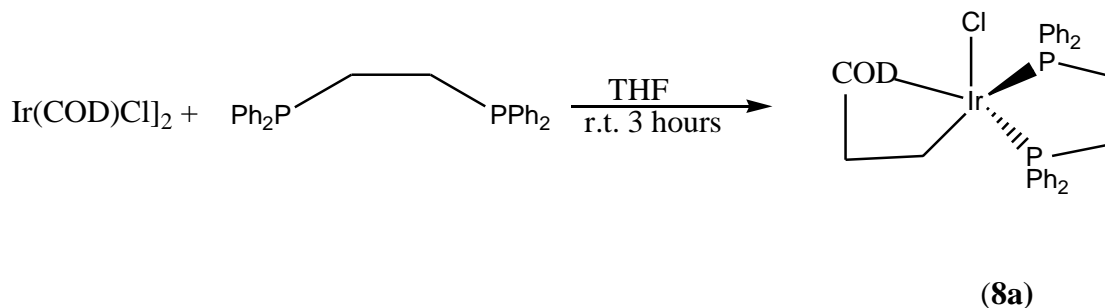
The complex, [Ir(COD)Cl]₂ was reacted with 1,2-bis(diphenylphosphino)ethane in THF for 3 hours to afford the red [Ir(COD)dppe(Cl)]. The complex, [Ir(COD)dppe(Cl)] was then treated with one equivalent of PPh₃ in THF for 24 hours to give the yellow , square planar[Ir(dppe)(PPh₃)Cl].

Scheme 28. The synthesis of [Ir(PPh₃)(dppe)Cl].(8b).

(**8a**)   (**8b**)
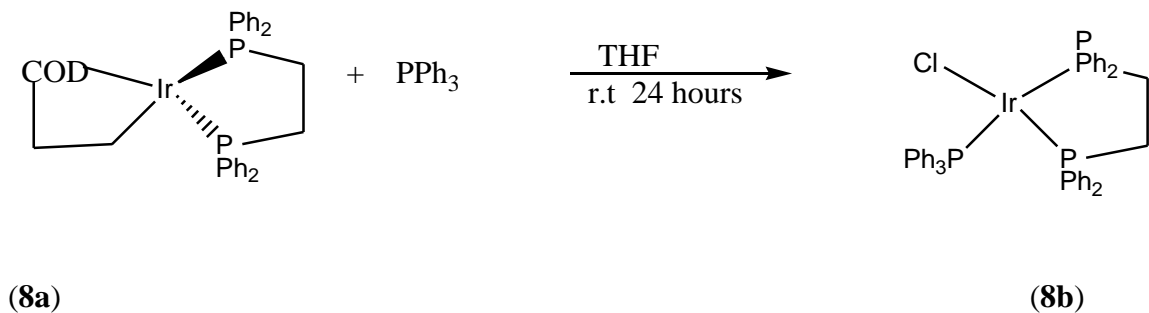
The yellow species, [Ir(dppe)(PPh₃)Cl], was extremely sensitive to oxidative addition of trace amounts of HCl in chloroform, water in any solvent. We were then able

to perform an oxidative addition with the H_2S_3 dithiolate ligand to afford the complex [Ir(dppe)HS$_3$].

Scheme 29. Oxidative addition of [Ir(dppe)(PPh$_3$)Cl] with H$_2$S$_3$.

(**8b**)   (**7a'**)
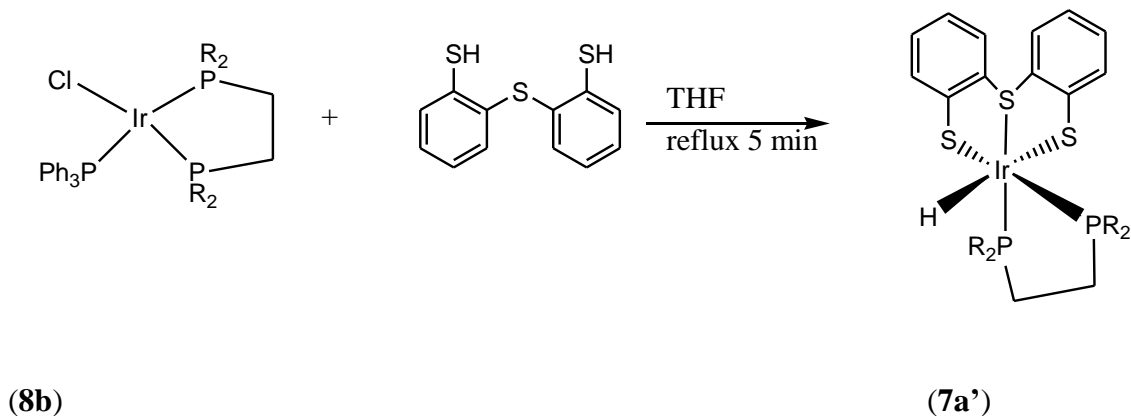
With this new synthetic pathway, we were then able to demonstrate bidentate tunability about the metal center. Interestingly, this synthetic route afforded (**7a'**), where unlike (**7a**), the hydride ligand is *trans* to the thiolate.

Scheme 30. Synthesis of complex [Ir(COD)Cl(1,2-bis(dipyrrolyl)phosphino)ethane]]

(**9a**)
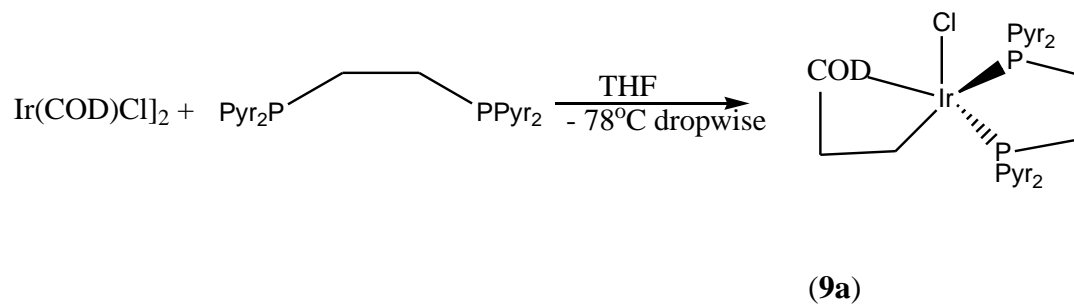
Using the same synthetic methodology, we used a much more electron-withdrawing bidentate phosphine system in the (dipyrolyl) phosphine and reacted it with the (COD) dimer at -78°C dropwise over a period of two hours to afford the bright yellow [Ir(COD)(PyrP)Cl] complex.   This was first attempted to be prepared as the (dppe) analogue was, at room temperature. This synthetic method however, gave a mixture of products.   Kinetic control was required to yield the pure desired species, [Ir(COD)(PyrP)Cl]. The next synthetic step was substitution of the final cyclooctadiene ligand with one PPh$_3$.

Scheme 31. Preparation of [Ir(PPh$_3$)Cl(1,2-bis(dipyrrolyl)phosphino)ethane]

(**6a**)   (**9b**)
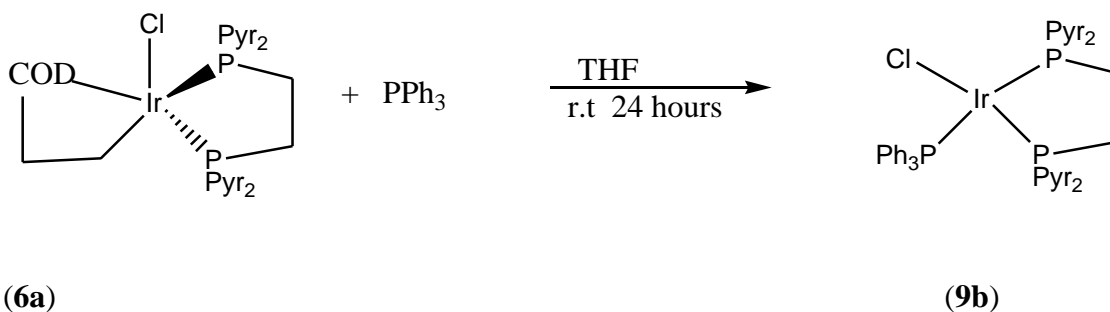
The substitution reaction was done at room temperature in THF for a period of 24 hours. This afforded the square planar, [Ir(PyrP)(PPh$_3$)Cl], which is still undergoing characterization. The reaction was done on such a small scale that determination of the yield is still not known.   The final step in this series of reaction steps would be to oxidatively add the dithiolate H$_2$S$_3$ ligand to give [Ir(PyrP)HS$_3$].

Scheme 32. Preparation of [Ir(PyrP)HS₃].

(**10a**)
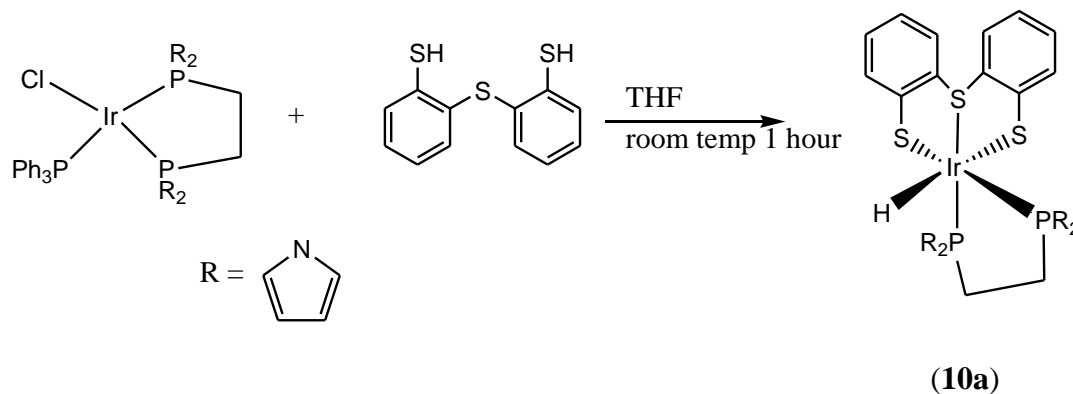
Conclusions

We have synthesized and fully characterized, including by single crystal X-ray crystallography, a new class of iridium(III) dithiolate complexes as well as a number of novel synthetic precursors. Preliminary findings suggest that some of the complexes are active catalysts for nucleophilic additions of weak acids to alkynes. We have discovered numerous synthetic routes to obtain similar system framework and with these new pathways have demonstrated great abilities of tuning the metal center for steric and electronic factors. Further investigation will focus on these aspects of tuning electronic and stereochemical properties of the complex by varying the nature of ancillary phosphine ligands. Also, a study of the types of substrate combinations that lead to selective formation of enol esters will be pursued.

Future Work

In the future, the full characterization of the many new complexes will be necessary. A class of new derivatives of this type is to be synthesized through using this novel synthetic approach. These new systems shall be tested for their electrophilic catalytic properties. A range of substrates shall be tested with these new catalysts. Hopefully, these new catalyts can be found to be of industrial or academic interest.

Experimental Section (part 2)

General Methods. Unless otherwise noted, all reactions and operations were carried out

under nitrogen atmosphere at room temperature using standard Schlenk techniques. Solvents were dried and distilled before use. As far as possible, reactions were monitored by IR or NMR spectroscopy. Spectra were recorded with the following instruments: IR (KBr pellets, solvent bands were compensated. NMR spectra were recorded at room temperature on a Varian 400MHz instrument. The ^{1}H and ^{13}C spectra were referenced to solvent resonance and are reported relative to TMS. ^{31}P shifts were referenced to an internal capillary tube containing 85% H_3PO_4. Elemental analyses (C, H) were sent off to be analyzed by Robinson Microlit corp. Starting materials (H_2S_3) ligand were prepared and described in the literature.[5] Starting material, [Ir(DMSO)$_3$(Cl)$_2$H], was prepared and

characterized in the literature.[7]   Starting material,[Ir(PPh₃)₃H(Cl)₂], was prepared and described in the literature.[6]

4a *Synthesis of[Ir(PPh₃)₂HS₃] (RK# 145)*

To a charged flask of nitrogen (1g, .9813 mmol) of, *[Ir(PPh₃)₃H(Cl)₂]* was placed along with 12 mL of dry THF. The yellow suspension was allowed to stir for a period. To a separate flask (0.106g, 1.962 mmol) of NaOCH₃ was placed along with 12 mL of dry MeOH. To this solution (0.245 g, .9813 mmol) H₂S₃ ligand was added. This bronze solution was stirred for 30 minutes. After this period the salt solution was added to the yellow suspension in THF. Subsequently this red/orange suspension was refluxed for 45 minutes. Afterwards the mixture was cooled and stripped to dryness under reduced pressure. The red/orange solid was washed with THF and then washed again with ethyl ether. The bright yellow product was then dried under vacuum: (yield 57%).

^{1}H NMR (CDCl₃, 400MHz): δ 7.5-6.4 (m, PC₆H₅), (m, (S₃H₈), -13.5 (dd, Ir-H). ^{31}P{^{1}H} NMR (CDCl₃): δ 2.4 (d, Ir-PPh3), -1.2 (d, Ir-PPh3). ^{13}C NMR (CDCl₃, 400MHz): δ 135-127 (m, ,PC₆H₅, S₃H₈)

Anal. Calcd. For C₄₈H₃₉P₂S₃Ir C, 59.67; H, 4.07. Found: C, 58.44; H, 3.78.

4a *Alternative synthesis of [Ir(PPh₃)₂HS₃] (RK# 139)*

To a flask charged with nitrogen (0.14 g, .233 mmol) of [Ir(DMSO)₂HS₃] was added. To that 0.12 g, of PPh₃ was placed. The system then had added to it 10 mL of THF and 6 mL of MeOH and the resulting solution was refluxed for 2 hours. It was then stripped to dryness by reduced pressure and triturated several times with THF to remove the free

DMSO that remained. The orange/yellow solid was then dried under reduced pressure and data was observed (yield 49%).

*Isomerization reaction of (**4a**) to (**4b**) (RK# 298-300)*

To a sealed screw cap NMR tube was placed an 800 µl of a solution of 0.04g of (**4a**) in 4 mL of C_6D_6. The tube was heated to 75 ^{o}C and allowed to react for a 24 hour period. The isomerization of complex (**4a**) to (**4b**) was monitored via the hydride region on a 400MHz-NMR instrument. The progress of the reaction was monitored by the integration of this region. The above stated reaction at 75 ^{o}C was also performed with one stoichiometric equivalent of PPh$_3$ added to the reaction vessel (RK#292).

(**4a**) ^{1}*H-NMR (C$_6$D$_6$,ppm): δ -13.5 (dd, Ir-H)*

(**4b**) ^{1}*H-NMR (C$_6$D$_6$,ppm): δ -12.5 (t, Ir-H)*

5a *Synthesis of [Ir(PPh$_3$)$_2$BrS$_3$] (RK# 282)*

To a flask charged with inert atmosphere, (0.25 g, .23 mmol) of [Ir(PPh$_3$)$_2$HS$_3$] was inserted. To that, 2 equivalents (0.12 g) of PPh$_3$ was added along with 1equivalent (0.057 g) of Et$_2$NCH$_2$Br.Then 30 mL of CH$_2$Cl$_2$ was placed. This yellow mixture was heated at reflux for one hour. It was then stripped to dryness and one equivalent of Et$_2$NCH$_2$Br (0.003 g) relative to the remaining starting material was placed along with 30 mL of CH$_2$Cl$_2$. Subsequently, the mixture was refluxed for another hour. It was then stripped to dryness and dissolved into 10 mL of C$_6$H$_6$. This solution was injected into a dry silica

column wetted with hexanes. It was then flash columned through using a gradient ratio of 4:2 hexanes to ethyl acetate (10 mL), then 7:3 mixture of hexanes to ethyl acetate (10 mL), then a 3:2 mixture of hexanes to ethyl acetate (10ml x 2), and finally a 1:1 ratio of hexanes to ethyl acetate (10ml x 3), or until all of the yellow material had been collected. This solution was then stripped to dryness and weighed: (yield 11.5%).

^{1}H NMR (CDCl$_3$, 400MHz): δ 8.2-6.4 (m, PC$_6$H$_5$), (7.5-6.4 (m, (S$_3$H$_8$). ^{31}P{^{1}H} NMR (CDCl$_3$): δ -18.5 (d, Ir-PPh$_3$), -29.6 (d, Ir-PPh$_3$). ^{13}C NMR (CDCl$_3$, 400MHz): δ 136-126 (m, PC$_6$H$_5$, S$_3$H$_8$)

Anal. Calcd. For C$_{48}$H$_{38}$BrIrP$_2$S$_3$. C, 55.16; H, 3.66. Found: C, 56.61; H, 3.76.

6a *Synthesis of [Ir(DMSO)$_2$HS$_3$] (RK# 155)*

To a charged flask of nitrogen (0.05 g, .100 mmol) of *[Ir(DMSO)$_3$(Cl)$_2$H]* was placed along with 14 mL of dry THF. To this, a solution of (0.108 g, .200 mmol) of NaOCH$_3$ and (0.025 g, .100 mmol) of H$_2$S$_3$ ligand in 10 mL MeOH was added. Upon this addition, the mixture turned an immediate orange. This orange solution was allowed to stir at room temperature for one hour. It was then stripped to dryness and heated in deep vacuum at 55 ^{o}C for 24 hours to remove the remaining free solvents. The complex was then dried under vacuum and data was observed (yield 77%).

^{1}H NMR (CDCl$_3$, 400MHz): δ 7.5-6.4 (m, (S$_3$H$_8$), 3.5 (s, SO(CH$_3$)$_2$), 3.1 (s, SO(CH$_3$)$_2$) -13.3 (s, Ir-H).

 Anal. Calcd. For C$_{16}$H$_{21}$IrO$_2$S$_5$ C, 32.14; H, 3.54. Found: C, 33.02; H, 3.27.

7a *Synthesis of [Ir(Dppe)HS₃] (RK# 190)*

To a flask charged with nitrogen gas (0.507 g, 1.019 mmol) of *[Ir(DMSO)₂HS₃]* was placed.

To that 0.333 g of Dppe was added. The vessel then had added to it, 28 mL of dry THF. This orange solution was allowed to stir under nitrogen at room temperature for 7 days. After which it was stripped to dryness with reduced pressure and was weighed (68 % yield).

^{1}H NMR (CDCl₃, 400MHz): δ 7.8-6.7 (m, PC_6H_5), 2.7 (br s, 2H), (PCH_2CH_2P), *-12.5 (t Ir-H)* ^{31}P{^{1}H} NMR (CDCl₃): δ 31.2 (s, Ir-PPh₂). ^{13}C NMR (CDCl₃, 400MHz): δ 135-127 (m, ,PC_6H_5, S_3H_8)

7b *Synthesis of [Ir(Dppe)HS₃] (RK#315)*

To a vial charged with nitrogen gas, 0.04 g of (**8b**) was placed. To that was added 10 mL of CH_2Cl_2 and the orange solution was allowed to stir for 30 minutes. After that period, one equivalent, 0.009 g of H_2S_3 ligand in 2 ml of CH_2Cl_2 was added to the vial. Upon addition, the orange solution changed to a light yellow color. This light yellow solution was allowed to stir at room temperature overnight. After this time, the system was dried and weighed (56% yield).

^{1}H NMR (CDCl$_3$, 400MHz): δ 7.8-6.7 (m, PC$_6$H$_5$), 2.7 (br s, 2H), (PCH$_2$CH$_2$P), *-13.7 (dd Ir-H)* ^{31}P{^{1}H} NMR (CDCl$_3$): δ 33.1 (d, Ir-PPh$_2$), 32.1 (d Ir-PPh$_2$). ^{13}C NMR (CDCl$_3$, 400MHz): δ 130-126 (m, ,PC$_6$H$_5$, S$_3$H$_8$)

8a *Synthesis of [Ir(dppe)(COD)Cl] (RK#306)*

To a flask charged with nitrogen gas, 2.06 g (3.066 mmol) of the complex, [Ir(COD)Cl]$_2$ was reacted with 2 equivalents (2.44 g) of 1,2-bis(diphenylphosphino)ethane, (dppe) in 44 mL of CH$_2$Cl$_2$ for 3 hours to afford the red [Ir(COD)dppe(Cl)]. This red material was then stripped to dryness under vacuum pressure and weighed (89% yield).

^{31}P-NMR (C$_6$D$_6$,ppm): δ 64 (s Ir-P dppe)

8b *Synthesis of [Ir(dppe)(PPh$_3$)Cl] (RK# 307)*

To a flask charged with nitrogen gas, 1 g of the complex [Ir(COD)dppe(Cl)] was placed. To that one equivalent of PPh$_3$ was added. The flask was then charged with 30 mL CH$_2$Cl$_2$. This mixture was allowed to react for 3 hours at room temperature. The yellow solution was then stripped to dryness and weighed. (82 % yield)

9a *Synthesis of [Ir(COD)(PyrP)Cl] (RK# 351)*

To a flask charged with nitrogen gas, 0.2 g (0.297 mmol) of [Ir(COD)Cl]$_2$ was placed. To that, 30 mL of THF was added. The red solution was then cooled to -78 ^{o}C and had added to it dropwise over a period of two hours, a solution of 2 equivalents (0.208 g) of dipyrolyl ligand in 80 mL of THF. After one hour of the addition, the red solution

became light yellow. After the addition was complete, the solution was stripped to dryness and weighed (78% yield).

^{31}P-NMR (C_6D_6 ,ppm): δ 101 (s Ir-P bis-Pyr)

9b *Synthesis of [Ir(PyrP)(PPh_3)Cl] (RK# 353)*

To a flask charged with nitrogen gas, 0.025 g (0.036 mmol) of [Ir(COD)(PyrP)Cl] was placed and 10 mL of THF was added. The yellow solution then had added to it one equivalent of PPh_3. The yellow solution was stirred overnight and after that period was stripped to dryness. Characterization of (**9b**) is currently ongoing. (45 % yield)

10a *Synthesis of [Ir(PyrP)HS_3] (RK# 359)*

To a flask of nitrogen gas, 0.303 g of (**9b**) was placed. To that, one equivalent of H_2S_3 ligand was added. This mixture then had added to it, 30 mL of THF. The resulting brown / yellow solution was stirred at room temperature for one hour. After this period, the solvent was evaporated and the brown crystalline material was dried and weighed (59% Yield).

^{1}H NMR (CDCl_3, 400MHz):   δ 7.6-5.6 (m, PNC_4H_4), (7.5-6.4 (m, (S_3H_8), 2.5 (br s, (PCH_2CH_2P), -12.5 (dd, Ir-H).   ^{31}P{^{1}H} NMR (CDCl_3):   δ 94 (d, $Ir-Pyr_2$), 92 (d, Ir-$Ppyr_2$).

References

Part 1

(1), Kamm, B.; Kamm, M.; Eds. *Biorefineries-Industrial Processes and Products*; Wiley-VCH: Weinheim, Germany, 2006.

(2), Leshkov, J.; Chheda, N.; Dumesic, A. *Science*. **2006**, 312, 1933–1937.

(3), Moreau, C.; Finiels, A.;Vanoye, L. *J.Mol. Catal. A: Chem*. **2006**, 253, 165-169.

(4), Watanabe, M.; *Green Chem*.,**2008**, 10, 799-805.

(5), Bianchini, C.; Peruzzini, M.; Zanobini, F. *J. Organomet. Chem.* **1988,**354.

(6), Crabtree, R. H. *Acc. Chem. Res*. **1990,** *23,* 95-101.

(7), Kubas, G. J.; Unkefer, C. J.; Swanson, B. 1.; Fukushima, E. J. *Am. Chem. Soc.* **1986**. *108.* 7000-7009.

(8), Sidle, A. R.; Newmark, R. A.; Korba, *G.* A.; Pignolet, L. H.; Boyle, P. D. *Inorg. Chem.* **1988**, *27,* 1593-1598.

(9), Bautista, M.T.; Morris, R.H. *J. Am. Chem. Soc.* **1991**, 113,4876-4887.

(10), Morris R.H.. *Inorg. Chem*. **1994**, 33, 6278-6288.

(11) Curtis, C.J.; Dubois, D.L. *J. Am. Chem. Soc*. **2002,** 124, 1918-1924.

(12), Drent, E.; Jager, W.W.; (Shell Oil Company), U.S. Patent 6,642,898, issued June 27, 2000.

(13), Che, T.M.; (Celanese Corp), U.S. Patent 4,642,394, issued Feb, 10, 1987.

(14), *Schlaf*, M. *Dalton Trans*. **2006**, 39, 4645-4653

(15), Cheng, T.; Bullock R. M. *Organometallics*. **2002**, 21, 2325–2331.

(16), Takei. *J. Organomet Chem.* 679 ,**2003,** 32-42.

(17), Dubois, D.L.; Curtis C.J. *J. Am. Chem. Soc.* **2002**, 124, 1918-1924.

(18), Hamilton, D.G.; Crabtree, R. H. *J. Am. Chem. Soc.* **1988**, *110,*4126-4133

(19), Hayashida, T. *J. Organomet Chem.* 692 (2007) 382–394

Part 2

(20), Sen, A.; Lai, T.W. *J.Am. Chem. Soc.* **1981**, 103, 4627-4629.

(21), Sen, A.; Lai, T.W.; Thomas, R.R. *J. Organomet. Chem.* **1988**, 358, 567-588.

(22), Arndtsen, B.A.; Bergman, R.G. *Science* **1995**, 270, 1970-1973

(23), Eisenberg, R, ; Albietz, P.J. *Inorg. Chem.* **2002**, 41, 2095-2108

(24), Heck, R. F.; Academic: New York, 1985.

(25), Poli, G.; Giambastiani, G.; Heumann, A. *Tetrahedron*, **2000**, *56*, 5959.

(26), Albietz, P.J.; Cleary, B.P.; Paw, W.; Eisenberg, R. *Inorg. Chem.* **2002**, *41*, 2095.

(27), Albietz, P.J.; Cleary, B.P.; Paw, W.; Eisenberg, R. *J. Am. Chem. Soc.* **2001**, *123*, 12091.

(28), Cleary, B. P.; Eisenberg, R. *Inorg. Chim. Acta* **1995**, *240*, 135.

(29), Crabtree, R.H.; Faller, J.W.; Mellea, M.F.; Quirk, J.M. *Organometallics* **1982**, *1*, 1361.

(30), Deeming, A. J.; Doherty, S.; Marshall, J. E.; Powell, J. L., Senior, A. M. *J. Chem. Soc. Dalton Trans.* **1993**, 1093.

(31), Shearer, J.; Jackson, H. L.; Schweitzer, D.; Rittenberg, D. K.; Leavy, T. M.; Kaminsky, W.; Scarrow, R. C.; Kovacs, J. A. *J. Am. Chem. Soc.* **2002**, *124*, 11428.

(32), Mascharak, P.K. *Coord. Chem. Revs.* **2002***, 225*, 201.

(33), Brennan, B. A.; Cummings, J. G.; Chase, D. B.; Turner, I. M., Jr.;
Nelson, M. J. *Biochemistry* **1996**, *35*, 10068-10077.

(34),   Shearer, J.; Kung, I.Y.; Lovell, S.; Kaminsky, W.; Kovacs, J.A. *J. Am. Chem. Soc.* **2001**, *123*, 463.

(35), Schweitzer, D.; Shearer, J.; Rittenberg, D.K.; Shoner, S.C.; Ellison, J.J.; Loloee, R.; Lovell, S.; Barnhart, D.; Kovacs, J.A. *Inorg. Chem.* 2002, *41*, 3128.

(36), Enders,D.; Reinhold, U. *Tetrahedron: Asymmetry* **1997**, *8*, 1895-1946.

(37), Kobyashi, M.; Nagasawa, T.; Yamada, H. *Tibtech* **1992**, *10*, 402.

(38), Zanella, A. W.; Ford, P. C. *Inorg. Chem*. **1975**, *14*, 42.

(39), Shearer, J.; Jackson, H. L.; Schweitzer, D.; Rittenberg, D. K.; Leavy, T. M.; Kaminsky, W.; Scarrow, R.C.; Kovacs, J.A. *J. Am. Chem. Soc.* **2002**, *124*, 11428.

(40), Rauchfuss, T.B.; Wilson, S.R. *Inorg. Chem*. **2002**, *41*, 6193.

(41), Douglas, W.; Nadasdi, T. *Coord. Chem. Rev*. **1996**, *147*, 147.

(42), Raper, E.S. *Coord. Chem. Rev*. **1997**, *165*, 475.

(43*),* Michelin, R.A.; Mozzon, M.; Bertani, R. *Coord. Chem. Rev*. **1996**, *147*, 299.

(44), Nakagawa, H.; Okimoto, Y.; Sakaguchi, S.; Ishii, Y. *Tett. Lett*. **2003**, *44*, 103.

(45), Sellmann, D. *Eur J. Inorg. Chem.* **1999**, 1715-1725

(46), James, B.; Morris, R.H.; Kvintovics, P. *CAN . J. Chem*. **1986**, *64*, 897-903

APPENDIX

Bond lengths and angles for the X-ray structure of cis-[Ru(dipyrrolylP)$_2$Cl$_2$] (2a).

Ru(1)-P(1)	Ru(1)-P(3)
2.3013(6)	2.3019(6)
Ru(1)-P(2)	Ru(1)-P(4)
2.3334(6)	2.3597(6)
Ru(1)-Cl(1)	Ru(1)-Cl(2)
2.4412(5)	2.4513(6)
P(1)-N(1)	P(1)-N(2)
1.7122(19)	1.739(2)
P(1)-C(1)	P(2)-N(4)
1.839(2)	1.701(2)
P(2)-N(3)	P(2)-C(2)
1.716(2)	1.820(2)
P(3)-N(5)	P(3)-N(6)
1.715(2)	1.722(2)
P(3)-C(3)	P(4)-N(7)
1.839(2)	1.709(2)
P(4)-N(8)	P(4)-C(4)
1.711(2)	1.822(2)
N(1)-C(5)	N(1)-C(8)
1.395(3)	1.403(3)
N(2)-C(9)	N(2)-C(12)
1.393(3)	1.395(3)
N(3)-C(16)	N(3)-C(13)
1.392(3)	1.392(3)
N(4)-C(17)	N(4)-C(20)
1.395(3)	1.398(3)
N(5)-C(24)	N(5)-C(21)
1.394(3)	1.395(3)
N(6)-C(28)	N(6)-C(25)
1.390(3)	1.398(3)
N(7)-C(29)	N(7)-C(32)
1.393(3)	1.395(3)
N(8)-C(33)	N(8)-C(36)
1.398(3)	1.398(3)
C(1)-C(2)	C(1)-H(1A)
1.527(3)	0.9900
C(1)-H(1B)	C(2)-H(2A)
0.9900	0.9900
C(2)-H(2B)	C(3)-C(4)
0.9900	1.534(3)
C(3)-H(3A)	C(3)-H(3B)
0.9900	0.9900
C(4)-H(4A)	C(4)-H(4B)
0.9900	0.9900
C(5)-C(6)	C(5)-H(5)
1.362(3)	0.9500
C(6)-C(7)	C(6)-H(6)

1.423(3)		0.9500	
C(7)-C(8)	1.359(3)	C(7)-H(7)	0.9500
C(8)-H(8)	0.9500	C(9)-C(10)	1.365(3)
C(9)-H(9)	0.9500	C(10)-C(11)	1.416(4)
C(10)-H(10)	0.9500	C(11)-C(12)	1.363(3)
C(11)-H(11)	0.9500	C(12)-H(12A)	0.9900
C(12)-H(12B)	0.9900	C(13)-C(14)	1.359(3)
C(13)-H(13)	0.9500	C(14)-C(15)	1.417(4)
C(14)-H(14)	0.9500	C(15)-C(16)	1.359(4)
C(15)-H(15)	0.9500	C(16)-H(16)	0.9500
C(17)-C(18)	1.362(4)	C(17)-H(17)	0.9500
C(18)-C(19)	1.423(4)	C(18)-H(18)	0.9500
C(19)-C(20)	1.363(3)	C(19)-H(19)	0.9500
C(20)-H(20)	0.9500	C(21)-C(22)	1.361(3)
C(21)-H(21)	0.9500	C(22)-C(23)	1.421(4)
C(22)-H(22)	0.9500	C(23)-C(24)	1.358(3)
C(23)-H(23)	0.9500	C(24)-H(24)	0.9500
C(25)-C(26)	1.362(3)	C(25)-H(25)	0.9500
C(26)-C(27)	1.422(4)	C(26)-H(26)	0.9500
C(27)-C(28)	1.358(4)	C(27)-H(27)	0.9500
C(28)-H(28)	0.9500	C(29)-C(30)	1.360(4)
C(29)-H(29)	0.9500	C(30)-C(31)	1.422(4)
C(30)-H(30)	0.9500	C(31)-C(32)	1.355(4)
C(31)-H(31)	0.9500	C(32)-H(32)	0.9500
C(33)-C(34)	1.364(4)	C(33)-H(33)	0.9500
C(34)-C(35)	1.421(4)	C(34)-H(34)	0.9500
C(35)-C(36)	1.358(3)	C(35)-H(35)	0.9500
C(36)-H(36)		C(1S)-Cl(2S)	

0.9500		1.762(4)
C(1S)-Cl(1S)	C(1S)-Cl(3S)	
1.771(4)	1.772(5)	
C(1S)-H(1S)	C(1S')-Cl(1')	
1.0000	1.723(19)	
C(1S')-Cl(2')	C(1S')-Cl(3')	
1.727(19)	1.76(2)	
C(1S')-H(1S')	C(2S)-Cl(4S)	
1.0000	1.728(18)	
C(2S)-Cl(5S)	C(2S)-Cl(6S)	
1.738(14)	1.752(18)	
C(2S)-H(2S)	C(2S')-Cl(8S)	
1.0000	1.744(19)	
C(2S')-Cl(7S)	C(2S')-Cl(9S)	
1.75(2)	1.768(18)	
C(2S')-H(2S')	C(3S)-Cl(10)	
1.0000	1.451(5)	
C(3S)-Cl(11)	C(3S)-Cl(11)#1	
1.740(6)	1.879(6)	
C(3S)-H(3S)	Cl(11)-C(3S)#1	
1.0000	1.879(6)	
	P(1)-Ru(1)-P(3)	
	89.49(2)	
P(1)-Ru(1)-P(2)	P(3)-Ru(1)-P(2)	
83.62(2)	102.59(2)	
P(1)-Ru(1)-P(4)	P(3)-Ru(1)-P(4)	
102.73(2)	82.63(2)	
P(2)-Ru(1)-P(4)	P(1)-Ru(1)-Cl(1)	
171.92(2)	92.15(2)	
P(3)-Ru(1)-Cl(1)	P(2)-Ru(1)-Cl(1)	
170.85(2)	86.540(19)	
P(4)-Ru(1)-Cl(1)	P(1)-Ru(1)-Cl(2)	
88.22(2)	165.71(2)	
P(3)-Ru(1)-Cl(2)	P(2)-Ru(1)-Cl(2)	
97.25(2)	82.624(19)	
P(4)-Ru(1)-Cl(2)	Cl(1)-Ru(1)-Cl(2)	
90.66(2)	83.194(19)	
N(1)-P(1)-N(2)	N(1)-P(1)-C(1)	
97.86(9)	100.67(10)	
N(2)-P(1)-C(1)	N(1)-P(1)-Ru(1)	
100.55(10)	123.75(7)	
N(2)-P(1)-Ru(1)	C(1)-P(1)-Ru(1)	
122.05(7)	107.93(7)	
N(4)-P(2)-N(3)	N(4)-P(2)-C(2)	
99.26(10)	104.77(10)	
N(3)-P(2)-C(2)	N(4)-P(2)-Ru(1)	
102.26(10)	118.85(7)	
N(3)-P(2)-Ru(1)	C(2)-P(2)-Ru(1)	
120.65(7)	108.86(8)	
N(5)-P(3)-N(6)	N(5)-P(3)-C(3)	
98.24(9)	101.82(10)	
N(6)-P(3)-C(3)	N(5)-P(3)-Ru(1)	
99.77(10)	122.15(7)	
N(6)-P(3)-Ru(1)	C(3)-P(3)-Ru(1)	

	122.28(7)		108.83(8)
N(7)-P(4)-N(8)	103.31(10)	N(7)-P(4)-C(4)	102.67(10)
N(8)-P(4)-C(4)	102.74(10)	N(7)-P(4)-Ru(1)	119.51(7)
N(8)-P(4)-Ru(1)	117.72(7)	C(4)-P(4)-Ru(1)	108.70(8)
C(5)-N(1)-C(8)	107.28(18)	C(5)-N(1)-P(1)	124.41(16)
C(8)-N(1)-P(1)	126.76(16)	C(9)-N(2)-C(12)	107.23(19)
C(9)-N(2)-P(1)	125.83(16)	C(12)-N(2)-P(1)	126.58(17)
C(16)-N(3)-C(13)	107.4(2)	C(16)-N(3)-P(2)	125.06(17)
C(13)-N(3)-P(2)	127.35(16)	C(17)-N(4)-C(20)	107.97(19)
C(17)-N(4)-P(2)	127.79(17)	C(20)-N(4)-P(2)	123.81(16)
C(24)-N(5)-C(21)	107.37(19)	C(24)-N(5)-P(3)	126.59(17)
C(21)-N(5)-P(3)	124.34(17)	C(28)-N(6)-C(25)	107.17(19)
C(28)-N(6)-P(3)	125.23(16)	C(25)-N(6)-P(3)	124.57(16)
C(29)-N(7)-C(32)	107.73(19)	C(29)-N(7)-P(4)	128.19(17)
C(32)-N(7)-P(4)	123.79(17)	C(33)-N(8)-C(36)	107.77(19)
C(33)-N(8)-P(4)	130.23(17)	C(36)-N(8)-P(4)	121.91(16)
C(2)-C(1)-P(1)	109.34(15)	C(2)-C(1)-H(1A)	109.8
P(1)-C(1)-H(1A)	109.8	C(2)-C(1)-H(1B)	109.8
P(1)-C(1)-H(1B)	109.8	H(1A)-C(1)-H(1B)	108.3
C(1)-C(2)-P(2)	107.99(15)	C(1)-C(2)-H(2A)	110.1
P(2)-C(2)-H(2A)	110.1	C(1)-C(2)-H(2B)	110.1
P(2)-C(2)-H(2B)	110.1	H(2A)-C(2)-H(2B)	108.4
C(4)-C(3)-P(3)	107.63(16)	C(4)-C(3)-H(3A)	110.2
P(3)-C(3)-H(3A)	110.2	C(4)-C(3)-H(3B)	110.2
P(3)-C(3)-H(3B)	110.2	H(3A)-C(3)-H(3B)	108.5
C(3)-C(4)-P(4)	107.99(15)	C(3)-C(4)-H(4A)	110.1
P(4)-C(4)-H(4A)	110.1	C(3)-C(4)-H(4B)	110.1
P(4)-C(4)-H(4B)		H(4A)-C(4)-H(4B)	

110.1		108.4	
	C(6)-C(5)-N(1)		C(6)-C(5)-H(5)
108.7(2)		125.6	
	N(1)-C(5)-H(5)		C(5)-C(6)-C(7)
125.6		107.6(2)	
	C(5)-C(6)-H(6)		C(7)-C(6)-H(6)
126.2		126.2	
	C(8)-C(7)-C(6)		C(8)-C(7)-H(7)
107.9(2)		126.1	
	C(6)-C(7)-H(7)		C(7)-C(8)-N(1)
126.1		108.5(2)	
	C(7)-C(8)-H(8)		N(1)-C(8)-H(8)
125.8		125.8	
	C(10)-C(9)-N(2)		C(10)-C(9)-H(9)
108.6(2)		125.7	
	N(2)-C(9)-H(9)		C(9)-C(10)-C(11)
125.7		107.8(2)	
	C(9)-C(10)-H(10)		C(11)-C(10)-H(10)
126.1		126.1	
	C(12)-C(11)-C(10)		C(12)-C(11)-H(11)
107.6(2)		126.2	
	C(10)-C(11)-H(11)		C(11)-C(12)-N(2)
126.2		108.8(2)	
	C(11)-C(12)-H(12A)		N(2)-C(12)-H(12A)
109.9		109.9	
	C(11)-C(12)-H(12B)		N(2)-C(12)-H(12B)
109.9		109.9	
	H(12A)-C(12)-H(12B)		C(14)-C(13)-N(3)
108.3		108.6(2)	
	C(14)-C(13)-H(13)		N(3)-C(13)-H(13)
125.7		125.7	
	C(13)-C(14)-C(15)		C(13)-C(14)-H(14)
107.7(2)		126.2	
	C(15)-C(14)-H(14)		C(16)-C(15)-C(14)
126.2		107.7(2)	
	C(16)-C(15)-H(15)		C(14)-C(15)-H(15)
126.1		126.1	
	C(15)-C(16)-N(3)		C(15)-C(16)-H(16)
108.6(2)		125.7	
	N(3)-C(16)-H(16)		C(18)-C(17)-N(4)
125.7		108.1(2)	
	C(18)-C(17)-H(17)		N(4)-C(17)-H(17)
126.0		126.0	
	C(17)-C(18)-C(19)		C(17)-C(18)-H(18)
108.1(2)		125.9	
	C(19)-C(18)-H(18)		C(20)-C(19)-C(18)
125.9		107.7(2)	
	C(20)-C(19)-H(19)		C(18)-C(19)-H(19)
126.2		126.2	
	C(19)-C(20)-N(4)		C(19)-C(20)-H(20)
108.2(2)		125.9	
	N(4)-C(20)-H(20)		C(22)-C(21)-N(5)
125.9		108.4(2)	
	C(22)-C(21)-H(21)		N(5)-C(21)-H(21)

78

Angle	Value	Angle	Value
	125.8		125.8
C(21)-C(22)-C(23)	107.8(2)	C(21)-C(22)-H(22)	126.1
C(23)-C(22)-H(22)	126.1	C(24)-C(23)-C(22)	107.6(2)
C(24)-C(23)-H(23)	126.2	C(22)-C(23)-H(23)	126.2
C(23)-C(24)-N(5)	108.8(2)	C(23)-C(24)-H(24)	125.6
N(5)-C(24)-H(24)	125.6	C(26)-C(25)-N(6)	108.5(2)
C(26)-C(25)-H(25)	125.7	N(6)-C(25)-H(25)	125.7
C(25)-C(26)-C(27)	107.7(2)	C(25)-C(26)-H(26)	126.2
C(27)-C(26)-H(26)	126.2	C(28)-C(27)-C(26)	107.5(2)
C(28)-C(27)-H(27)	126.3	C(26)-C(27)-H(27)	126.3
C(27)-C(28)-N(6)	109.1(2)	C(27)-C(28)-H(28)	125.4
N(6)-C(28)-H(28)	125.4	C(30)-C(29)-N(7)	108.2(2)
C(30)-C(29)-H(29)	125.9	N(7)-C(29)-H(29)	125.9
C(29)-C(30)-C(31)	107.8(2)	C(29)-C(30)-H(30)	126.1
C(31)-C(30)-H(30)	126.1	C(32)-C(31)-C(30)	107.8(2)
C(32)-C(31)-H(31)	126.1	C(30)-C(31)-H(31)	126.1
C(31)-C(32)-N(7)	108.4(2)	C(31)-C(32)-H(32)	125.8
N(7)-C(32)-H(32)	125.8	C(34)-C(33)-N(8)	108.0(2)
C(34)-C(33)-H(33)	126.0	N(8)-C(33)-H(33)	126.0
C(33)-C(34)-C(35)	107.9(2)	C(33)-C(34)-H(34)	126.0
C(35)-C(34)-H(34)	126.0	C(36)-C(35)-C(34)	107.9(2)
C(36)-C(35)-H(35)	126.1	C(34)-C(35)-H(35)	126.1
C(35)-C(36)-N(8)	108.4(2)	C(35)-C(36)-H(36)	125.8
N(8)-C(36)-H(36)	125.8	Cl(2S)-C(1S)-Cl(1S)	108.1(3)
Cl(2S)-C(1S)-Cl(3S)	110.1(2)	Cl(1S)-C(1S)-Cl(3S)	110.9(2)
Cl(2S)-C(1S)-H(1S)	109.2	Cl(1S)-C(1S)-H(1S)	109.2
Cl(3S)-C(1S)-H(1S)	109.2	Cl(1')-C(1S')-Cl(2')	126.6(19)
Cl(1')-C(1S')-Cl(3')		Cl(2')-C(1S')-Cl(3')	

94.9(11)	110.7(14)
Cl(1')-C(1S')-H(1S') 107.7	Cl(2')-C(1S')-H(1S') 107.7
Cl(3')-C(1S')-H(1S') 107.7	Cl(4S)-C(2S)-Cl(5S) 112.0(10)
Cl(4S)-C(2S)-Cl(6S) 108.9(9)	Cl(5S)-C(2S)-Cl(6S) 109.1(10)
Cl(4S)-C(2S)-H(2S) 108.9	Cl(5S)-C(2S)-H(2S) 108.9
Cl(6S)-C(2S)-H(2S) 108.9	Cl(8S)-C(2S')-Cl(7S) 111.6(13)
Cl(8S)-C(2S')-Cl(9S) 110.7(8)	Cl(7S)-C(2S')-Cl(9S) 109.3(11)
Cl(8S)-C(2S')-H(2S') 108.4	Cl(7S)-C(2S')-H(2S') 108.4
Cl(9S)-C(2S')-H(2S') 108.4	Cl(10)-C(3S)-Cl(11) 129.2(4)
Cl(10)-C(3S)-Cl(11)#1 115.1(4)	Cl(11)-C(3S)-Cl(11)#1 106.3(3)
Cl(10)-C(3S)-H(3S) 100.1	Cl(11)-C(3S)-H(3S) 100.1
Cl(11)#1-C(3S)-H(3S) 100.1	C(3S)-Cl(11)-C(3S)#1 31.8(3)

Bond lengths and angles for the X-ray structure of trans-[Ru(dipyrrolylP)₂Cl₂] (2a').

Ru(1)-P(2)#1 2.3123(4)	Ru(1)-P(2) 2.3123(4)
Ru(1)-P(1)#1 2.3365(4)	Ru(1)-P(1) 2.3365(4)
Ru(1)-Cl(1) 2.4199(4)	Ru(1)-Cl(1)#1 2.4199(4)
P(1)-N(1) 1.7150(14)	P(1)-N(2) 1.7218(14)
P(1)-C(9) 1.8555(17)	P(2)-N(4) 1.7036(14)
P(2)-N(3)	P(2)-C(10)

1.7185(14)	1.8289(17)
N(1)-C(4) 1.404(2)	N(1)-C(1) 1.404(2)
C(1)-C(2) 1.360(2)	C(1)-H(1) 0.9500
C(2)-C(3) 1.426(2)	C(2)-H(2) 0.9500
C(3)-C(4) 1.358(2)	C(3)-H(3) 0.9500
C(4)-H(4) 0.9500	N(2)-C(8) 1.395(2)
N(2)-C(5) 1.399(2)	C(5)-C(6) 1.362(2)
C(5)-H(5) 0.9500	C(6)-C(7) 1.423(3)
C(6)-H(6) 0.9500	C(7)-C(8) 1.365(2)
C(7)-H(7) 0.9500	C(8)-H(8) 0.9500
C(9)-C(10) 1.532(2)	C(9)-H(9A) 0.9900
C(9)-H(9B) 0.9900	C(10)-H(10A) 0.9900
C(10)-H(10B) 0.9900	N(3)-C(11) 1.391(2)
N(3)-C(14) 1.392(2)	C(11)-C(12) 1.363(2)
C(11)-H(11) 0.9500	C(12)-C(13) 1.421(3)
C(12)-H(12) 0.9500	C(13)-C(14) 1.363(2)
C(13)-H(13) 0.9500	C(14)-H(14) 0.9500
N(4)-C(18) 1.394(2)	N(4)-C(15) 1.394(2)
C(15)-C(16) 1.361(2)	C(15)-H(15) 0.9500
C(16)-C(17) 1.421(2)	C(16)-H(16) 0.9500
C(17)-C(18) 1.359(2)	C(17)-H(17) 0.9500
C(18)-H(18) 0.9500	
P(2)#1-Ru(1)-P(2) 180.00(2)	P(2)#1-Ru(1)-P(1)#1 81.875(14)
P(2)-Ru(1)-P(1)#1 98.125(14)	P(2)#1-Ru(1)-P(1) 98.126(14)
P(2)-Ru(1)-P(1) 81.875(14)	P(1)#1-Ru(1)-P(1) 180.0
P(2)#1-Ru(1)-Cl(1) 83.999(14)	P(2)-Ru(1)-Cl(1) 96.001(14)
P(1)#1-Ru(1)-Cl(1) 80.630(13)	P(1)-Ru(1)-Cl(1) 99.371(13)
P(2)#1-Ru(1)-Cl(1)#1	P(2)-Ru(1)-Cl(1)#1

96.001(14)		83.999(14)
P(1)#1-Ru(1)-Cl(1)#1 99.370(13)		P(1)-Ru(1)-Cl(1)#1 80.629(13)
Cl(1)-Ru(1)-Cl(1)#1 180.0		N(1)-P(1)-N(2) 97.46(7)
N(1)-P(1)-C(9) 99.66(7)		N(2)-P(1)-C(9) 103.63(7)
N(1)-P(1)-Ru(1) 123.27(5)		N(2)-P(1)-Ru(1) 119.12(5)
C(9)-P(1)-Ru(1) 110.49(5)		N(4)-P(2)-N(3) 100.06(7)
N(4)-P(2)-C(10) 104.08(7)		N(3)-P(2)-C(10) 101.02(7)
N(4)-P(2)-Ru(1) 118.36(5)		N(3)-P(2)-Ru(1) 122.40(5)
C(10)-P(2)-Ru(1) 108.33(5)		C(4)-N(1)-C(1) 107.09(13)
C(4)-N(1)-P(1) 121.83(11)		C(1)-N(1)-P(1) 119.12(11)
C(2)-C(1)-N(1) 108.61(15)		C(2)-C(1)-H(1) 125.7
N(1)-C(1)-H(1) 125.7		C(1)-C(2)-C(3) 107.73(15)
C(1)-C(2)-H(2) 126.1		C(3)-C(2)-H(2) 126.1
C(4)-C(3)-C(2) 107.98(15)		C(4)-C(3)-H(3) 126.0
C(2)-C(3)-H(3) 126.0		C(3)-C(4)-N(1) 108.54(15)
C(3)-C(4)-H(4) 125.7		N(1)-C(4)-H(4) 125.7
C(8)-N(2)-C(5) 107.84(13)		C(8)-N(2)-P(1) 127.34(11)
C(5)-N(2)-P(1) 124.69(11)		C(6)-C(5)-N(2) 108.23(15)
C(6)-C(5)-H(5) 125.9		N(2)-C(5)-H(5) 125.9
C(5)-C(6)-C(7) 107.86(15)		C(5)-C(6)-H(6) 126.1
C(7)-C(6)-H(6) 126.1		C(8)-C(7)-C(6) 107.79(15)
C(8)-C(7)-H(7) 126.1		C(6)-C(7)-H(7) 126.1
C(7)-C(8)-N(2) 108.27(15)		C(7)-C(8)-H(8) 125.9
N(2)-C(8)-H(8) 125.9		C(10)-C(9)-P(1) 113.22(11)
C(10)-C(9)-H(9A) 108.9		P(1)-C(9)-H(9A) 108.9
C(10)-C(9)-H(9B) 108.9		P(1)-C(9)-H(9B) 108.9
H(9A)-C(9)-H(9B) 107.7		C(9)-C(10)-P(2) 111.93(11)
C(9)-C(10)-H(10A)		P(2)-C(10)-H(10A)

109.2		109.2	
	C(9)-C(10)-H(10B)		P(2)-C(10)-H(10B)
109.2		109.2	
	H(10A)-C(10)-H(10B)		C(11)-N(3)-C(14)
107.9		107.97(14)	
	C(11)-N(3)-P(2)		C(14)-N(3)-P(2)
124.82(11)		126.07(12)	
	C(12)-C(11)-N(3)		C(12)-C(11)-H(11)
108.26(15)		125.9	
	N(3)-C(11)-H(11)		C(11)-C(12)-C(13)
125.9		107.79(16)	
	C(11)-C(12)-H(12)		C(13)-C(12)-H(12)
126.1		126.1	
	C(14)-C(13)-C(12)		C(14)-C(13)-H(13)
107.71(16)		126.1	
	C(12)-C(13)-H(13)		C(13)-C(14)-N(3)
126.1		108.27(15)	
	C(13)-C(14)-H(14)		N(3)-C(14)-H(14)
125.9		125.9	
	C(18)-N(4)-C(15)		C(18)-N(4)-P(2)
107.44(14)		123.54(12)	
	C(15)-N(4)-P(2)		C(16)-C(15)-N(4)
129.01(12)		108.48(15)	
	C(16)-C(15)-H(15)		N(4)-C(15)-H(15)
125.8		125.8	
	C(15)-C(16)-C(17)		C(15)-C(16)-H(16)
107.74(15)		126.1	
	C(17)-C(16)-H(16)		C(18)-C(17)-C(16)
126.1		107.67(15)	
	C(18)-C(17)-H(17)		C(16)-C(17)-H(17)
126.2		126.2	
	C(17)-C(18)-N(4)		C(17)-C(18)-H(18)
108.65(15)		125.7	
	N(4)-C(18)-H(18)		
125.7			

_____

Bond lengths and angles for the X-ray structure of [Ir(PPh₃)₂HS₃](4a).

Ir(1)-P(1)		Ir(1)-P(2)	
2.303(3)		2.314(3)	
	Ir(1)-S(2)		Ir(1)-S(1)
2.353(3)		2.388(3)	
	Ir(1)-S(3)		S(1)-C(1)
2.418(4)		1.744(15)	
	S(2)-C(6)		S(2)-C(7)
1.772(15)		1.783(14)	
	S(3)-C(12)		C(1)-C(6)
1.762(16)		1.391(19)	
	C(1)-C(2)		C(2)-C(3)
1.42(2)		1.36(2)	
	C(2)-H(2)		C(3)-C(4)
0.9500		1.399(18)	
	C(3)-H(3)		C(4)-C(5)
0.9500		1.39(2)	
	C(4)-H(4)		C(5)-C(6)
0.9500		1.42(2)	
	C(5)-H(5)		C(7)-C(12)
0.9500		1.39(2)	
	C(7)-C(8)		C(8)-C(9)
1.439(19)		1.40(2)	
	C(8)-H(8)		C(9)-C(10)
0.9500		1.36(3)	
	C(9)-H(9)		C(10)-C(11)
0.9500		1.38(2)	
	C(10)-H(10)		C(11)-C(12)
0.9500		1.40(2)	
	C(11)-H(11)		P(1)-C(25)
0.9500		1.796(14)	
	P(1)-C(19)		P(1)-C(13)
1.822(13)		1.830(15)	
	C(13)-C(14)		C(13)-C(18)
1.39(2)		1.417(18)	
	C(14)-C(15)		C(14)-H(14)
1.40(2)		0.9500	
	C(15)-C(16)		C(15)-H(15)
1.40(2)		0.9500	
	C(16)-C(17)		C(16)-H(16)
1.39(2)		0.9500	
	C(17)-C(18)		C(17)-H(17)
1.38(2)		0.9500	
	C(18)-H(18)		C(19)-C(20)
0.9500		1.383(18)	
	C(19)-C(24)		C(20)-C(21)
1.39(2)		1.37(2)	

C(20)-H(20) 0.9500		C(21)-C(22) 1.37(3)	
C(21)-H(21) 0.9500		C(22)-C(23) 1.40(2)	
C(22)-H(22) 0.9500		C(23)-C(24) 1.37(2)	
C(23)-H(23) 0.9500		C(24)-H(24) 0.9500	
C(25)-C(30) 1.41(2)		C(25)-C(26) 1.41(2)	
C(26)-C(27) 1.39(2)		C(26)-H(26) 0.9500	
C(27)-C(28) 1.41(3)		C(27)-H(27) 0.9500	
C(28)-C(29) 1.37(3)		C(28)-H(28) 0.9500	
C(29)-C(30) 1.39(2)		C(29)-H(29) 0.9500	
C(30)-H(30) 0.9500		P(2)-C(43) 1.796(12)	
P(2)-C(31) 1.828(14)		P(2)-C(37) 1.852(15)	
C(31)-C(32) 1.41(2)		C(31)-C(36) 1.439(19)	
C(32)-C(33) 1.38(2)		C(32)-H(32) 0.9500	
C(33)-C(34) 1.37(2)		C(33)-H(33) 0.9500	
C(34)-C(35) 1.40(2)		C(34)-H(34) 0.9500	
C(35)-C(36) 1.36(2)		C(35)-H(35) 0.9500	
C(36)-H(36) 0.9500		C(37)-C(42) 1.389(19)	
C(37)-C(38) 1.389(18)		C(38)-C(39) 1.42(2)	
C(38)-H(38) 0.9500		C(39)-C(40) 1.36(2)	
C(39)-H(39) 0.9500		C(40)-C(41) 1.365(19)	
C(40)-H(40) 0.9500		C(41)-C(42) 1.39(3)	
C(41)-H(41) 0.9500		C(42)-H(42) 0.9500	
C(43)-C(44) 1.400(19)		C(43)-C(48) 1.426(18)	
C(44)-C(45) 1.425(19)		C(44)-H(44) 0.9500	
C(45)-C(46) 1.39(2)		C(45)-H(45) 0.9500	
C(46)-C(47) 1.41(2)		C(46)-H(46) 0.9500	
C(47)-C(48) 1.408(18)		C(47)-H(47) 0.9500	

C(48)-H(48) 0.9500		C(1S)-Cl(3S) 1.726(19)	
C(1S)-Cl(2S) 1.78(2)		C(1S)-Cl(1S) 1.79(2)	
C(1S)-H(1S) 1.0000			
P(1)-Ir(1)-P(2) 100.39(12)		P(1)-Ir(1)-S(2) 165.51(14)	
P(2)-Ir(1)-S(2) 90.44(12)		P(1)-Ir(1)-S(1) 84.72(12)	
P(2)-Ir(1)-S(1) 174.14(12)		S(2)-Ir(1)-S(1) 85.02(12)	
P(1)-Ir(1)-S(3) 101.90(13)		P(2)-Ir(1)-S(3) 90.05(12)	
S(2)-Ir(1)-S(3) 87.56(13)		S(1)-Ir(1)-S(3) 86.07(12)	
C(1)-S(1)-Ir(1) 102.6(5)		C(6)-S(2)-C(7) 101.3(6)	
C(6)-S(2)-Ir(1) 103.2(5)		C(7)-S(2)-Ir(1) 104.4(5)	
C(12)-S(3)-Ir(1) 102.6(5)		C(6)-C(1)-C(2) 116.8(14)	
C(6)-C(1)-S(1) 122.2(12)		C(2)-C(1)-S(1) 121.0(11)	
C(3)-C(2)-C(1) 121.1(14)		C(3)-C(2)-H(2) 119.4	
C(1)-C(2)-H(2) 119.4		C(2)-C(3)-C(4) 122.2(16)	
C(2)-C(3)-H(3) 118.9		C(4)-C(3)-H(3) 118.9	
C(5)-C(4)-C(3) 118.0(17)		C(5)-C(4)-H(4) 121.0	
C(3)-C(4)-H(4) 121.0		C(4)-C(5)-C(6) 120.1(14)	
C(4)-C(5)-H(5) 120.0		C(6)-C(5)-H(5) 120.0	
C(1)-C(6)-C(5) 121.7(14)		C(1)-C(6)-S(2) 119.8(11)	
C(5)-C(6)-S(2) 118.5(11)		C(12)-C(7)-C(8) 121.1(13)	
C(12)-C(7)-S(2) 121.7(10)		C(8)-C(7)-S(2) 117.2(12)	
C(9)-C(8)-C(7) 117.9(16)		C(9)-C(8)-H(8) 121.1	
C(7)-C(8)-H(8) 121.1		C(10)-C(9)-C(8) 120.7(15)	
C(10)-C(9)-H(9) 119.7		C(8)-C(9)-H(9) 119.7	
C(9)-C(10)-C(11) 120.8(15)		C(9)-C(10)-H(10) 119.6	
C(11)-C(10)-H(10) 119.6		C(10)-C(11)-C(12) 121.8(16)	
C(10)-C(11)-H(11) 119.1		C(12)-C(11)-H(11) 119.1	

C(7)-C(12)-C(11) 117.7(14)		C(7)-C(12)-S(3) 123.6(11)	
C(11)-C(12)-S(3) 118.7(13)		C(25)-P(1)-C(19) 104.7(7)	
C(25)-P(1)-C(13) 98.0(7)		C(19)-P(1)-C(13) 103.7(6)	
C(25)-P(1)-Ir(1) 122.3(4)		C(19)-P(1)-Ir(1) 112.5(4)	
C(13)-P(1)-Ir(1) 113.3(5)		C(14)-C(13)-C(18) 117.3(14)	
C(14)-C(13)-P(1) 124.0(10)		C(18)-C(13)-P(1) 118.6(12)	
C(13)-C(14)-C(15) 121.9(14)		C(13)-C(14)-H(14) 119.1	
C(15)-C(14)-H(14) 119.1		C(14)-C(15)-C(16) 119.8(16)	
C(14)-C(15)-H(15) 120.1		C(16)-C(15)-H(15) 120.1	
C(17)-C(16)-C(15) 119.1(14)		C(17)-C(16)-H(16) 120.5	
C(15)-C(16)-H(16) 120.5		C(18)-C(17)-C(16) 120.8(14)	
C(18)-C(17)-H(17) 119.6		C(16)-C(17)-H(17) 119.6	
C(17)-C(18)-C(13) 121.1(15)		C(17)-C(18)-H(18) 119.5	
C(13)-C(18)-H(18) 119.5		C(20)-C(19)-C(24) 116.1(13)	
C(20)-C(19)-P(1) 124.3(12)		C(24)-C(19)-P(1) 119.5(10)	
C(21)-C(20)-C(19) 121.4(15)		C(21)-C(20)-H(20) 119.3	
C(19)-C(20)-H(20) 119.3		C(22)-C(21)-C(20) 122.0(15)	
C(22)-C(21)-H(21) 119.0		C(20)-C(21)-H(21) 119.0	
C(21)-C(22)-C(23) 117.8(15)		C(21)-C(22)-H(22) 121.1	
C(23)-C(22)-H(22) 121.1		C(24)-C(23)-C(22) 119.5(16)	
C(24)-C(23)-H(23) 120.3		C(22)-C(23)-H(23) 120.3	
C(23)-C(24)-C(19) 123.1(14)		C(23)-C(24)-H(24) 118.5	
C(19)-C(24)-H(24) 118.5		C(30)-C(25)-C(26) 117.7(14)	
C(30)-C(25)-P(1) 124.1(11)		C(26)-C(25)-P(1) 118.0(12)	
C(27)-C(26)-C(25) 120.7(16)		C(27)-C(26)-H(26) 119.7	
C(25)-C(26)-H(26) 119.7		C(26)-C(27)-C(28) 120.9(16)	
C(26)-C(27)-H(27) 119.6		C(28)-C(27)-H(27) 119.6	

C(29)-C(28)-C(27) 118.1(16)		C(29)-C(28)-H(28) 120.9	
C(27)-C(28)-H(28) 120.9		C(28)-C(29)-C(30) 122.0(19)	
C(28)-C(29)-H(29) 119.0		C(30)-C(29)-H(29) 119.0	
C(29)-C(30)-C(25) 120.5(16)		C(29)-C(30)-H(30) 119.8	
C(25)-C(30)-H(30) 119.8		C(43)-P(2)-C(31) 101.7(6)	
C(43)-P(2)-C(37) 104.9(7)		C(31)-P(2)-C(37) 104.7(6)	
C(43)-P(2)-Ir(1) 109.1(4)		C(31)-P(2)-Ir(1) 117.5(5)	
C(37)-P(2)-Ir(1) 117.1(4)		C(32)-C(31)-C(36) 118.8(13)	
C(32)-C(31)-P(2) 123.0(11)		C(36)-C(31)-P(2) 118.2(11)	
C(33)-C(32)-C(31) 119.9(16)		C(33)-C(32)-H(32) 120.0	
C(31)-C(32)-H(32) 120.0		C(34)-C(33)-C(32) 121.4(17)	
C(34)-C(33)-H(33) 119.3		C(32)-C(33)-H(33) 119.3	
C(33)-C(34)-C(35) 119.2(16)		C(33)-C(34)-H(34) 120.4	
C(35)-C(34)-H(34) 120.4		C(36)-C(35)-C(34) 121.8(15)	
C(36)-C(35)-H(35) 119.1		C(34)-C(35)-H(35) 119.1	
C(35)-C(36)-C(31) 118.8(15)		C(35)-C(36)-H(36) 120.6	
C(31)-C(36)-H(36) 120.6		C(42)-C(37)-C(38) 118.7(14)	
C(42)-C(37)-P(2) 119.7(10)		C(38)-C(37)-P(2) 121.6(11)	
C(37)-C(38)-C(39) 119.0(13)		C(37)-C(38)-H(38) 120.5	
C(39)-C(38)-H(38) 120.5		C(40)-C(39)-C(38) 120.6(13)	
C(40)-C(39)-H(39) 119.7		C(38)-C(39)-H(39) 119.7	
C(39)-C(40)-C(41) 120.6(16)		C(39)-C(40)-H(40) 119.7	
C(41)-C(40)-H(40) 119.7		C(40)-C(41)-C(42) 119.6(15)	
C(40)-C(41)-H(41) 120.2		C(42)-C(41)-H(41) 120.2	
C(41)-C(42)-C(37) 121.5(13)		C(41)-C(42)-H(42) 119.3	
C(37)-C(42)-H(42) 119.3		C(44)-C(43)-C(48) 116.7(11)	
C(44)-C(43)-P(2) 123.3(10)		C(48)-C(43)-P(2) 119.8(10)	

C(43)-C(44)-C(45) 122.0(14)	C(43)-C(44)-H(44) 119.0
C(45)-C(44)-H(44) 119.0	C(46)-C(45)-C(44) 118.5(14)
C(46)-C(45)-H(45) 120.7	C(44)-C(45)-H(45) 120.7
C(45)-C(46)-C(47) 122.3(13)	C(45)-C(46)-H(46) 118.9
C(47)-C(46)-H(46) 118.9	C(46)-C(47)-C(48) 117.3(14)
C(46)-C(47)-H(47) 121.3	C(48)-C(47)-H(47) 121.3
C(47)-C(48)-C(43) 123.0(13)	C(47)-C(48)-H(48) 118.5
C(43)-C(48)-H(48) 118.5	Cl(3S)-C(1S)-Cl(2S) 111.6(11)
Cl(3S)-C(1S)-Cl(1S) 110.9(13)	Cl(2S)-C(1S)-Cl(1S) 108.2(10)
Cl(3S)-C(1S)-H(1S) 108.7	Cl(2S)-C(1S)-H(1S) 108.7
Cl(1S)-C(1S)-H(1S) 108.7	

_____

Bond lengths and angles for the X-ray structure of isomerized [Ir(PPh₃)₂HS₃](4b).

Ir(1)-P(2) 2.3106(9)	Ir(1)-P(1) 2.3136(9)
Ir(1)-S(3) 2.3832(9)	Ir(1)-S(1) 2.3872(9)
Ir(1)-S(2) 2.3929(9)	Ir(1)-H(1) 1.34(3)
S(1)-C(1) 1.752(4)	S(2)-C(7) 1.782(4)
S(2)-C(6) 1.792(4)	S(3)-C(12) 1.753(4)

P(1)-C(13)		P(1)-C(19)
1.834(4)		1.838(4)
P(1)-C(25)		P(2)-C(43)
1.843(4)		1.829(4)
P(2)-C(37)		P(2)-C(31)
1.837(4)		1.847(4)
C(1)-C(6)		C(1)-C(2)
1.396(6)		1.413(6)
C(2)-C(3)		C(2)-H(2)
1.372(6)		0.9500
C(3)-C(4)		C(3)-H(3)
1.400(7)		0.9500
C(4)-C(5)		C(4)-H(4)
1.384(6)		0.9500
C(5)-C(6)		C(5)-H(5)
1.397(6)		0.9500
C(7)-C(8)		C(7)-C(12)
1.394(6)		1.398(6)
C(8)-C(9)		C(8)-H(8)
1.387(6)		0.9500
C(9)-C(10)		C(9)-H(9)
1.390(7)		0.9500
C(10)-C(11)		C(10)-H(10)
1.387(6)		0.9500
C(11)-C(12)		C(11)-H(11)
1.402(6)		0.9500
C(13)-C(14)		C(13)-C(18)
1.390(6)		1.407(6)
C(14)-C(15)		C(14)-H(14)
1.393(6)		0.9500
C(15)-C(16)		C(15)-H(15)
1.380(7)		0.9500
C(16)-C(17)		C(16)-H(16)
1.391(7)		0.9500
C(17)-C(18)		C(17)-H(17)
1.396(6)		0.9500
C(18)-H(18)		C(19)-C(24)
0.9500		1.389(6)
C(19)-C(20)		C(20)-C(21)
1.404(6)		1.395(6)
C(20)-H(20)		C(21)-C(22)
0.9500		1.382(6)
C(21)-H(21)		C(22)-C(23)
0.9500		1.395(6)
C(22)-H(22)		C(23)-C(24)
0.9500		1.391(6)
C(23)-H(23)		C(24)-H(24)
0.9500		0.9500
C(25)-C(30)		C(25)-C(26)
1.388(6)		1.409(6)
C(26)-C(27)		C(26)-H(26)
1.377(6)		0.9500
C(27)-C(28)		C(27)-H(27)
1.391(6)		0.9500

C(28)-C(29) 1.383(6)	C(28)-H(28) 0.9500
C(29)-C(30) 1.392(6)	C(29)-H(29) 0.9500
C(30)-H(30) 0.9500	C(31)-C(36) 1.393(5)
C(31)-C(32) 1.398(6)	C(32)-C(33) 1.390(5)
C(32)-H(32) 0.9500	C(33)-C(34) 1.386(6)
C(33)-H(33) 0.9500	C(34)-C(35) 1.377(6)
C(34)-H(34) 0.9500	C(35)-C(36) 1.394(6)
C(35)-H(35) 0.9500	C(36)-H(36) 0.9500
C(37)-C(42) 1.393(5)	C(37)-C(38) 1.408(5)
C(38)-C(39) 1.394(6)	C(38)-H(38) 0.9500
C(39)-C(40) 1.384(6)	C(39)-H(39) 0.9500
C(40)-C(41) 1.394(6)	C(40)-H(40) 0.9500
C(41)-C(42) 1.395(6)	C(41)-H(41) 0.9500
C(42)-H(42) 0.9500	C(43)-C(48) 1.394(6)
C(43)-C(44) 1.404(5)	C(44)-C(45) 1.382(6)
C(44)-H(44) 0.9500	C(45)-C(46) 1.379(6)
C(45)-H(45) 0.9500	C(46)-C(47) 1.386(6)
C(46)-H(46) 0.9500	C(47)-C(48) 1.386(6)
C(47)-H(47) 0.9500	C(48)-H(48) 0.9500
C(1S1)-C(6S1) 1.374(7)	C(1S1)-C(2S1) 1.389(8)
C(1S1)-H(1S1) 0.9500	C(2S1)-C(3S1) 1.370(8)
C(2S1)-H(2S1) 0.9500	C(3S1)-C(4S1) 1.378(7)
C(3S1)-H(3S1) 0.9500	C(4S1)-C(5S1) 1.394(6)
C(4S1)-H(4S1) 0.9500	C(5S1)-C(6S1) 1.390(6)
C(5S1)-H(5S1) 0.9500	C(6S1)-H(6S1) 0.9500
C(2S2)-C(1S2) 1.373(7)	C(2S2)-C(3S2) 1.385(7)
C(2S2)-H(2S2) 0.9500	C(3S2)-C(1S2)#1 1.377(7)

C(3S2)-H(3S2) 0.9500		C(1S2)-C(3S2)#1 1.377(7)
C(1S2)-H(1S2) 0.9500		
P(2)-Ir(1)-P(1) 99.68(3)		P(2)-Ir(1)-S(3) 167.77(3)
P(1)-Ir(1)-S(3) 91.09(3)		P(2)-Ir(1)-S(1) 82.48(3)
P(1)-Ir(1)-S(1) 173.87(3)		S(3)-Ir(1)-S(1) 86.24(3)
P(2)-Ir(1)-S(2) 99.82(3)		P(1)-Ir(1)-S(2) 98.44(3)
S(3)-Ir(1)-S(2) 84.17(3)		S(1)-Ir(1)-S(2) 86.78(3)
P(2)-Ir(1)-H(1) 85.0(14)		P(1)-Ir(1)-H(1) 85.9(15)
S(3)-Ir(1)-H(1) 90.0(16)		S(1)-Ir(1)-H(1) 88.6(15)
S(2)-Ir(1)-H(1) 172.8(19)		C(1)-S(1)-Ir(1) 104.03(14)
C(7)-S(2)-C(6) 101.82(18)		C(7)-S(2)-Ir(1) 103.20(14)
C(6)-S(2)-Ir(1) 104.59(14)		C(12)-S(3)-Ir(1) 103.28(14)
C(13)-P(1)-C(19) 103.67(18)		C(13)-P(1)-C(25) 97.87(17)
C(19)-P(1)-C(25) 103.09(17)		C(13)-P(1)-Ir(1) 114.87(12)
C(19)-P(1)-Ir(1) 115.90(13)		C(25)-P(1)-Ir(1) 118.84(13)
C(43)-P(2)-C(37) 103.00(18)		C(43)-P(2)-C(31) 102.71(17)
C(37)-P(2)-C(31) 100.22(17)		C(43)-P(2)-Ir(1) 111.37(12)
C(37)-P(2)-Ir(1) 114.00(13)		C(31)-P(2)-Ir(1) 123.11(12)
C(6)-C(1)-C(2) 117.0(4)		C(6)-C(1)-S(1) 124.5(3)
C(2)-C(1)-S(1) 118.5(3)		C(3)-C(2)-C(1) 121.3(4)
C(3)-C(2)-H(2) 119.4		C(1)-C(2)-H(2) 119.4
C(2)-C(3)-C(4) 120.9(4)		C(2)-C(3)-H(3) 119.6
C(4)-C(3)-H(3) 119.6		C(5)-C(4)-C(3) 119.1(4)
C(5)-C(4)-H(4) 120.5		C(3)-C(4)-H(4) 120.5
C(4)-C(5)-C(6) 119.9(4)		C(4)-C(5)-H(5) 120.1
C(6)-C(5)-H(5) 120.1		C(1)-C(6)-C(5) 122.0(4)
C(1)-C(6)-S(2) 119.9(3)		C(5)-C(6)-S(2) 118.1(3)

C(8)-C(7)-C(12) 122.1(4)	C(8)-C(7)-S(2) 118.6(3)
C(12)-C(7)-S(2) 119.4(3)	C(9)-C(8)-C(7) 120.2(4)
C(9)-C(8)-H(8) 119.9	C(7)-C(8)-H(8) 119.9
C(8)-C(9)-C(10) 118.2(4)	C(8)-C(9)-H(9) 120.9
C(10)-C(9)-H(9) 120.9	C(11)-C(10)-C(9) 121.8(4)
C(11)-C(10)-H(10) 119.1	C(9)-C(10)-H(10) 119.1
C(10)-C(11)-C(12) 120.6(4)	C(10)-C(11)-H(11) 119.7
C(12)-C(11)-H(11) 119.7	C(7)-C(12)-C(11) 117.1(4)
C(7)-C(12)-S(3) 122.0(3)	C(11)-C(12)-S(3) 120.9(3)
C(14)-C(13)-C(18) 118.5(4)	C(14)-C(13)-P(1) 123.9(3)
C(18)-C(13)-P(1) 117.6(3)	C(13)-C(14)-C(15) 120.7(4)
C(13)-C(14)-H(14) 119.6	C(15)-C(14)-H(14) 119.6
C(16)-C(15)-C(14) 120.2(4)	C(16)-C(15)-H(15) 119.9
C(14)-C(15)-H(15) 119.9	C(15)-C(16)-C(17) 120.4(4)
C(15)-C(16)-H(16) 119.8	C(17)-C(16)-H(16) 119.8
C(16)-C(17)-C(18) 119.4(4)	C(16)-C(17)-H(17) 120.3
C(18)-C(17)-H(17) 120.3	C(17)-C(18)-C(13) 120.8(4)
C(17)-C(18)-H(18) 119.6	C(13)-C(18)-H(18) 119.6
C(24)-C(19)-C(20) 118.9(4)	C(24)-C(19)-P(1) 122.5(3)
C(20)-C(19)-P(1) 118.5(3)	C(21)-C(20)-C(19) 120.4(4)
C(21)-C(20)-H(20) 119.8	C(19)-C(20)-H(20) 119.8
C(22)-C(21)-C(20) 120.5(4)	C(22)-C(21)-H(21) 119.8
C(20)-C(21)-H(21) 119.8	C(21)-C(22)-C(23) 119.1(4)
C(21)-C(22)-H(22) 120.5	C(23)-C(22)-H(22) 120.5
C(24)-C(23)-C(22) 120.9(4)	C(24)-C(23)-H(23) 119.5
C(22)-C(23)-H(23) 119.5	C(19)-C(24)-C(23) 120.2(4)
C(19)-C(24)-H(24) 119.9	C(23)-C(24)-H(24) 119.9

C(30)-C(25)-C(26)		C(30)-C(25)-P(1)
118.4(4)		123.4(3)
C(26)-C(25)-P(1)		C(27)-C(26)-C(25)
118.1(3)		120.5(4)
C(27)-C(26)-H(26)		C(25)-C(26)-H(26)
119.8		119.8
C(26)-C(27)-C(28)		C(26)-C(27)-H(27)
120.5(4)		119.8
C(28)-C(27)-H(27)		C(29)-C(28)-C(27)
119.8		119.7(4)
C(29)-C(28)-H(28)		C(27)-C(28)-H(28)
120.2		120.2
C(28)-C(29)-C(30)		C(28)-C(29)-H(29)
120.0(4)		120.0
C(30)-C(29)-H(29)		C(25)-C(30)-C(29)
120.0		120.9(4)
C(25)-C(30)-H(30)		C(29)-C(30)-H(30)
119.5		119.5
C(36)-C(31)-C(32)		C(36)-C(31)-P(2)
118.2(4)		124.1(3)
C(32)-C(31)-P(2)		C(33)-C(32)-C(31)
117.7(3)		120.9(4)
C(33)-C(32)-H(32)		C(31)-C(32)-H(32)
119.5		119.5
C(34)-C(33)-C(32)		C(34)-C(33)-H(33)
120.2(4)		119.9
C(32)-C(33)-H(33)		C(35)-C(34)-C(33)
119.9		119.5(4)
C(35)-C(34)-H(34)		C(33)-C(34)-H(34)
120.3		120.3
C(34)-C(35)-C(36)		C(34)-C(35)-H(35)
120.6(4)		119.7
C(36)-C(35)-H(35)		C(31)-C(36)-C(35)
119.7		120.7(4)
C(31)-C(36)-H(36)		C(35)-C(36)-H(36)
119.7		119.7
C(42)-C(37)-C(38)		C(42)-C(37)-P(2)
118.5(4)		122.7(3)
C(38)-C(37)-P(2)		C(39)-C(38)-C(37)
118.8(3)		120.2(4)
C(39)-C(38)-H(38)		C(37)-C(38)-H(38)
119.9		119.9
C(40)-C(39)-C(38)		C(40)-C(39)-H(39)
120.8(4)		119.6
C(38)-C(39)-H(39)		C(39)-C(40)-C(41)
119.6		119.6(4)
C(39)-C(40)-H(40)		C(41)-C(40)-H(40)
120.2		120.2
C(40)-C(41)-C(42)		C(40)-C(41)-H(41)
119.8(4)		120.1
C(42)-C(41)-H(41)		C(37)-C(42)-C(41)
120.1		121.1(4)
C(37)-C(42)-H(42)		C(41)-C(42)-H(42)
119.4		119.4

C(48)-C(43)-C(44) 117.2(4)		C(48)-C(43)-P(2) 122.5(3)
C(44)-C(43)-P(2) 120.2(3)		C(45)-C(44)-C(43) 121.3(4)
C(45)-C(44)-H(44) 119.4		C(43)-C(44)-H(44) 119.4
C(46)-C(45)-C(44) 120.2(4)		C(46)-C(45)-H(45) 119.9
C(44)-C(45)-H(45) 119.9		C(45)-C(46)-C(47) 119.9(4)
C(45)-C(46)-H(46) 120.0		C(47)-C(46)-H(46) 120.0
C(48)-C(47)-C(46) 119.6(4)		C(48)-C(47)-H(47) 120.2
C(46)-C(47)-H(47) 120.2		C(47)-C(48)-C(43) 121.7(4)
C(47)-C(48)-H(48) 119.1		C(43)-C(48)-H(48) 119.1
C(6S1)-C(1S1)-C(2S1) 120.2(5)		C(6S1)-C(1S1)-H(1S1) 119.9
C(2S1)-C(1S1)-H(1S1) 119.9		C(3S1)-C(2S1)-C(1S1) 120.3(5)
C(3S1)-C(2S1)-H(2S1) 119.8		C(1S1)-C(2S1)-H(2S1) 119.8
C(2S1)-C(3S1)-C(4S1) 119.9(4)		C(2S1)-C(3S1)-H(3S1) 120.0
C(4S1)-C(3S1)-H(3S1) 120.0		C(3S1)-C(4S1)-C(5S1) 120.3(4)
C(3S1)-C(4S1)-H(4S1) 119.9		C(5S1)-C(4S1)-H(4S1) 119.9
C(6S1)-C(5S1)-C(4S1) 119.4(4)		C(6S1)-C(5S1)-H(5S1) 120.3
C(4S1)-C(5S1)-H(5S1) 120.3		C(1S1)-C(6S1)-C(5S1) 119.9(5)
C(1S1)-C(6S1)-H(6S1) 120.1		C(5S1)-C(6S1)-H(6S1) 120.1
C(1S2)-C(2S2)-C(3S2) 119.4(4)		C(1S2)-C(2S2)-H(2S2) 120.3
C(3S2)-C(2S2)-H(2S2) 120.3		C(1S2)#1-C(3S2)-C(2S2) 120.4(5)
C(1S2)#1-C(3S2)-H(3S2) 119.8		C(2S2)-C(3S2)-H(3S2) 119.8
C(2S2)-C(1S2)-C(3S2)#1 120.2(4)		C(2S2)-C(1S2)-H(1S2) 119.9
C(3S2)#1-C(1S2)-H(1S2) 119.9		

_____

Bond lengths and angles for [Ir(Br)(S₃)(PPh₃)₂] (5a).

Ir(1)-S(2)	Ir(1)-P(2)
2.3106(17)	2.3387(17)
Ir(1)-S(3)	Ir(1)-S(1)
2.3510(17)	2.3528(16)
Ir(1)-P(1)	Ir(1)-Br(1)
2.3749(17)	2.5664(9)
P(1)-C(19)	P(1)-C(13)
1.822(7)	1.826(6)
P(1)-C(25)	P(2)-C(31)
1.829(6)	1.787(7)
P(2)-C(43)	P(2)-C(37)
1.818(6)	1.850(6)
S(1)-C(1)	S(2)-C(7)
1.730(6)	1.767(6)
S(2)-C(2)	C(1)-C(2)
1.780(6)	1.382(9)
C(1)-C(6)	C(2)-C(3)
1.405(9)	1.375(9)
S(3)-C(8)	C(3)-C(4)
1.721(6)	1.369(9)
C(3)-H(3)	C(4)-C(5)
0.9500	1.402(10)
C(4)-H(4)	C(5)-C(6)
0.9500	1.359(10)
C(5)-H(5)	C(6)-H(6)
0.9500	0.9500
C(7)-C(12)	C(7)-C(8)
1.377(9)	1.383(9)
C(8)-C(9)	C(9)-C(10)
1.391(9)	1.368(10)
C(9)-H(9)	C(10)-C(11)
0.9500	1.386(10)
C(10)-H(10)	C(11)-C(12)
0.9500	1.365(10)
C(11)-H(11)	C(12)-H(12)
0.9500	0.9500
C(13)-C(18)	C(13)-C(14)
1.389(9)	1.396(9)
C(14)-C(15)	C(14)-H(14)
1.364(9)	0.9500
C(15)-C(16)	C(15)-H(15)
1.393(10)	0.9500
C(16)-C(17)	C(16)-H(16)
1.371(10)	0.9500
C(17)-C(18)	C(17)-H(17)
1.364(9)	0.9500
C(18)-H(18)	C(19)-C(24)
0.9500	1.387(9)
C(19)-C(20)	C(20)-C(21)

1.400(9)		1.363(10)	
	C(20)-H(20)		C(21)-C(22)
0.9500		1.375(10)	
	C(21)-H(21)		C(22)-C(23)
0.9500		1.379(10)	
	C(22)-H(22)		C(23)-C(24)
0.9500		1.349(10)	
	C(23)-H(23)		C(24)-H(24)
0.9500		0.9500	
	C(25)-C(26)		C(25)-C(30)
1.363(9)		1.398(10)	
	C(26)-C(27)		C(26)-H(26)
1.382(9)		0.9500	
	C(27)-C(28)		C(27)-H(27)
1.383(11)		0.9500	
	C(28)-C(29)		C(28)-H(28)
1.340(10)		0.9500	
	C(29)-C(30)		C(29)-H(29)
1.380(9)		0.9500	
	C(30)-H(30)		C(31)-C(32)
0.9500		1.393(9)	
	C(31)-C(36)		C(32)-C(33)
1.405(8)		1.355(10)	
	C(32)-H(32)		C(33)-C(34)
0.9500		1.381(9)	
	C(33)-H(33)		C(34)-C(35)
0.9500		1.367(9)	
	C(34)-H(34)		C(35)-C(36)
0.9500		1.356(9)	
	C(35)-H(35)		C(36)-H(36)
0.9500		0.9500	
	C(37)-C(42)		C(37)-C(38)
1.387(9)		1.393(9)	
	C(38)-C(39)		C(38)-H(38)
1.381(9)		0.9500	
	C(39)-C(40)		C(39)-H(39)
1.387(10)		0.9500	
	C(40)-C(41)		C(40)-H(40)
1.388(10)		0.9500	
	C(41)-C(42)		C(41)-H(41)
1.385(9)		0.9500	
	C(42)-H(42)		C(43)-C(48)
0.9500		1.369(9)	
	C(43)-C(44)		C(44)-C(45)
1.382(9)		1.393(9)	
	C(44)-H(44)		C(45)-C(46)
0.9500		1.345(10)	
	C(45)-H(45)		C(46)-C(47)
0.9500		1.365(10)	
	C(46)-H(46)		C(47)-C(48)
0.9500		1.386(9)	
	C(47)-H(47)		C(48)-H(48)
0.9500		0.9500	
	C(1B1)-C(2B1)		C(1B1)-C(3B1)#1

	1.375(12)		1.386(13)
C(1B1)-H(1B1)	0.9500	C(2B1)-C(3B1)	1.351(13)
C(2B1)-H(2B1)	0.9500	C(3B1)-C(1B1)#1	1.386(13)
C(3B1)-H(3B1)	0.9500	C(1B2)-C(6B2)	1.368(14)
C(1B2)-C(2B2)	1.384(15)	C(1B2)-H(1B2)	0.9500
C(2B2)-C(3B2)	1.349(14)	C(2B2)-H(2B2)	0.9500
C(3B2)-C(4B2)	1.382(12)	C(3B2)-H(3B2)	0.9500
C(4B2)-C(5B2)	1.375(11)	C(4B2)-H(4B2)	0.9500
C(5B2)-C(6B2)	1.350(13)	C(5B2)-H(5B2)	0.9500
C(6B2)-H(6B2)	0.9500		
S(2)-Ir(1)-P(2)	171.47(5)	S(2)-Ir(1)-S(3)	87.74(6)
P(2)-Ir(1)-S(3)	85.01(6)	S(2)-Ir(1)-S(1)	87.47(5)
P(2)-Ir(1)-S(1)	96.84(5)	S(3)-Ir(1)-S(1)	88.59(6)
S(2)-Ir(1)-P(1)	89.36(6)	P(2)-Ir(1)-P(1)	98.15(6)
S(3)-Ir(1)-P(1)	175.36(5)	S(1)-Ir(1)-P(1)	87.66(6)
S(2)-Ir(1)-Br(1)	82.89(4)	P(2)-Ir(1)-Br(1)	92.35(4)
S(3)-Ir(1)-Br(1)	88.07(5)	S(1)-Ir(1)-Br(1)	169.91(4)
P(1)-Ir(1)-Br(1)	95.17(5)	C(19)-P(1)-C(13)	101.6(3)
C(19)-P(1)-C(25)	101.8(3)	C(13)-P(1)-C(25)	101.3(3)
C(19)-P(1)-Ir(1)	119.79(19)	C(13)-P(1)-Ir(1)	110.7(2)
C(25)-P(1)-Ir(1)	118.9(2)	C(31)-P(2)-C(43)	108.0(3)
C(31)-P(2)-C(37)	100.9(3)	C(43)-P(2)-C(37)	101.0(3)
C(31)-P(2)-Ir(1)	113.42(19)	C(43)-P(2)-Ir(1)	115.31(19)
C(37)-P(2)-Ir(1)	116.5(2)	C(1)-S(1)-Ir(1)	104.0(2)
C(7)-S(2)-C(2)	99.6(3)	C(7)-S(2)-Ir(1)	103.7(2)
C(2)-S(2)-Ir(1)	104.8(2)	C(2)-C(1)-C(6)	118.8(6)
C(2)-C(1)-S(1)	123.3(5)	C(6)-C(1)-S(1)	117.9(5)
C(3)-C(2)-C(1)		C(3)-C(2)-S(2)	

122.1(6)		118.0(5)	
	C(1)-C(2)-S(2)		C(8)-S(3)-Ir(1)
119.9(5)		103.5(2)	
	C(4)-C(3)-C(2)		C(4)-C(3)-H(3)
118.4(6)		120.8	
	C(2)-C(3)-H(3)		C(3)-C(4)-C(5)
120.8		120.7(6)	
	C(3)-C(4)-H(4)		C(5)-C(4)-H(4)
119.6		119.6	
	C(6)-C(5)-C(4)		C(6)-C(5)-H(5)
120.5(6)		119.8	
	C(4)-C(5)-H(5)		C(5)-C(6)-C(1)
119.8		119.4(6)	
	C(5)-C(6)-H(6)		C(1)-C(6)-H(6)
120.3		120.3	
	C(12)-C(7)-C(8)		C(12)-C(7)-S(2)
122.0(6)		116.7(5)	
	C(8)-C(7)-S(2)		C(7)-C(8)-C(9)
121.2(5)		119.0(6)	
	C(7)-C(8)-S(3)		C(9)-C(8)-S(3)
122.8(5)		118.2(5)	
	C(10)-C(9)-C(8)		C(10)-C(9)-H(9)
118.7(6)		120.6	
	C(8)-C(9)-H(9)		C(9)-C(10)-C(11)
120.6		121.6(6)	
	C(9)-C(10)-H(10)		C(11)-C(10)-H(10)
119.2		119.2	
	C(12)-C(11)-C(10)		C(12)-C(11)-H(11)
120.2(6)		119.9	
	C(10)-C(11)-H(11)		C(11)-C(12)-C(7)
119.9		118.5(6)	
	C(11)-C(12)-H(12)		C(7)-C(12)-H(12)
120.7		120.7	
	C(18)-C(13)-C(14)		C(18)-C(13)-P(1)
119.8(6)		118.3(5)	
	C(14)-C(13)-P(1)		C(15)-C(14)-C(13)
121.8(5)		119.7(6)	
	C(15)-C(14)-H(14)		C(13)-C(14)-H(14)
120.1		120.1	
	C(14)-C(15)-C(16)		C(14)-C(15)-H(15)
120.2(7)		119.9	
	C(16)-C(15)-H(15)		C(17)-C(16)-C(15)
119.9		119.6(6)	
	C(17)-C(16)-H(16)		C(15)-C(16)-H(16)
120.2		120.2	
	C(18)-C(17)-C(16)		C(18)-C(17)-H(17)
121.1(7)		119.5	
	C(16)-C(17)-H(17)		C(17)-C(18)-C(13)
119.5		119.6(6)	
	C(17)-C(18)-H(18)		C(13)-C(18)-H(18)
120.2		120.2	
	C(24)-C(19)-C(20)		C(24)-C(19)-P(1)
118.0(6)		120.5(5)	
	C(20)-C(19)-P(1)		C(21)-C(20)-C(19)

	121.1(5)		121.3(6)
C(21)-C(20)-H(20)	119.3	C(19)-C(20)-H(20)	119.3
C(20)-C(21)-C(22)	119.4(6)	C(20)-C(21)-H(21)	120.3
C(22)-C(21)-H(21)	120.3	C(21)-C(22)-C(23)	119.7(7)
C(21)-C(22)-H(22)	120.1	C(23)-C(22)-H(22)	120.1
C(24)-C(23)-C(22)	121.2(6)	C(24)-C(23)-H(23)	119.4
C(22)-C(23)-H(23)	119.4	C(23)-C(24)-C(19)	120.4(6)
C(23)-C(24)-H(24)	119.8	C(19)-C(24)-H(24)	119.8
C(26)-C(25)-C(30)	118.3(6)	C(26)-C(25)-P(1)	120.3(5)
C(30)-C(25)-P(1)	121.3(5)	C(25)-C(26)-C(27)	120.3(7)
C(25)-C(26)-H(26)	119.8	C(27)-C(26)-H(26)	119.8
C(26)-C(27)-C(28)	120.3(7)	C(26)-C(27)-H(27)	119.8
C(28)-C(27)-H(27)	119.8	C(29)-C(28)-C(27)	120.1(6)
C(29)-C(28)-H(28)	119.9	C(27)-C(28)-H(28)	119.9
C(28)-C(29)-C(30)	120.0(7)	C(28)-C(29)-H(29)	120.0
C(30)-C(29)-H(29)	120.0	C(29)-C(30)-C(25)	120.9(7)
C(29)-C(30)-H(30)	119.6	C(25)-C(30)-H(30)	119.6
C(32)-C(31)-C(36)	118.4(6)	C(32)-C(31)-P(2)	121.1(5)
C(36)-C(31)-P(2)	120.4(5)	C(33)-C(32)-C(31)	120.5(6)
C(33)-C(32)-H(32)	119.8	C(31)-C(32)-H(32)	119.8
C(32)-C(33)-C(34)	119.8(6)	C(32)-C(33)-H(33)	120.1
C(34)-C(33)-H(33)	120.1	C(35)-C(34)-C(33)	121.1(6)
C(35)-C(34)-H(34)	119.4	C(33)-C(34)-H(34)	119.4
C(36)-C(35)-C(34)	119.6(6)	C(36)-C(35)-H(35)	120.2
C(34)-C(35)-H(35)	120.2	C(35)-C(36)-C(31)	120.7(6)
C(35)-C(36)-H(36)	119.7	C(31)-C(36)-H(36)	119.7
C(42)-C(37)-C(38)	118.9(5)	C(42)-C(37)-P(2)	121.6(5)
C(38)-C(37)-P(2)		C(39)-C(38)-C(37)	

	119.3(5)		120.2(6)
C(39)-C(38)-H(38)	119.9	C(37)-C(38)-H(38)	119.9
C(38)-C(39)-C(40)	121.1(6)	C(38)-C(39)-H(39)	119.5
C(40)-C(39)-H(39)	119.5	C(39)-C(40)-C(41)	118.6(6)
C(39)-C(40)-H(40)	120.7	C(41)-C(40)-H(40)	120.7
C(42)-C(41)-C(40)	120.6(6)	C(42)-C(41)-H(41)	119.7
C(40)-C(41)-H(41)	119.7	C(41)-C(42)-C(37)	120.5(6)
C(41)-C(42)-H(42)	119.7	C(37)-C(42)-H(42)	119.7
C(48)-C(43)-C(44)	117.0(6)	C(48)-C(43)-P(2)	118.4(4)
C(44)-C(43)-P(2)	124.5(5)	C(43)-C(44)-C(45)	120.5(6)
C(43)-C(44)-H(44)	119.8	C(45)-C(44)-H(44)	119.8
C(46)-C(45)-C(44)	121.4(6)	C(46)-C(45)-H(45)	119.3
C(44)-C(45)-H(45)	119.3	C(45)-C(46)-C(47)	118.9(6)
C(45)-C(46)-H(46)	120.5	C(47)-C(46)-H(46)	120.5
C(46)-C(47)-C(48)	120.1(7)	C(46)-C(47)-H(47)	120.0
C(48)-C(47)-H(47)	120.0	C(43)-C(48)-C(47)	122.0(6)
C(43)-C(48)-H(48)	119.0	C(47)-C(48)-H(48)	119.0
C(2B1)-C(1B1)-C(3B1)#1	120.6(9)	C(2B1)-C(1B1)-H(1B1)	119.7
C(3B1)#1-C(1B1)-H(1B1)	119.7	C(3B1)-C(2B1)-C(1B1)	120.1(8)
C(3B1)-C(2B1)-H(2B1)	119.9	C(1B1)-C(2B1)-H(2B1)	119.9
C(2B1)-C(3B1)-C(1B1)#1	119.3(8)	C(2B1)-C(3B1)-H(3B1)	120.4
C(1B1)#1-C(3B1)-H(3B1)	120.4	C(6B2)-C(1B2)-C(2B2)	120.0(10)
C(6B2)-C(1B2)-H(1B2)	120.0	C(2B2)-C(1B2)-H(1B2)	120.0
C(3B2)-C(2B2)-C(1B2)	119.2(9)	C(3B2)-C(2B2)-H(2B2)	120.4
C(1B2)-C(2B2)-H(2B2)	120.4	C(2B2)-C(3B2)-C(4B2)	120.4(8)
C(2B2)-C(3B2)-H(3B2)	119.8	C(4B2)-C(3B2)-H(3B2)	119.8
C(5B2)-C(4B2)-C(3B2)	120.4(8)	C(5B2)-C(4B2)-H(4B2)	119.8
C(3B2)-C(4B2)-H(4B2)		C(6B2)-C(5B2)-C(4B2)	

119.8	118.8(8)
C(6B2)-C(5B2)-H(5B2) 120.6	C(4B2)-C(5B2)-H(5B2) 120.6
C(5B2)-C(6B2)-C(1B2) 121.3(8)	C(5B2)-C(6B2)-H(6B2) 119.4
C(1B2)-C(6B2)-H(6B2) 119.4	

VITA

Ryan Robley Ketcham was born in Baltimore, MD, in the United States of America in 1981. In 1984 his family moved to Jacksonville Beach, FL. There he enjoyed the waves of the Atlantic Ocean until he was 7 years of age. He lived in Kentucky for 4 years exploring his grandfather's farm until he was 12 years old. He then moved to live with his father in Washington, DC. At this time his interest in science and chemistry began to blossom. He graduated high school in 1999 at Jeb Stuart High in Baileys Crossroads, VA. He then worked in the Heating and Air-conditioning trade for some time until he decided to travel around the world in the year 2000. He then enjoyed a back-packing trip around Europe and Japan for almost a year. After these travels, he then moved to Miami, FL to work with his cousin in pool maintenance and air-conditioning repair. He joined the University of Kentucky as chemistry major in the year 2002. In 2003 he studied marine biology in pristine coral reefs of Puerto Rico. In 2005 he suffered a severe head injury that sufficiently slowed down academic accomplishments for a period. Still, he was able to study abroad in Viña del Mar, Chile for a semester and then graduate with a Bachelors of Arts in Chemistry in 2008 with honors. After working with Dr.Folami. T.

Ladipo on transition metal catalytic chemistry research for most of his academic career, he finally was awarded a Masters of Science in Chemistry in the year 2011.